Modification of lipid biosynthesis in *Populus* x *canescens* and characterization of transgenic lines

Dissertation

zur Erlangung des mathematisch-naturwissenschaftlichen

Doktorgrades

"Doctor rerum naturalium"

der Georg-August-Universität Göttingen

im Promotionsprogramm Materialforschung Holz

der Georg-August University School of Science (GAUSS)

Vorgelegt von

Gerrit-Jan Strijkstra

Varel, 2020

Betreuungsausschuss

Prof. Dr. Andrea Polle

(Forstbotanik und Baumphysiologie, Büsgen-Institut, Universität Göttingen)

Prof. Dr. Carsten Mai

(Holzbiologie und Holzprodukte, Büsgen-Institut, Universität Göttingen)

Prof. Dr. Cynthia A. Volkert

(Physik, Institut für Materialphysik, Universität Göttingen)

Mitglieder der Prüfungskommission

Referentin:

Prof. Dr. Andrea Polle

(Forstbotanik und Baumphysiologie, Büsgen-Institut, Universität Göttingen)

Koreferent:

Dr. habil. Thomas Teichmann

(Schwann-Schleiden Research Center, Abteilung Zellbiologie der Pflanze, Universität Göttingen)

Weitere Mitglieder der Prüfungskommission

Prof. Dr. H. Militz

(Holzbiologie und Holzprodukte, Büsgen-Institut, Universität Göttingen)

Prof. Dr. C. Mai

(Holzbiologie und Holzprodukte, Büsgen-Institut, Universität Göttingen)

Prof. Dr. C. Volkert

(Physik, Institut für Materialphysik, Universität Göttingen)

Dr. C. Eckert

(Forstbotanik und Baumphysiologie, Büsgen-Institut, Universität Göttingen)

List of contents

List of figures

List of abbreviations

ANOVA	Analysis of Variance
bp	Base pairs of nucleotides
cDNA	Complementary DNA
CTAB	Cetyltrimethylammoniumbromide
ddH_2O	Double deionized water
DNA	Desoxyribonucleic Acid
DNTPs	Desoxy-nucleotide triphosphates
(DX)	Developing xylem, tissue
EDTA	Ethylenediaminetetraacetic acid
et al.	Et alia (Latin) = and others
FAE	Formaldehyde: Acetic Acid: Ethanol
FW	Fresh weight
g_s	Stomatal conductance
h	Hours
H_2O	Water
L	Litre
(L)	Leaf, tissue
$MgCl_2$	Magnesium chloride
min	Minute
ml	Millilitre
mm	Millimetre
mol	Mole
MPa	Megapascal
mRNA	Messenger RNA
MS medium	Murashige & Skoog medium
mx	Mature xylem
Nm	Nanometer
µg	Microgram
µL	Microliter
µm	Micrometer
µM	Micromolar
OE	Overexpression

°C	Degree Celsius
P. trichocarpa	*Populus trichocarpa*
P. x *canescens*	*Populus* x *canescens*
PCR	Polymerase chain reaction
qRT-PCR	Quantitative real –time PCR
(R)	Root, tissue
rcf	relative centrifugal force (1 rcf = 9.81 $m*s^{-1}$)
Rif	Rifampicine
RNA	Ribonucleic acid
RNase	Ribonuclease
rpm	revolutions per minute
RT	Room temperature
s	Seconds
SE	Standard error
SWC	Soil water content
Taq	*Thermus aquaticum*
Tm	Melting temperature
UV	Ultra violet
V	Voltage
v/v	Volume/volume
VLA	Vessel lumen area
WT	Wild type
w/v	Weight/volume
YEB	Yeast extract broth
Ψ	Pre-dawn water potential

Abstract

Lipid-derived hydrocarbons have many important tasks in land plants. They prevent uncontrolled water loss as constituents of the hydrophobic properties of the cuticula. Another important task of lipid-derived hydrocarbons is the storage of energy. A common, lipid-derived plant storage compound is triacylglycerol (TAG). In woody plants, TAGs are localized in the stem in ray cells and utilized to power cambial reactivation in spring. The storage pools in the stem of woody plants are used not only to cope with seasonal changes but also to encounter sudden stress events such as wounding, extreme cold and drought periods. Regarding climate change, especially drought events are expected more frequently and may require enhanced protection against water loss. In woody perennial plants, TAG and wax synthesis and their physiological consequences for wood properties and stress resistance are poorly understood.

The main goal of this thesis was to generate transgenic *P.* x *canescens* trees with enhanced amounts of wax esters and TAGs in vegetative tissues and to investigate the impact of these modifications on growth, biomass production, wood properties and physiological performance. Two main hypotheses were tested: (a) enhanced amounts of wax esters or TAGs increase the hydrophobicity of wood evident from reduced wood swelling, thereby, affecting an important technological feature of wood, and (b) the accumulation of wax esters in the cuticula enhances the drought resistance of transgenic trees. Therefore, two key genes involved in wax ester and TAG synthesis were expressed in poplar: (i) a wax ester synthase derived from the desert shrub *Simmondsia chinensis* (*ScWS*) and (ii) the Arabidopsis diacylglycerol *O*-acyltransferase 1 (*AtDGAT1*), the key enzyme in TAG production via the Kennedy pathway. Efforts were undertaken to co-express two further genes to increase the yield of lipids: the *Marinobacter aquaolei* fatty alcohol reductase (*MaFAR*) in combination with the *ScWS* and the transcription factor *WRINKLED1* of Arabidopsis (*AtWRI1*) in combination with *AtDGAT*. The genes were expressed in poplar under the 35S promoter or the DX15 promoter, the latter being cloned and characterized in this study. While the commonly used 35S promoter was expected to lead to constitutive overexpression of the target gene, the DX15 promoter was demonstrated to express the target gene strongly in wood. Although a co-expression of two genes could not be achieved, presumably due to the size of the resulting constructs, several viable transgenic lines of *Populus* x *canescens* were produced overexpressing *ScWS* or *AtDGAT1*. The constitutive overexpression of the *ScWS* under the 35S promoter led to significant physiological changes of the transgenic plants. Compared to the wildtype, transgenic plants showed a lower stomatal conductance caused by smaller stomata, but similar photosynthesis rates. In long term experiments, the *35S::ScWS* expressing plants showed slightly decreased water consumption, and enhanced water use efficiency. The biomass production was significantly influenced negatively by overexpression of *ScWS* in young plants under only during long term growth under greenhouse conditions. Gas chromatography–mass

spectrometry analyses revealed a significant decrease in wax ester precursor molecules on the surface of leaves and – to a lower extent – also on the surface of stems. To test the drought responses of the ScWS-overexpressing poplar lines, the plants were exposed to mild and severe drought stress conditions. Under sudden, severe drought conditions, the transgenic plants showed an enhanced vitality compared to WT plants. Under mild drought conditions, the pre-dawn leaf water potential of the transgenic plants was slightly lower than that of the wildtype plants. Anatomical studies of wood that had been produced during long term mild drought revealed no differences between the transgenic lines and the wildtype. Taken together, we speculate that overexpression of the wax ester synthase might deplete the precursor molecule pool due to higher wax biosynthesis. The synthesis of other compounds being part in the cuticular wax layer (e.g. alkanes) might thus be limited. Since the cuticular composition has been demonstrated to be controlled by drought stress in many annual plants, feed-back mechanisms of an altered cuticular composition might have induced a mild drought stress in the transgenic polar plants. This might have resulted in “pre-acclimation” and subsequently in plants with higher resistance under severe stress.

Transformation of poplars with *AtDGAT1* yielded only viable plants under the tissue-specific DX15 promoter but not under the 35S promoter. Previous studies in annual plants suggested that overexpression of *DGAT1* resulted only in an enhanced accumulation of TAGs when the production of the precursor molecules for TAGs were enhanced by co-expression of a second gene, such as the transcription factor WRI1 or the enzyme FAR. Therefore, we speculate that a constitutive overexpression of *AtDGAT1* without enhancing the precursor pool might unbalance the lipid metabolism too harshly, thereby, precluding the production of viable lines of *35S::AtDGAT1*. However, when expressed tissue-specific with the DX15 promoter, the impact might be sufficiently limited to prevent effects on the poplar’s physiology. This idea was supported by the observation that the presence of lipid droplets in ray cells and other xylem regions of the *DX15*::*AtDGAT1* transgenic poplar was not different from that in the wildtype. No significant differences were found in growth rates, biomass production and wood formation, but the water uptake of dry wood was significantly decreased.

In conclusion, the overexpression of *ScWS* led to improved drought performance in poplar and the overexpression of At*DGAT1* in developing xylem improved a technological wood feature since the swelling of dry wood was diminished compared to the wildtype. In future studies, the impact of these transgenic modifications on the composition of the lipid profiles and the wax load on the plant´s surfaces have to be further characterized. It will also be important to clarify the links between drought signals, stomatal size and wax production. This thesis, thereby, opens new perspectives not only for the development of trees with improved wood properties but also for the selection of trees for future, drier climatic conditions.

Zusammenfassung

Fette, Wachse und andere lipidartige, langkettige Kohlenwasserstoffe erfüllen in Landpflanzen wichtige Aufgaben, z.B. in Form der Kutikula als Schutz vor unkontrolliertem Wasserverlust oder in Form von Speicherverbindungen, die Energie und organische Moleküle für den Stoffwechsel liefern. Dabei nehmen Triacylglyceride (TAGs) eine Schlüsselstellung ein. Sie finden sich als Energiespeicher in Samen, ebenso wie in vegetativen Geweben. Im Holz von Bäumen werden TAGs in den Strahlzellen bevorratet, wo sie zur Kohlenstoff- und Energieversorgung für die Reaktivierung des Kambiums im Frühjahr essentiell sind. Neben saisonalen Veränderungen werden diese Speicherpools auch verwendet, um plötzlichen Stressereignissen wie Verletzungen, extremer Kälte und Dürreperioden zu begegnen. Insbesondere Dürreereignisse werden im Zuge des Klimawandels immer häufiger erwartet und machen einen verbesserten Schutz vor Wasserverlust unabdingbar. In mehrjährigen Holzpflanzen sind die Biosyntheseprozesse für TAGs und Wachse, sowie ihre physiologischen Auswirkungen für die Holzeigenschaften und die Stressresistenz jedoch kaum bekannt.

Das Hauptziel dieser Arbeit war es, transgene *P.* x *canescens* mit erhöhten Mengen an Wachsestern und TAGs in vegetativen Geweben zu erzeugen und die Auswirkungen dieser Modifikationen auf Wachstum, Biomasseproduktion, Holzeigenschaften und Physiologie zu untersuchen. Dabei wurden zwei Hypothesen verfolgt: (a) Erhöhte Mengen an Wachsestern oder TAGs erhöhen die Hydrophobizität von Holz. (b) In transgenen Pappeln reichern sich Wachsester auf der Cuticula an und erhöhen die Trockenstressresistenz.

Um diese Hypothesen zu testen, sollten folgende zwei Schlüsselgene, die an der Wachsester- und TAG-Synthese beteiligt sind, in Pappeln überexprimiert werden: (i) eine Wachsestersynthase von *Simmondsia chinensis,* einer Wüstenstaude (*ScWS*), sowie (ii) die Arabidopsis-Diacylglycerol-O-Acyltransferase 1 (*AtDGAT1*), das Schlüsselenzym in der TAG-Synthese. Durch Ko-transformation weiterer Gene des Lipidstoffwechsels wurde weiterhin versucht, einer Limitierung der nötigen Vorstufen für diese Stoffwechselpfade entgegenzuwirken und somit die Lipidsynthese zu erhöhen. Hierzu wurde die Fettalkohol-Reduktase aus *Marinobacter aquaolei* (*MaFAR*) in Kombination mit der *ScWS*, sowie der Transkriptionsfaktor WRINKLED1 aus Arabidopsis (*AtWRI1*) in Kombination mit der *AtDGAT1* verwendet.

Die Zielgene (*ScWS, AtDGAT1*) wurden in Pappeln unter dem 35S-Promotor oder dem in dieser Studie klonierten sowie charakterisierten DX15-Promotor exprimiert. Diese Ansätze dienten dazu, neben der konstitutiven Expression des Gens unter dem 35S-Promoter in allen Geweben, auch eine spezifische Expression im Xylem mittels des DX15-Promoters zu ermöglichen. Die Ko-Expression von zwei Genen konnte vermutlich aufgrund der Größe der resultierenden Konstrukte nicht erreicht werden. Jedoch wurden zahlreiche, lebensfähige transgene Linien von *Populus* x *canescens* hergestellt, die *ScWS* oder

AtDGAT1 überexprimierten. Die konstitutive Überexpression der *ScWS* unter dem 35S-Promotor führte zu signifikanten physiologischen Veränderungen der transgenen Pflanzen. Im Vergleich zum Wildtyp wurde eine geringere stomatäre Leitfähigkeit bedingt durch eine kleinere Größe der Stomata festgestellt. Die Photosyntheserate der überexprimierenden *ScWS*-Linien war im Vergleich zum Wildtyp nicht beeinflusst. In Langzeitversuchen zeigten die *ScWS*-überexprimierenden Pappeln einen leicht verringerten Wasserverbrauch und eine verbesserte Wassernutzungseffizienz. Hierbei wurde auch die Biomasseproduktion durch die Überexpression von *ScWS* in jungen Pflanzen unter Gewächshausbedingungen signifikant negativ beeinflusst. Analysen mittels Gaschromatographie mit Massenspektrometrie-Kopplung zeigten eine signifikante Abnahme von Vorstufen für Wachsester auf der Oberfläche von Blättern und - in geringerem Maße - auch auf der Oberfläche des Stamms.

Um die Reaktionen der *ScWS*-überexprimierenden Pappellinien auf Trockenstress zu testen, wurden die Pflanzen mildem, langanhaltendem sowie schwerem, akutem Trockenstress ausgesetzt. Unter schwerem, akutem Trockenstress zeigten die transgenen Pflanzen im Vergleich zum Wildtyp eine erhöhte Vitalität. Unter langanhaltendem, mildem Trockenstress war das nach Erholung in der Dunkelphase vor Tagesbeginn gemessene Wasserpotential („pre-dawn“) der Blätter der transgenen Pflanzen geringfügig niedriger als das vom Wildtyp. Die Untersuchung der Holzanatomie ergab keine Unterschiede zwischen den transgenen Linien und dem Wildtyp.

Diese Ergebnisse lassen sich folgendermaßen interpretieren: Eine Überexpression der Wachsestersynthase könnte den Pool an Vorläufermolekülen minimieren haben und daher die Synthese anderer Verbindungen, die Teil der kutikulären Wachsschicht sind (z. B. Alkane), limitieren. Da gezeigt wurde, dass die kutikuläre Zusammensetzung in vielen einjährigen Pflanzen durch Trockenstress kontrolliert wird, könnten Rückkopplungsmechanismen einer veränderten kutikulären Zusammensetzung ein mildes Trockenstress-Signal in den transgenen Pflanzen induziert haben und damit zu einer „Vorakklimatisierung“ der transgenen Pflanzen führen. Diese könnten deshalb zu einer höheren Resistenz unter akutem Trockenstress zeigen, hätten aber keinen Vorteil, wenn eine Akklimatisierung unter moderatem Stress möglich ist.

Die Transformation von Pappeln mit *AtDGAT1* ergab nur unter dem gewebespezifischen DX15-Promotor lebensfähige Pflanzen, nicht jedoch unter dem 35S-Promotor. Frühere Studien an einjährigen Pflanzen zeigten, dass eine Überexpression von DGAT1 nur zu einer verstärkten Akkumulation von TAGs führt, wenn die Produktion der Vorläufermoleküle für TAG durch Ko-expression eines zweiten Gens wie des Transkriptionsfaktors WRI1 oder des Enzyms FAR gesteigert wurde. Daher vermuten wir, dass eine konstitutive Überexpression von *AtDGAT1* mittels des 35S-Promoters ohne Erhöhung des Pools an Vorstufen den Lipidstoffwechsel stark aus dem Gleichgewicht bringt und deshalb keine lebensfähigen Linien erzeugt werden konnten. Wenn *AtDGAT1*

jedoch gewebespezifisch mittels des DX15-Promotors exprimiert wird, ist die Wirkung offenbar ausreichend begrenzt, um eine zu starke Auswirkung auf die Physiologie der Pflanze zu erzeugen. Gestützt wird diese These dadurch, dass sich die Menge der Lipidakkumulation in Strahlzellen und anderen Xylemregionen von *AtDGAT1*-überexprimierenden Pappeln ebenfalls nicht signifikant zur Lipidakkumulation von Wildtyp Pappeln unterschied. Weiterhin wurden zwischen *DX15::*AT*DGAT1* Linien und dem Wildtyp keine signifikanten Unterschiede in Bezug auf Wachstumsraten, Biomasseproduktion und Holzbildung gefunden. Die Wasseraufnahme von trockenem Holz zeigte sich jedoch signifikant verringert.

Zusammenfassend lässt sich festhalten, dass die Überexpression von *ScWS* unter dem 35S-Promoter zu einer verbesserten Trockenstressresistenz von Pappeln und die Xylem-spezifische Überexpression von *AtDGAT1* zu einer verringerten Holzquellung führt. Eine weitergehende Charakterisierung der Lipidakkumulation sowie der Wachszusammensetzung und -menge der Kutikula durch die veränderte Lipid- und Wachsbiosynthese sollte Gegenstand weitergehender Studien sein. Hierzu ist eine Klärung der Zusammenhänge von Trockenstress-Signalen, Größe der Stomata und Wachssynthese notwendig.

Die vorliegende Arbeit eröffnet damit nicht nur neue Perspektiven hinsichtlich der Entwicklung von verbesserten Holzeigenschaften, sondern auch für Bäume mit verbessertem Trockenstressverhalten unter zukünftigen, trockeneren klimatischen Bedingungen.

1. Introduction

1.1. The Role of lipids in woody plants

1.1.1. Waxes and wax-like hydrocarbons: essential for land plants

Lipids are forming a diverse and essential group of natural compounds involved in many functions in the cell, as structural components of the cell membrane, as signalling agents, as precursors for carbon skeletons and as an important storage form for energy. A very important role in preventing water loss is played by wax esters, neutral and highly hydrophobic lipids accumulated on the plant's surface in the cuticula. The cuticula is formed of cutin, impregnated with waxes and covered with a mixture of epicuticular hydrophobic aliphatic wax-like hydrocarbons (Figure 1 B, C) of varying chain length from C16 to C36 (Stark and Tian, 2018).

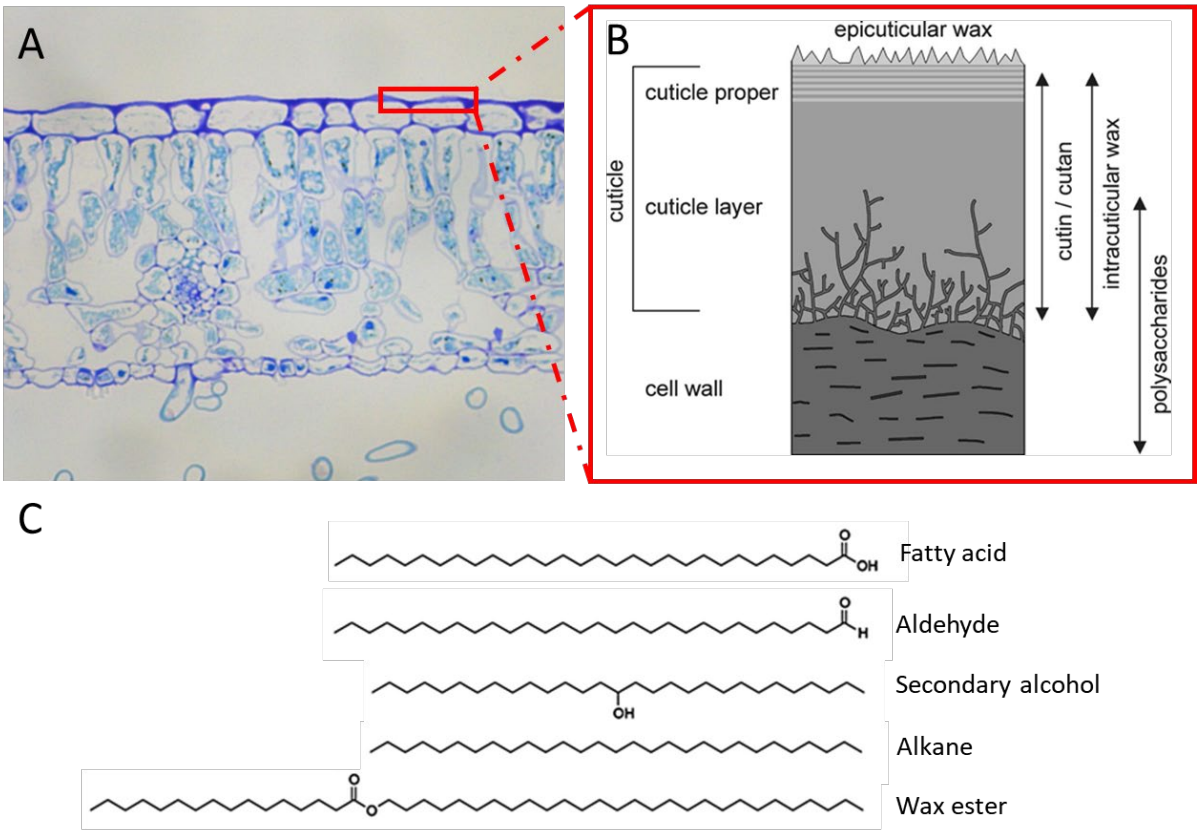

Figure 1: Schematic overview plant cuticula. A.: Cross section of a leaf of *P.* x *canescens*, stained with Fuchsin-Chryosidine-Astra blue. **B.:** Schematic overview of the cuticula's structure. **C.:** Selection of lipid-derived compounds found in the cuticula. Figure derived from Stark and Tian (2018).

Alongside the transpiration regulation, waxes also contribute to abiotic and biotic stress defences such as UV radiation (Jiang et al., 2009) or drought (Bourdenx et al., 2011). Drought has been demonstrated to increase the cuticular wax load (Shepherd and Griffiths, 2006) and alter its composition. For example, in Arabidopsis (Kosma et al., 2009) and in tobacco (Cameron et al., 2006) drought caused an increased wax load. In Arabidopsis, the amount of cuticular waxes was found to be increased up to

80 %, whereas primarily wax alkanes were affected. Interestingly, abscisic acid treatment demonstrated only little effects on wax load and cutin composition, compared to a water deficit treatment (Kosma et al., 2009).

In woody species, several studies have been executed regarding the wax quantity and composition of different tree species. Maiti et al. (2016) have found a broad variability of total epicuticular wax load in several woody species and shrubs; a classification could be drawn in high- (*Diospyros texana*; 607.65 µg/cm^2), medium- (*Quercus polymorph*; 199.40 µg/cm^2), and low- (*Ehretia anacua*; 17.58 µg/cm^2) wax load tree species (Maiti and Rodriguez, 2016). Although the cuticular composition has been screened and described in *Pinus radiata* (Franich et al., 1985) and linked to seasonal variations in temperate deciduous tree species such as *Fagus sylvatica* and *Acer pseudoplatanus* (Sachse et al., 2009), in tree species a comprehensive knowledge is not yet achieved.

In *Populus* species, GC-MS studies revealed the most abundant compounds to be odd chain alkanes and alcohols; wax esters, however, were not investigated (Dost 2014). More detailed studies regarding the cuticula wax composition or overexpression of wax ester synthesis genes in *Populus* species have not been accomplished so far (December 2019).

1.1.2. Lipids as energy and carbon storage in perennial plants

Lipids, predominately triacylglycerols (TAG), are well suited molecules to store energy and carbon due to their high density, hydrophobicity and easy dissimilation (Cagliari et al., 2011). Storage TAGs can be found in all plant phyla. TAGs consist of three fatty acid residues of varying length and composition (Figure 2) and are mostly stored in seeds. Lipids are utilized in seed tissues of many plant species to power germination and as a time-limited energy and carbon source. Recent research focussed mainly on the possibility to increase TAG content of seed tissues, as TAGs are a valulable biological resource for the production of biofuels, lubricants and food oil production in conventional crop production (Durrett et al., 2008). However, the natural production of TAGs is often limited, despite the ability of plants for assimilation, accumulation, and dissimilation of TAGs in vegetative tissues. Instead, predominately starch is utilized for carbon and energy storage.

In addition to storage functions of lipids in seed tissues, perennial woody plants must further ensure a certain amount of carbon and energy in vital tissues to straddle time periods of no or low photosynthetic activity, for examples when coping with seasonal changes between winter and summer. In deciduous tree species, the most important vegetative tissue to be maintained by carbon supply is the cambium, whose reactivation in spring consumes a lot of energy. According to the main storage compounds found in stems, some tree genera have been classified as “starch -” and others as “fat -“ trees already a long time ago (Sinnott, 1918). However, cambial reactivation has been

demonstrated to be powered by starch (Giovannelli et al., 2011) and lipids as well (Sauter and Cleve, 1994), indicating that both compounds play vital roles in the tree´s life.

Lipids in vegetative stem tissues are accumulated in oleosomes in parenchyma cells but have also been found in meristems such as the cambium. In *Cryptomeria japonica*, the oleosome size in cambial tissue during cambial reactivation was demonstrated to be decreased by 75%; the size of lipid droplets decreased in ray and fusiform cambium from cambial reactivation to the start of xylem differentiation (Begum et al., 2010). In *Populus* x *canadensis* (Moench 'robusta'), oleosomes present in ray parenchyma cells increased in summer, persisted during winter and decreased during cambial reactivation in spring (Sauter and Cleve, 1994). Microarray analyses of ray cells of *Populus* x *canescens* revealed 20 genes involved in fatty acid metabolism that were upregulated in early spring, indicating an increased glyoxylate cycle activity (Larisch et al., 2012). Therefore, Larisch et al. (2012) speculated that carbon derived from dissimilated TAGs might participate in gluconeogenesis underlining the carbon and energy storage function of glycerolipids. Also, it has been hypothesized by Paux et al. (2004) that precursors or intermediate compounds of lipid dissimilation could take part indirectly in cellulose synthesis of *Eucalyptus* xylem secondary cell walls, forming a possible link to channel carbon from lipids towards wood production (Eckert et al., 2019). Similar as to wax esters, the biosynthesis, regulation and dissimilation of TAGs in tree species has rarely been studied.

1.2. Biosynthetic pathways for plant lipids

1.2.1. Wax ester accumulation in seeds: Wax ester synthase (*WS*)

Wax esters do not only play a role in cuticula formation but have also been discovered as storage compounds (Miwa, 1971) in the desert shrub Jojoba (*Simmondsia chinensis*). In Jojoba, monounsaturated wax esters with chain length of C16-C26 (Sham and Aly, 2012) account for about 50 % of the seed dry weight (Miwa, 1971). Jojoba oil is known for its oxidation stability; Jojoba-derived wax esters are utilized in cosmetic industry, as lubricant and have been discussed for replacing triacylglycerols for biofuel production (Jetter and Kunst, 2008). Therefore, the jojoba wax ester synthase (*ScWS*) has been used in biotechnological studies (Kalscheuer et al., 2006).

Wax esters are produced by condensing fatty alcohols with acyl-CoA (Figure 2). The availability of fatty acids *in planta* is limiting the production yield (Iven et al., 2016). Fatty alcohols are synthesized by a fatty acyl-CoA reductase (FAR) via reduction of an acyl-CoA (Figure 2). Several different FARs have been tested for their productivity to channel fatty alcohols towards the ScWS to improve the overall yield (Iven et al., 2016). The ScWS is localized in the ER membrane and FAR is situated in cytosol. Expression of fusion constructs containing a WS and a FAR as well as a simple co-expression of WS and FAR both led to higher wax ester content (Yu et al., 2018). A FAR from *Marinobacter aquaolei* (*MaFAR*) has been

found to be a suitable protein with specificity to monounsaturated substrates (Iven et al., 2013), providing a suitable two-step gene setup for enhanced wax ester synthesis.

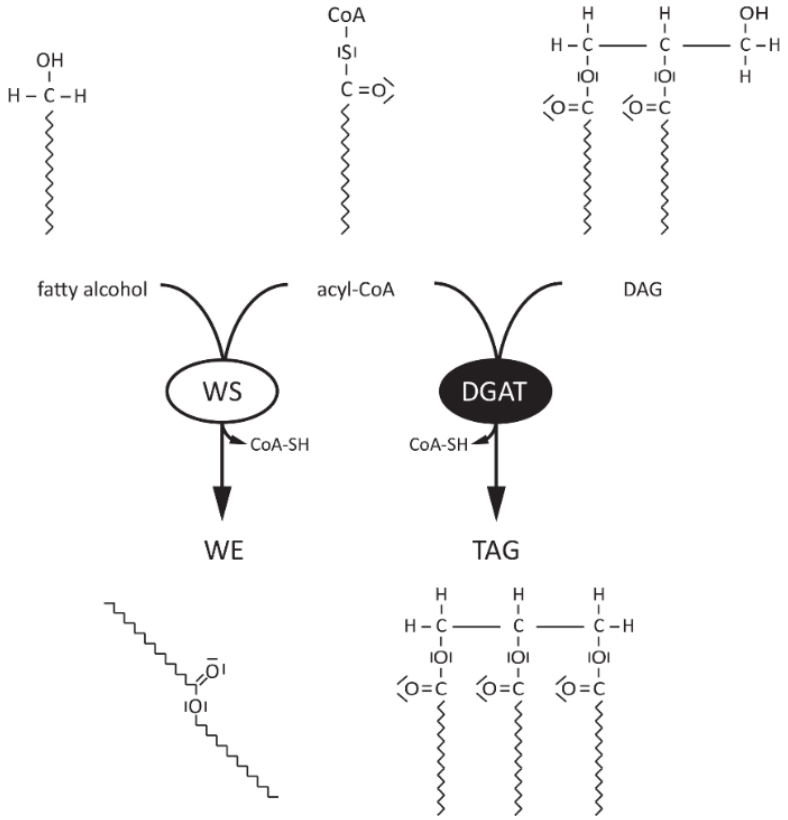

Figure 2: Production of both wax ester (WE) and triacylglycerols (TAG) require acyl-CoA. The amount of free fatty alcohols limits the yield of wax ester. Forming TAG, the diacylglycerol (**DAG**) pool is mostly believed to limit TAG synthesis. Picture derived from Kawelke and Feussner (2015).

1.2.2. Biosynthesis of wax esters

Wax esters are synthesized by acyl-CoA:wax alcohol acyltransferases (WSD), utilizing fatty alcohols and acyl-CoA as precursor molecules (Figure 3). Several different WSDs with different metabolic tasks have been discovered so far. In Arabidopsis, a complex network of 11 WSDs regulates wax synthesis and wax deposition of different tissues such as the surface of flowers, siliques and leaves (WSD1), whereas in roots no wax ester increase was found after overexpression of WSD 10 (Patwari et al., 2019). WSDs have been shown to affect petal development (WSD11), (Takeda et al., 2014) and several WSDs were demonstrated to be affected by ABA and drought stress, with partly opposite effects. For example, ABA increased wax deposition on leaves through WSD1 (Cui et al., 2016) but decreased expression of WSD10 in roots (Patwari et al., 2019). Some WSDs (WSD 6, 7) were demonstrated not to take part in surface wax ester synthesis at all (Patwari et al., 2019). However, WSDs strongly contribute to the outer wax layer of plants through synthesis of wax esters (Figure 3).

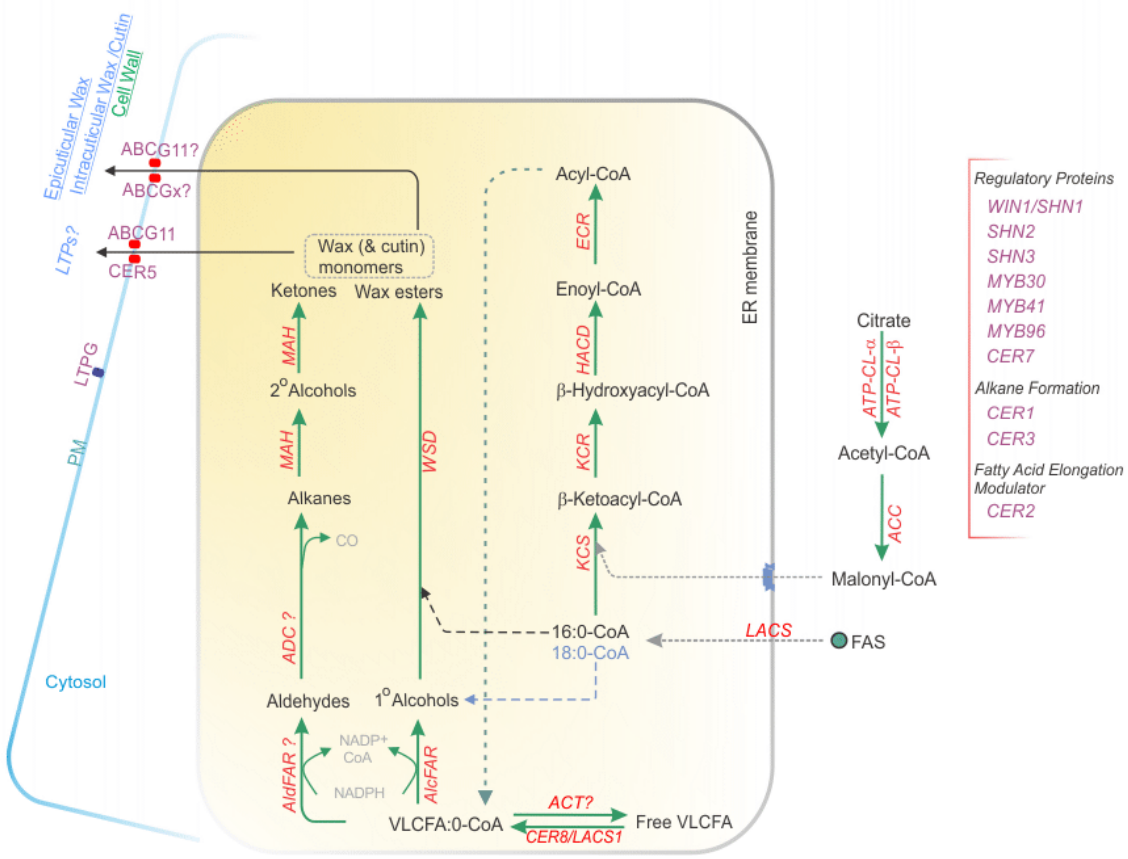

Figure 3: The synthesis pathway of surface wax esters in Arabidopsis. Wax ester synthase (**WSD**) converts primary alcohols (**1° alcohols**) and acyl-CoA to wax esters. Very long chain fatty acids (**VLCFA**) are precursors of two wax synthesis pathways: the decarbonylation pathway, forming predominately alkanes and the acyl reduction pathway, forming primary alcohols and wax esters. Several regulatory transcription factors are involved in regulation of surface waxes in Arabidopsis and are mainly linked to osmotic stress (**MYB41**, Hoang et al., 2012), ABA response (**MYB30**, Zheng et al., 2012) and directly to wax biosynthesis (**MYB96**, Seo and Park, 2011). Abbr.: **ABCG:** ATP-binding cassette transporter G subfamily; **ACC:** acetyl-CoA carboxylase; **ADC:** aldehyde decarbonylase; **AlcFAR:** alcohol-forming fatty acyl-CoA reductase; **AldFAR:** aldehyde-forming fatty acyl-CoA reductase; **ATP-CL-α(β):** ATP citrate lyase α(β) subunit; **CER5:** ECERIFERUM 5; **ECR:** enoyl-CoA reductase; **HACD:** hydroxyacyl-CoA dehydrase; **KCS:** ketoacyl-CoA synthase; **KCR:** ketoacyl-CoA reductase; **LACS:** long-chain acyl-CoA synthetase; **LTP:** lipid transfer protein; **LTPG:** GPI-anchored lipid transfer protein; **MAH:** midchain alkane hydroxylase; **MAO:** midchain alkanol oxidase; **MCD:** malonyl-CoA decarboxylase; **THS:** acyl-CoA thiOEsterase; **VLCFA:** very long-chain fatty acid; **WS:** wax synthase; **WSD:** bifunctional wax ester synthase/diacylglycerol acyltransferase. Picture derived from Li-Beisson et al. (2010).

1.2.3. DGAT1 as the major player in TAG synthesis

The production of both lipidic compounds, wax esters and TAGs, use acetyl-CoA as a precursor (Fig. 2). The key step in TAG production (Figure 4) via the Kennedy pathway (Kennedy, 1961) is performed by the diacylglycerol *O*-acyltransferase (DGAT1), which converts diacylglycerol and acetyl-CoA to triacylglycerol (TAG, Hobbs et al., 1999). DGAT1 is a ubiquitous enzyme in major eukaryotes and specifically in higher plants (Turchetto-Zolet et al., 2011); homologs of the *DGAT1* gene family have been described in many annual land plants (Bouvier-Navé et al., 2000) and in woody species *Vernicia fordii* (Shockey et al., 2006). In *Populus trichocarpa, DGAT1* homologs have been found as well (Wang et al., 2013).

In Arabidopsis and tobacco, DGAT1 has been discovered to alter oil composition and quantity in seed tissues (Katavic et al., 1995, Zhang et al., 2005). Overexpression of *DGAT1* under a seed-specific promoter led to an increased quantity of TAG in seeds of Arabidopsis (Jako et al., 2001) and Brassicaceae species (Savadi et al., 2015; Weselake et al., 2008). As limiting step in TAG synthesis, DGAT1 has been demonstrated to be affected by environmental stress. In Arabidopsis seedlings, stress-induced *DGAT1* expression was increased in response to treatments with either ABA, JA, SA, or NaCl as well as under nitrogen deprivation (Kong et al., 2013). The regulation of DGAT1 was identified to consist of a synergistic effect of the two transcription factors ABI4 and ABI5, forming a direct link to ABA as a regulating "supervisor" (Kong et al., 2013).

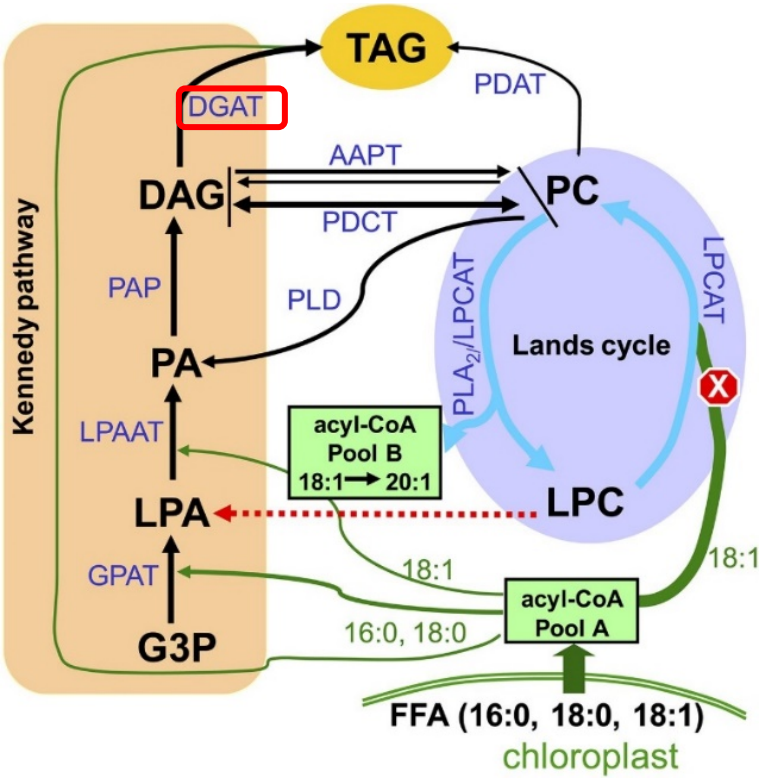

Figure 4: Schematic overview of triacylglycerol (TAG) synthesis in plants. Two different pathways are known to interact in order to produce TAG: The Kennedy pathway synthesizes TAG from *de novo* synthesized diacylglycerol (**DAG**) via the diacylglycerol acyltransferase (**DGAT**, highlighted in red). In the Lands cycle, a phosphatidylcholine: diacylglycerol acyltransferase (**PDAT**) converts phosphatidylcholine (**PC**) to synthesize TAG. Both pathways are interacting in order to adjust metabolic limitations of precursor molecules. **PC:** Phosphatidylcholine; **LPC:** Lysophosphatidic acid**; LPCAT:** Acyl-CoA:lysophosphatidylcholine acyltransferase; **FFA:** free fatty acids; **G3P:**; Glyceraldehyde 3-phosphate; **GPAT:** Glycerolphosphate-O-acyltransferase; **LPA:** Lysophosphatidic acid; **LPAAT:** Lysophosphatidic acid acyltransferase; **PA:** Phosphatidic acid; **PAP:** Phosphatidic Acid Phosphatase; **AAPT:** Aminoalcoholphosphotransferase; **PDCT:** PC:diacylglycerol cholinephosphotransferase; **PLD**: Phospholipase D. Figure derived from Wang et al. (2012).

In vegetative tissues of Arabidopsis, an increased *DGAT1* transcript level was found during leaf senescence, presumably to recycle sequestered fatty acids from galactolipid origin (Kaup et al., 2002). An enhanced accumulation of TAG in vegetative tissues such as leaves and stem parts was achieved by ectopic expression of *DGAT1* in *Jatropha curcas* (Maravi et al., 2016) and tobacco (Nookaraju et al.,

2014). However, the co-expression of transcription factors (e.g. *WRI1*, see 1.2.4, or *LEC2*) was mandatory to boost lipid biosynthesis and achieve significant TAG accumulation (Nookaraju et al., 2014). Therefore, DGAT1 may be a good candidate to stimulate TAG synthesis in vegetative tissues of poplar.

1.2.4. Transcription factor WRI1: Co-transformation boosts lipid synthesis

The transcription factor WRINKLED1 (WRI1), an APETALA2/ethylene-responsive element binding protein (AP2/EREBP), was demonstrated to be a highly conserved ubiquitous regulator in oil accumulating tissues of various plant species (Grimberg et al., 2015, Ma et al., 2013). Firstly described in Arabidopsis, malfunctioning WRI1 led to a reduction of up to 80% in seed lipid content (Focks and Benning, 1998), indicating its importance in the regulation of genes involved in carbon partitioning to TAG synthesis (Cernac and Benning, 2004). Further transcriptomic analyses of overexpressed WRI1 in tobacco revealed an upregulation of genes connected to fatty acid synthesis, -degradation and phosphoenolpyruvate metabolism (Figure 5), while genes involved in starch degradation were down-regulated (Grimberg et al., 2015).

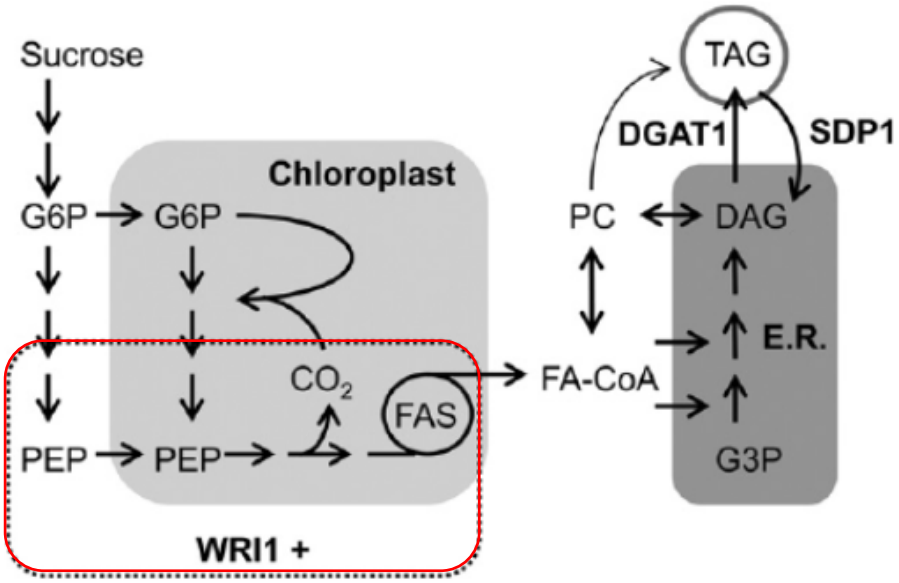

Figure 5: Schematic overview of WRI1 involvement in TAG production. WRI1 is a transcription factor that positively regulates genes of fatty acid synthesis and thus increases the pool of free FA-CoA, precursor of TAG (indicated in red). Synergistic effects through co-expression with *DGAT1* have been observed (1.2.4). **E.R.:** endoplasmic reticulum; **FA-CoA:** fatty acyl-CoA; **FAS:** fatty acid synthase; **PEP:** phosphoenolpyruvate; **G6P:** Glucose-6-phosphate; **PC:** phosphatidylcholine; **DAG:** diacylglycerol; **DGAT:** diacylglycerol acyltransferase; **SDP1:** sugar-dependent 1**.** Figure derived from Van Erp et al. (2014).

Since the synthesis of TAG requires acyl-CoA and DAG (Figure 2), these precursor molecules are limiting the overall yield of TAG production in various TAG-accumulating species, such as the algae *Chromera velia* (Huerlimann et al., 2014), Arabidopsis (Bates et al., 2009) and traditional crops such as soybean (Bates et al., 2009). Because DAG can be formed *de novo* via the Kennedy pathway or by

utilizing PC in the Lands cycle (Figure 4), the preference for the utilized pathways varies in different species; in crops like soybean (Bates et al., 2009) or linseed (Dyer et al., 2008), PC-derived TAG is preferred. In the woody species *Cocoa*, *de novo* produced DAG is preferred (Griffiths and Harwood, 1991). In *Populus* species, the preference of the utilized DAG pathway is unknown. Although WRI1 is positively affecting the synthesis of FA-CoA and FA upstream (Figure 5) and thus is contributing to both TAG-pathways (Kennedy and Lands cycle), this transcription factor also positively regulated LPAAT WRI1 of *Elais guineensis* (Figure 4) (Yeap et al., 2017). When co-transformed with DGAT1, WRI1 had synergistic effects on TAG production in seeds of *Lepidium campestre* (Ivarson et al., 2017a) and in leaves of Arabidopsis (Vanhercke et al., 2013), sugarcane (Zale et al., 2016) and tobacco (Nookaraju et al., 2014). Therefore, WRI1 is apparently essential to persistently enhance TAG levels in vegetative tissues.

1.3. The role of abscisic acid and cuticular changes in drought stress

Abscisic acid (ABA) is a phytohormone well known for its extensive functions in plants. Additionally to its involvement in developmental procedures in non-stress conditions, e.g. seed and bud dormancy and germination (Hilhorst and Karssen, 1992), leaf senescence (Zhao et al., 2016) and seasonality in perennial plants (Tylewicz et al., 2018), various abiotic stresses such as soil salinity (Cramer, 2002), cold tolerance (Ishitani et al., 1997) and freezing resistance (Chen and Gusta, 1983) are managed by ABA. In short-term drought events, ABA was demonstrated to play a major role in maintaining the water balance: Increasing ABA levels were linked to the reduction of stomatal conductance and photosynthesis yield (Jones and Mansfield, 1970; Negin and Moshelion, 2016) by the regulation of AREB (ABA-Responsive Element Binding protein) transcription factors (Hubbard et al., 2010). In long-term drought stress conditions, ABA was found to contribute to stress adaptation by affecting the morphology of stomata, leading to a reduced size of stomata without affecting the photosynthesis capacity (Franks and Farquhar, 2001). Adjustment of the water balance also occurs in other tissues, e.g. by the short-term regulation of root water uptake (Kumar et al., 2018) or long-term regulation of the root growth (Sharp and LeNoble, 2002). Besides maintaining the water balance in short- and long-term conditions by adjustment of transpiration, ABA is also involved in reducing evaporation in long-term drought conditions: several studies with different plant species showed increased cuticula thickness in response to ABA to decrease water loss in drought stress situations, e.g. tree tobacco (Cameron et al., 2006), tomato (Martin et al., 2017) and Arabidopsis (Macková et al., 2013; Patwari et al., 2019). The transcription factor MYB96 is demonstrated to connect ABA to changes in cuticular composition in long-term drought stress conditions (Seo and Park, 2011). Although the regulation of the cuticular composition can be affected by drought stress via ABA, little is known about feed-back effects of an altered cuticula towards ABA signalling. Since this study predominately focusses on the

effects of an altered cuticular composition by putatively boosting the wax ester synthesis downstream of the ABA signalling network, addressing a feed-back mechanism might be of interest.

1.4. Objectives

The main goal of this study was to increase lipid-derived compounds, namely wax esters and triacylglycerols, in vegetative tissues in the woody species *P.* x *canescens.* The phenotypes of the different transgenic poplar plants produced in this study were investigated with a focus on (I) drought tolerance and (II) lipid accumulation in wood. Therefore, two different promoters have been utilized: the ubiquitous 35S promoter to increase lipid-derived compounds in all tissues and the xylem specific promoter DX15, to enhance hydrophobic compounds specifically in wood.

P. x *canescens* was selected for this study because it is a suitable model organism for wood characteristics (Eckert et al., 2019). As a perennial deciduous tree species, poplar requires strong regulation of its carbon flux and energy turnover in vegetative tissues, for instance, during seasonal changes (Larisch et al., 2012). Since poplar is storing energy in lipid droplets (Sauter and Cleve, 1994), it is the model-of-choice to investigate lipid synthesis and accumulation in wood. *Populus* species are further useful as woody model plant because of their fast growth, ease of handling tissue cultures, transformation capability and fully sequenced genome, e.g. *P. trichocarpa* (Tuskan et al., 2006) and *P.* x *canescens* (Mader et al., 2016). In this study, *P.* x *canescens* (*P. alba* x *tremula*, clone INRA 717-1B4) was utilized to produce transgenic plants.

Two major genes of interest have been chosen for expression in poplar trees: Firstly, a DIACYLGLYCEROL *O*-ACYLTRANSFERASE (1.2.3) of Arabidopsis origin (further referred to as *AtDGAT1*) to push accumulation of TAGs, a common storage compound in wood of poplar trees. Secondly, a WAX ESTER SYNTHASE from jojoba (1.2.1, further referred to as *ScWS*) was used as an alternative transformation target to enhance wax accumulation.

In *Populus*, wax esters are usually channelled to the cuticula, where they are deposited. Thus, no active breakdown in vegetative tissues of poplar plants is expected to take place. To avoid limitation of wax ester biosynthesis by lacking precursors, several attempts were done to co-express genes with impact on the pool of precursor molecules: the transcription factor WRI1 was used with the intention to boost lipid synthesis and channel carbon towards the DGAT1 and FAR to increase free fatty alcohols utilized by the WS. As a possible outcome of overexpression of wax ester biosynthetic pathways, an accumulation of wax esters in the cuticula was expected. Since the cuticula is a major barrier to avoid water loss, the thesis focused on studying on the characterization of growth, biomass and physiological performance of *P.* x *canescens* under drought conditions.

2. Material and Methods

2.1. Schematic overview on the preparation of binary vectors

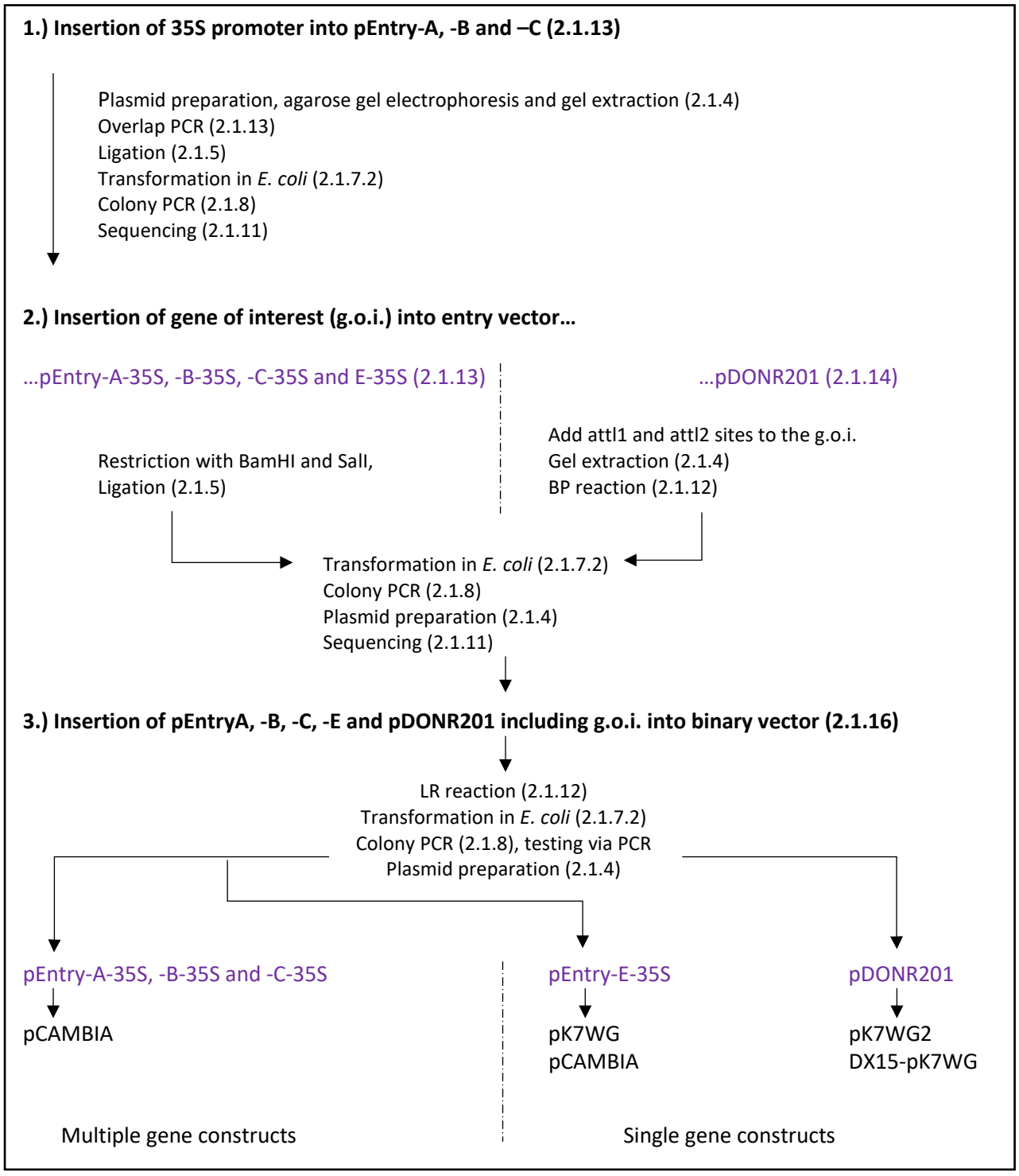

Figure 6: Schematic overview of steps performed for preparation of the different binary vectors. Every single step is described in detail in the later chapters, as indicated in brackets (). Main steps are shown in bold and refer to the preparation of entry vectors (1), the insertion of genes to the entry vectors (2) and the insertion of entry vectors with inserted genes of interest into binary vectors (3). For an overview, a complete list of each binary construct produced within this work, see Table 13.

2.1.1. Origin of genetic material

All genes utilized for the preparation of transgenic plants (Table 1) were a kind gift by Prof. Dr. I. Feussner (Department for Plant Biochemistry, Albrecht-von-Haller-Institute for Plant Sciences, University of Goettingen).

Gateway entry vectors pEntryA, -B, -C and -E and the binary vector pCAMBIA32.0G were a kind gift by Prof. Dr. I. Feussner (Department for Plant Biochemistry, Albrecht-von-Haller-Institute for Plant Sciences, University of Goettingen). Gateway entry vector pDONR201 and the pK7WG binary vector system were purchased from the manufacturer (VIB, Gent, Belgium).

The 35S promoters were either obtained from Prof. Dr. I. Feussner (Department for Plant Biochemistry, Albrecht-von-Haller-Institute for Plant Sciences, University of Goettingen) or from VIB (Gent, Belgium) as part of the pK7WG binary vector system (Table 13). The DX15 promoter was prepared within this work (2.1.15) from *P. trichocarpa* plants (stock, Department of Forest Botany and Tree Physiology, Goettingen, Germany).

Table 1: Genes utilized for poplar transformation.

Genes	Organism, origin	Referred to	Purpose
WRINKLED1	*A. thaliana*	*AtWRI1*	transcription factor
DIACYLGLYCEROL *O*-ACYLTRANSFERASE	*A. thaliana*	*AtDGAT1*	enzyme
FATTY ACYL REDUCTASE	*Marinobacter aquaeolei*	*MaFAR*	enzyme
WAX ESTER SYNTHASE	*Simmondsia chinensis*	*ScWS*	enzyme

2.1.2. Chemicals

Chemicals were obtained from Roth (Karlsruhe, Germany), if not stated otherwise.

2.1.3. Antibiotics

To select positively transformed *E. coli*, *Agrobacteria* and poplar plants and to neutralize *Agrobacteria* during the transformation (2.2.4), several different antibiotics were utilized as stated in Table 2. Antibiotics were obtained from Duchefa (Haarlem, Netherlands).

Table 2: Antibiotics utilized within this work. Antibiotics are used for selection for vectors or neutralisation of *agrobacteria*. *Ticarcillin and clavulanic acid in a ratio of 15:1 will be further referred to as Timentin® (Duchefa, Haarlem, Netherlands).

Antibiotic	Concentration [µg/ml]	Organism	Purpose	for / of	Vector
Spectinomycin	50	*E. coli*	selection	entry vector	pEntry A, -B, -C, -E
Rifampicin	20	*A. tumefasciens*	selection	*agrobacteria*	Cromosomal
Gentamicin	25				Ti plasmid
Streptomycin	50			binary vector	pK7WG2 / pCAMBIA
Kanamycin	50	*P.* x *canescens*	selection	binary vector	pK7WG2 / pCAMBIA
*Timentin®	200		neutralisation	*agrobacteria*	-
Cefotaxime	250				

2.1.4. Plasmid preparation, agarose gel electrophoresis and gel extraction

Plasmid extraction was done from 2 ml overnight culture of *E. coli* (37°C, LB-media) with a MiniPrep kit (Quiagen, Hilden, Germany).

Agarose gel electrophoresis of PCR products was done with 1.2 % agarose in TRIS-Acetate-EDTA-buffer (TAE) buffer. Ethidium bromide (approximately 3 µl) was added directly to the gel before the agarose settled in a gel chamber. DNA samples were loaded with 10 x loading buffer. DNA ladder (GeneRuler™, Thermo Scientific, Braunschweig, Germany) was used in a 10x loading dye solution. Electrophoresis was performed at 100 – 120 V for 15 to 30 min (Bio-Rad Laboratories, Inc., Hercules, U.S.A).

Gel extraction of PCR products was done with the gel extraction kit of Macherey & Nagel (Düren, Germany) according to the manufacturer's protocol.

2.1.5. Restriction digests, ligation

Restriction digests of PCR products and vectors were done in accordance to the manufacturer's protocol of the restriction enzymes (Thermo Scientific, Braunschweig, Germany) up to 16 h at 37°C.

Table 3: Ingredients of a typical double digestion with HindIII and SalI.

Ingredients	Amount
Tango Buffer (2X)	8 µl
Template DNA	10-150 ng
HindIII	75 U
SalI	15 U
H_2O	up to 40 µl

Ligation of restricted PCR products and vectors occurred with a T4 Ligase (Thermo Scientific, Braunschweig, Germany) at 16°C for a minimum of 2h or overnight according to the protocol of the manufacturer.

Table 4: Ingredients of a typical T4-mediated ligation (blunt end).

Ingredients	Amount
Linear vector DNA	100 ng
Insert DNA	100-500 ng
T4 Ligase Buffer (2X)	5 µl
T4 DNA Ligase	1 U

2.1.6. Polymerase chain reaction (PCR)

A standard PCR for cloning purposes was done with the *Pfu®* proofreading polymerase (Thermo Scientific, Braunschweig, Germany), while *Taq®* polymerase (Thermo Scientific, Braunschweig, Germany) was used for colony PCR and for proof-of-concept (Table 5a). PCR (Table b) occurred in a Thermocyler® (Eppendorf, Hamburg, Germany). Annealing temperature was adjusted to the primer melting temperature (tm). Extension occurred typically at 60 s/kb of expected amplicon at 72°C.

Table 5a: Ingredients for PCR with *Pfu®* and *Taq®* polymerase.

Ingredients	*Pfu®* polymerase	*Taq®* polymerase
H20, nuclease free	up to 50 µl	up to 50 µl
10 X Pfu® Buffer including MgSO4	5 µl	-
10 X Taq® Buffer	-	5µl
dNTP Mix	0.2 mM each	0.2 mM each
Forward primer	10 mM	10 mM
Reverse primer	10 mM	10 mM
Template DNA	10 - 1000 ng	10 - 1000 ng
Pfu DNA polymerase	2.5 U	1.25 U

Table 5b: Standard PCR scheme with typical values.

	Temperature [°C]	T [sec]	Cycles
Initial denaturation	95 - 98	240	
Denaturation	95 - 98	60	25 - 45 X
Annealing	primer dependent	120	
Extension	72	60 s/kb	
	72	600	

2.1.7. Escherichia coli (*E. coli*)

In this work, *E. coli* strain DH5α (stock, Department of Forest Botany and Tree Physiology, Goettingen, Germany) was utilized for cloning procedures. For Gateway-cloning, ccdB–resistant *E. coli* strains DB3.1 (stock, department of Forest Botany and Tree Physiology, Goettingen, Germany) and One Shot® ccdB Survival™ 2 T1R (Thermo Fisher, USA) were used (Table 6).

Table 6: Chromosomal genotypes of *E. coli*-strains used in this work.

Strain	Genotype
DH5α	*fhuA2 lac(del)U169 phoA glnV44 Φ80' lacZ(del)M15 gyrA96 recA1 relA1 endA1 thi-1 hsdR17*
DB3.1	*gyrA462 endA1 Δ(sr1-recA) mcrB mrr hsdS20 glnV44 (=supE44) ara14 galK2 lacY1 proA2 rpsL20 xyl5 leuB6 mtl1*
One Shot 2T1^{r}	F^{-}*mcr*A Δ(*mrr-hsd*RMS-*mcr*BC) Φ80*lac*ZΔM15 Δ*lac*X74 *rec*A1 *ara*Δ139 Δ(*ara-leu*)7697 *gal*U *gal*K *rps*L (Str^{R}) *end*A1 *nup*G *fhu*A::*IS2*

Lysogeny broth medium (LB) or 2X yeast-extract tryptone medium (2X YT) was used for *E. coli* cultivation (Table 7). Petri dishes contained LB or 2X YT media including 20 g/L micro agar (Beckton, Dickinson and company, Sparks, MD, U.S.A).

Table 7: Ingredients for 1 L LB – and 2X YT media.

	amount [g]	
Ingredients	LB	2X YT
Tryptone	10	16
Yeast extract	5	10
NaCl	10	5
Agar	20	20

2.1.7.1. *Generation of chemically competent E. coli*

E. coli cells from stock culture were cultured in 2 ml LB at 37°C overnight. This starter culture was transferred into 200 mL LB, which was then incubated at 37°C for 3 hours on a shaker. The OD_{600} was measured with a spectrophotometer (Eppendorf, Hamburg, Germany). When the OD_{600} reached 0.3 to 0.5, the incubation was stopped and the suspension was chilled on ice for 20 min, swirling occasionally. Cells were centrifuged at 3000 rpm in a table top centrifuge (Eppendorf, Hamburg, Germany) for 10 min at 4°C and afterwards gently re-suspended in 20 ml of precooled 0.05 M $CaCl_2$. After an incubation period of 20 min on ice, the suspension was centrifuged at 3000 g for 10 min at

4°C. Precipitated cells were re-suspended gently in 8 ml 15 % (v/v) glycerol with 0.05 M $CaCL_2$. The cell suspension was aliquoted (200 µl) in reaction tubes, frozen in liquid N_2 and stored at -80°C.

2.1.7.2. *Transformation of E. coli*

Aliquoted chemically competent *E. coli* were thawed at 37°C for 3-5 min before approximately 100 ng plasmid DNA was added. After incubation for 30 min on ice while swirling occasionally, cells were heat–shocked at 42°C for 90 sec. After chilling on ice for additional 2 to 3 min, 800 µl YT – media was added and the suspension was incubated for 1 h at 37°C on a thermoshaker. After incubation, an aliquot of 200 µl of the suspension was plated on Petri dishes containing LB media and the required antibiotics (Table 2). The remaining suspension was centrifuged in a table top centrifuge (Eppendorf, Hamburg, Germany) at 3000 rpm for 2 min, 750 µl of the supernatant was discarded and the rest was re - suspended and plated on a second Petri dish. The Petri dishes were then incubated at 37°C overnight.

2.1.8. Colony PCR

E. coli and *Agrobacteria* were tested for a positive transformation of the desired vectors by colony PCR. A colony of previously grown *E. coli* or *Agrobacteria* was picked with a sterile toothpick and transferred into the PCR mixture, consisting of 12 µl REDTaq® ReadyMix™ PCR Reaction Mix (Merck KGaA, Darmstadt, Germany), 1 µl forward primer, 1 µl reverse primer and 10 µl H_2O. The primers are listed in Table 8. The same toothpick was then used to spread the bacteria onto a new Petri dish with the referring selection antibiotics for further incubation. To run the PCR, the initial denaturation of the PCR was set to 240 s at 98°C, denaturation was adjusted to 60 s at 98° C.

2.1.9. Genomic DNA isolation

Approximately 100 mg of frozen leaf material was ground in a reaction vessel with a ball mill (MM 200, Retsch GmbH, Haan, Germany) utilizing steel beads. Milling occurred two times for 30 s at maximum speed. The container holding the reaction tubes was cooled down in liquid N_2 to keep the samples frozen during milling.

DNA isolation was done according to the protocol of the DNA isolation kit (Quiagen GmbH, Hilden, Germany). Purity and concentration of DNA was measured with a spectrophotometer (NanoDrop 2000, Thermo Fisher Scientific, Braunschweig, Germany) at A_{260} and A_{280}.

2.1.10. Screening

Each line was tested by PCR for positive insertion of the gene of interest, before Sanger sequencing was performed to test the correct sequence. Plants transformed with the pEntry Gateway system were screened only for the gene (e.g. *35S::ScWS* K60, Figure 25), whereas plants transformed with the DX15 promoter were screened for the gene of interest and the promoter DX15 (e.g. *DX15::AtDGAT1* K76, Figure 7). Primers used for screening purposes are shown in Table 8. To screen for a correct insertion

of the *AtDGAT1* and promoter, each line was tested for the insertion of the gene (primer 1, 2), the sequence from the right border to the 5'-end of promoter (primer 27, 22) and the entire sequence from right to left border of the pK7WG construct (primer 27, 56). Plants transformed with *DX15::ScWS* were screened for the insertion of the gene (primer 7, 8) and the sequence from the right border to the 5'-end of the promoter (primer 27, 22).

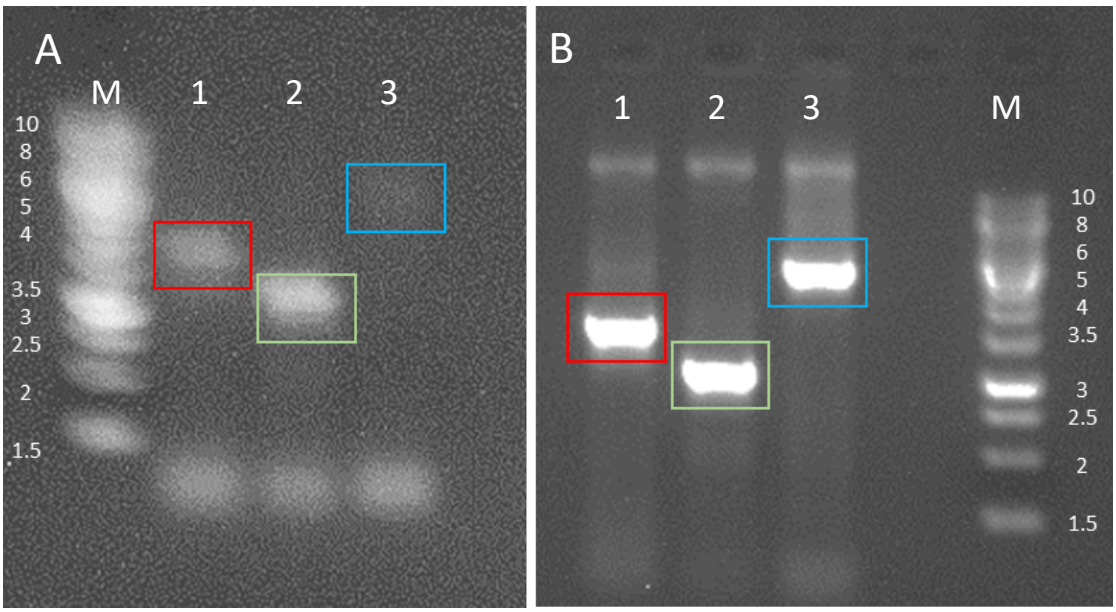

Figure 7: Example for PCR screening for correct insertion of gene (red box), promoter (green box) and insertion of pK7WG construct (blue box). A.: PCR screening of plant line K76I. **B.:** Positive control of plasmid DNA. M: Marker, 1: *AtDGAT1*, 2: promoter DX15, 3: sequence from right border to left border of pK7WG construct. Primers are listed in Table 8.

Table 8: Primers used for screening PCR.

Designation	Number	Destination	Sequence
AtDGAT-fwd	1	*AtDGAT1*	TTTTTGTCGACATGGCGATTTTGG
AtDGAT-Sal1-rev	2	*AtDGAT1*	TTTTTGTCGACTCATGACATCGATCCTTTTCGG
ScWS-fwd	7	*ScWS*	TTTTTGTCGACATGGAGGTGGAG
ScWS-Sal1-rev	8	*ScWS*	TTTTTGTCGACTCACCACCCCAACAAACC
22-DX15 Promoter SacI rev	22	DX15	TTTTTGAGCTCAAGATGAAAGATTGTGGCCTC
pK7WG_F (RB)	27	Vector	GCGGGAAACGACAATCTG
56_p7wg2	56	Vector	TTGCGGACTCTAGCATGG

2.1.11. DNA Verification

The verification of positive insertion of promoter and genes of interest into entry and binary vectors as well as positively transformed plants was done via Sanger sequencing (Microsynth AG, Balgach, Switzerland).

2.1.12. LR and BP reactions

LR and BP reactions were conducted with the Gateway® LR Clonase II™ or Gateway® BP Clonase II™ kit (Fisher Scientific, Braunschweig, Germany) following the manufacturer's protocol.

For LR reaction, 100 ng destination vector and 100 ng of entry vector were combined. Tris-EDTA buffer (pH 8.0) was added to an end volume of 8 µl. After adding 2 µl of LR Clonase® II, the reaction mixture was incubated for one hour or overnight at 25°C. One µl proteinase K solution (Fisher Scientific, Braunschweig, Germany) was added for termination of the reaction at 37°C for 10 min. One µl of the reaction was then used for transformation into *E. coli.*

For BP reaction, 100 ng donor and 100 ng of the purified PCR product containing the attB-sites was used. The reaction was adjusted to 8 µl volume with TE buffer (pH 8.0). Two µl of BP Clonase II™ was added and the reaction mixture was incubated at 25°C for 1 hour. The reaction was terminated by adding one µl Proteinase K solution (Fisher Scientific, Braunschweig, Germany) followed by incubation at 37°C for 10 min. One µl of the reaction was then used for transformation into liquid cultures of *E. coli.*

2.1.13. Preparation of pEntry donor vectors

To introduce the 35S promoter into the pEntry vectors A, B and C, several overlap PCRs were conducted. Because the pEntry B-and C donor vectors were intended to be inserted in the mid-section of multiple gene constructs (Figure 9), the attachment sites are critical for correct insertion. Therefore, a DNA-overhang of 5-10 bp compatible to the 35S promoter as well as a HindIII restriction site were amplified fitting to the respective attachment site (attR4 for B, attL3 for C) via PCR. The HindIII restriction site was located upstream to the attachment site.

The 35S promoter was amplified from a pEntryE-35S donor vector. A SalI restriction site was inserted downstream of the 35S promoter via PCR as well as a fitting overhang to the attachment sites (attR4 for B, attL3 for C). Both products were fused by PCR afterwards.

The final products contained the 35S promoter with the respective Att-site and HindIII recognition site at the 5´ end and a SalI recognition site at the 3´- end. Both sites were ligated blunt-end into the pJET 1.2 vector and were transformed introduced into *E. coli* (2.1.7.2). Colonies were determined by colony PCR (2.1.8) and positively transformed colonies were used for plasmid preparation and sequencing (2.1.11). Positive and sequence-verified plasmids were then restricted with HindIII and SalI (Thermo Scientific, Germany). The target vectors pEntryB and pEntryC were also restricted with HindIII and SalI. Inserts and the respective pEntry vectors were ligated afterwards at 16°C for 16 h on a Thermocyler® (Eppendorf, Hamburg, Germany), following the manufacturer´s protocol.

The 35S promoter could be directly inserted into the pEntryA-vector, since the attL1 site is present in the pEntryE-35S as well. Therefore, the pEntryE-35S was digested with HindIII and SalI and the product was ligated (2.1.5) into a prepared pEntryA vector.

Since the pEntryE vector had already a 35S promoter and the matching restriction sites, this vector could be used directly for insertion of the genes of interest.

The genes of interest were ligated into the multiple cloning site of the finished pEntry vectors. For this purpose, the genes of interest as well as the pEntry vectors were restricted with the restriction enzymes BamHI and SalI (Thermo Scientific, Braunschweig, Germany) and ligated afterwards as described in (2.1.5). Entry vectors were sequenced (2.1.11) before insertion into the binary vector.

Table 9: Primer used for overlap PCR.

Designation	Purpose	PCR on…	Sequence
attR4-HindIII.for	HindIII insertion	pEntryB	GGCCATGCAAGCTTCATAGTGACTGGATATGTTGTGTTTTACAG
attR4-35Sov-rev	Overhang		CTCTAGCCAATACGCCAACTTTGTATAGAAAAGTTG
attR4-35S-ov-for	Overhang	pEntryE-35S	TTCTATACAAAGTTGGCGTATTGGCTAGAGCAGCTTG
35S-SalI-rev	SalI insertion		ACGGTCGACAGAGATAGATTTGTAGAGAGAGAC
attL3-HindIII.for	HindIII insertion	pEntryC	GGCCATGCAAGCTTAAATAATGATTTTATTTTGACTG
attL3-35Sov-rev	Overhang		CTCTAGCCAATACGCCAACTTTATTATACAAAGTTGG
attL3-35S-ov-for	Overhang	pEntryE-35S	TGTATAATAAAGTTGGCGTATTGGCTAGAGCAGCTTG
35S-SalI-rev	SalI insertion		ACGGTCGACAGAGATAGATTTGTAGAGAGAGAC

2.1.14. Preparation of pDONR201 donor vectors

To insert the genes of interest into the pDONR201 entry vector, attl1 and attl2 sites were added via PCR to the gene of interest. Amplicons of the gene including the attachment sites were then inserted to the pDONR201 entry vector via BP reaction, as described in (2.1.12). Entry vectors were sequenced before insertion into the binary vector (2.1.11).

Table 10: Primers used for BP reaction of the genes of interest into the pDONR201 entry vector. The BP attachment sites are highlighted in bold type font.

Purpose	Designation	Amplicon	Sequence
Cloning	AtDGAT-fwd	attL1/attL2	**GGGGACAAGTTTGTACAAAAAAGCAGGCTTA**GTCGACATGGCGATTTTGG
	AtDGAT-rev		**GGGGACCACTTTGTACAAGAAAGCTGGGTTC**TCATGACATCGATCCTTTTCGG
	AtWRI1-fwd	attL1/attL2	**GGGGACAAGTTTGTACAAAAAAGCAGGCTTA**GTCGACATGAAGAAGCGC
	AtWRI1-rev		**GGGGACCACTTTGTACAAGAAAGCTGGGTTC**TCAGACCAAATAGTTACAAGAAACC
	MaFAR-fwd	attL1/attL2	**GGGGACAAGTTTGTACAAAAAAGCAGGCTTA**GTCGACATGGCAATCCAGC
	MaFAR-rev		**GGGGACCACTTTGTACAAGAAAGCTGGGTTC**TCATGCCGCTTTTTTACGTTG
	ScWS-fwd	attL1/attL2	**GGGGACAAGTTTGTACAAAAAAGCAGGCTTA**GTCGACATGGAGGTGGAG
	ScWS-rev		**GGGGACCACTTTGTACAAGAAAGCTGGGTTC**TCACCACCCCAACAAACC
Sequencing	SeqL-A	*pDONR201*	TCGCGTTAACGCTAGCATGGATCTC
	SeqL-B		GTAACATCAGAGATTTTGAGACAC

2.1.15. Preparation of vector pK7WG-DX15

DNA extracts (2.1.9) of three individual *P. trichocarpa* plants were used to amplify the promoter region. To insert the promoter into the pK7WG binary vector, the restriction sites HindIII (3') and SacI (5') were added directly via PCR. Amplification of the DX15 promoter region from genomic DNA was done with a hot start PCR including BSA and Taq®-polymerase (Table 11 and Table 12). PCR was conducted with 100 ng DNA. The amplicon was restricted and ligated upstream of the attR1 attachment site of the pK7WG binary vector. The genes of interest were then added to the finished vector via LR reaction () of pDONR201-entry vectors.

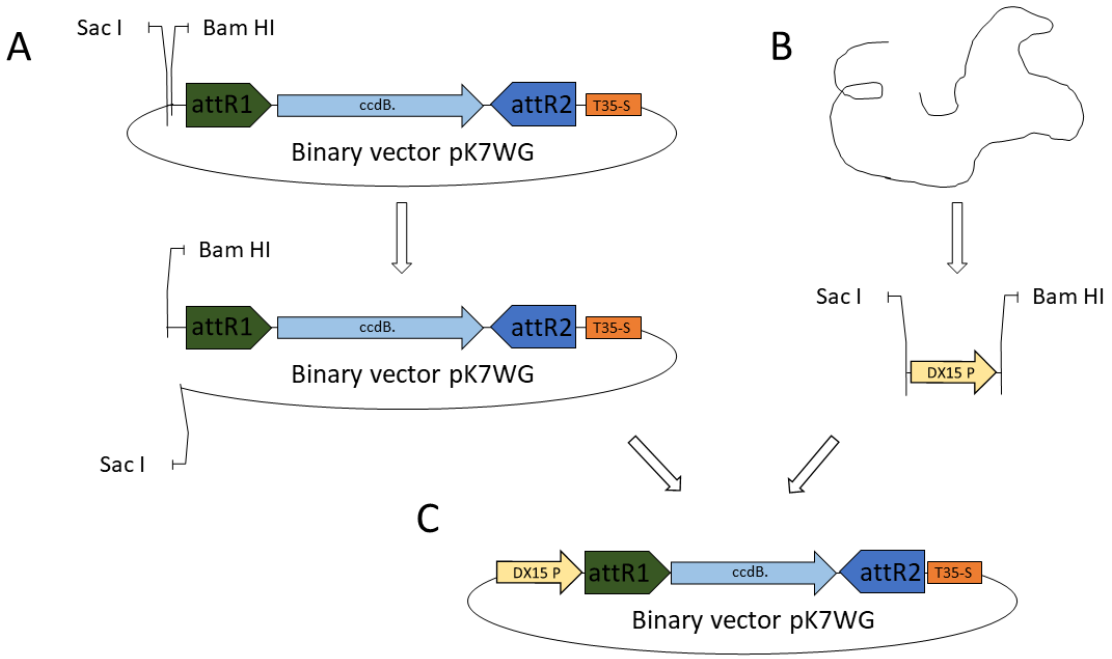

Figure 8: Cloning scheme for DX15-pK7WG. A.: The binary vector pK7WG was restricted with SacI and BamHI upstream of the attachment site. B.: DX15 promoter region was amplified from genomic DNA of *P. trichocarpa*, including the restriction sites Sac I and Bam HI C.: DX15 promoter region was ligated into binary vector pK7WG.

Table 11: Ingredients for the PCR of the promoter region DX15.

Ingredients	Volume (µl)	Conc. of stock solution
H2O* (nuclease free)	27	-
Genomic DNA	2	10 – 1000 ng
Primer fwd.	1	10 nM
Primer rev.	1	10 nM
BSA	2.5	10% (100 mg/mL)
Taq ® buffer (10X)	5	10 x
MgCL2	6	25 mM
dNTPs	5	2 mM
Taq® polymerase	0.5	1 U

*Nuclease free water was purchased from AppliChem, Darmstadt, Germany.

Table 12: Hot start PCR setup for promoter amplification.

Step	Temp [°C]	T [min]	Remarks	Cycles
Hot start	99	5	Pre-denaturation	
Cooling	72	pause	loading Taq® polymerase	
Initial	94	5		
Denaturation	94	0.5		35 X
Annealing	60	1		
Extension	72	2		
Final	72	5		
Cool	4	∞		

2.1.16. Preparation of binary vectors

Binary vectors used for plant transformation were cloned by utilizing the Gateway® system. Entry vectors pEntryA,-B,-C and -E, as well as pDONR201, were used as donor vectors (Figure 11).

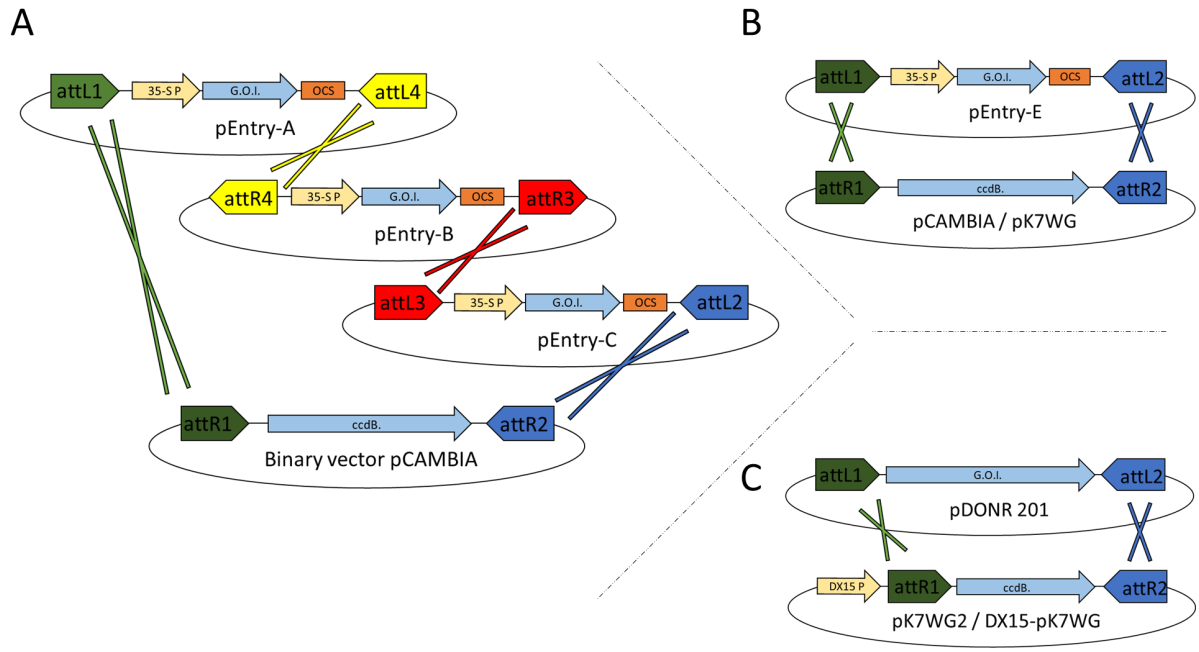

Figure 9: Gateway cloning scheme of binary vectors used in this work. A.: Multiple gene constructs were cloned by utilizing pEntry vectors containing a 35S promoter and the gene of interest into a pCAMBIA binary vector. B.: Single gene constructs were made by utilizing pEntry-E entry vector containing a 35S promoter and the gene of interest, inserted into the pK7WG or pCAMBIA binary vector. C.: Single gene constructs with the DX15 promoter were exclusively made with the pDONR201 entry vector containing the gene of interest.

The pEntry donor vector system was used to insert the 35S promoter and gene of interest collectively. This system was used predominantly to produce multiple gene constructs in the pCAMBIA vector (Figure 9A), but as well for single gene constructs in the pK7WG vector (Figure 9B) by using the pEntry-E entry vector. The pDONR201 vector system was exclusively used to introduce genes into binary vectors that contained already a promoter, such as the pK7WG2 or the DX15-pK7WG (Figure 9 C). For a complete overview about all produced binary vectors, see Table 13.

Table 13: Composition of all binary constructs prepared for agrobacteria mediated transformation. 15 constructs have been produced with different compositions of promoters, gene setups, entry and binary vectors. Two different 35S promoter were used (Figure 11). The 35S promoter in constructs K 30 to K 60 was inserted to the pEntry entry vector system and was obtained from Prof. Dr. Feussner (Department for Plant Biochemistry, Albrecht-von-Haller-Institute for Plant Sciences, University of Goettingen). The second 35S promoter was obtained from the pK7WG2 vector system from VIB (Gent, Belgium), as indicated with an asterisk. The DX15 promoter was prepared in this work (2.1.15).

Promoter	Gene setup	Binary vector	Entry vector	Construct No.
35S	*AtWRI1, AtDGAT1*	pCAMBIA 23.0G	pENTRY	K 30
	AtWRI1, MaFAR, ScWS	pCAMBIA 23.0G	pENTRY	K 32
	MaFAR, ScWS	pCAMBIA 23.0G	pENTRY	K 31
	AtWRI1	pCAMBIA 23.0G	pENTRY	K 61
	AtDGAT1	pCAMBIA 23.0G	pENTRY	K 62
	ScWS	pCAMBIA 23.0G	pENTRY	K 64
	AtWRI1	pK7WG	pENTRY	K 57
	AtDGAT1	pK7WG	pENTRY	K 58
	ScWS	pK7WG	pENTRY	K 60
35S*	*AtDGAT1*	pK7WG2	pDONR201	K 70
	MaFAR	pK7WG2	pDONR201	K 71
	ScWS	pK7WG2	pDONR201	K 72
DX15	*AtDGAT1*	pK7WG-DX15	pDONR201	K 76
	MaFAR	pK7WG-DX15	pDONR201	K 77
	ScWS	pK7WG-DX15	pDONR201	K 78

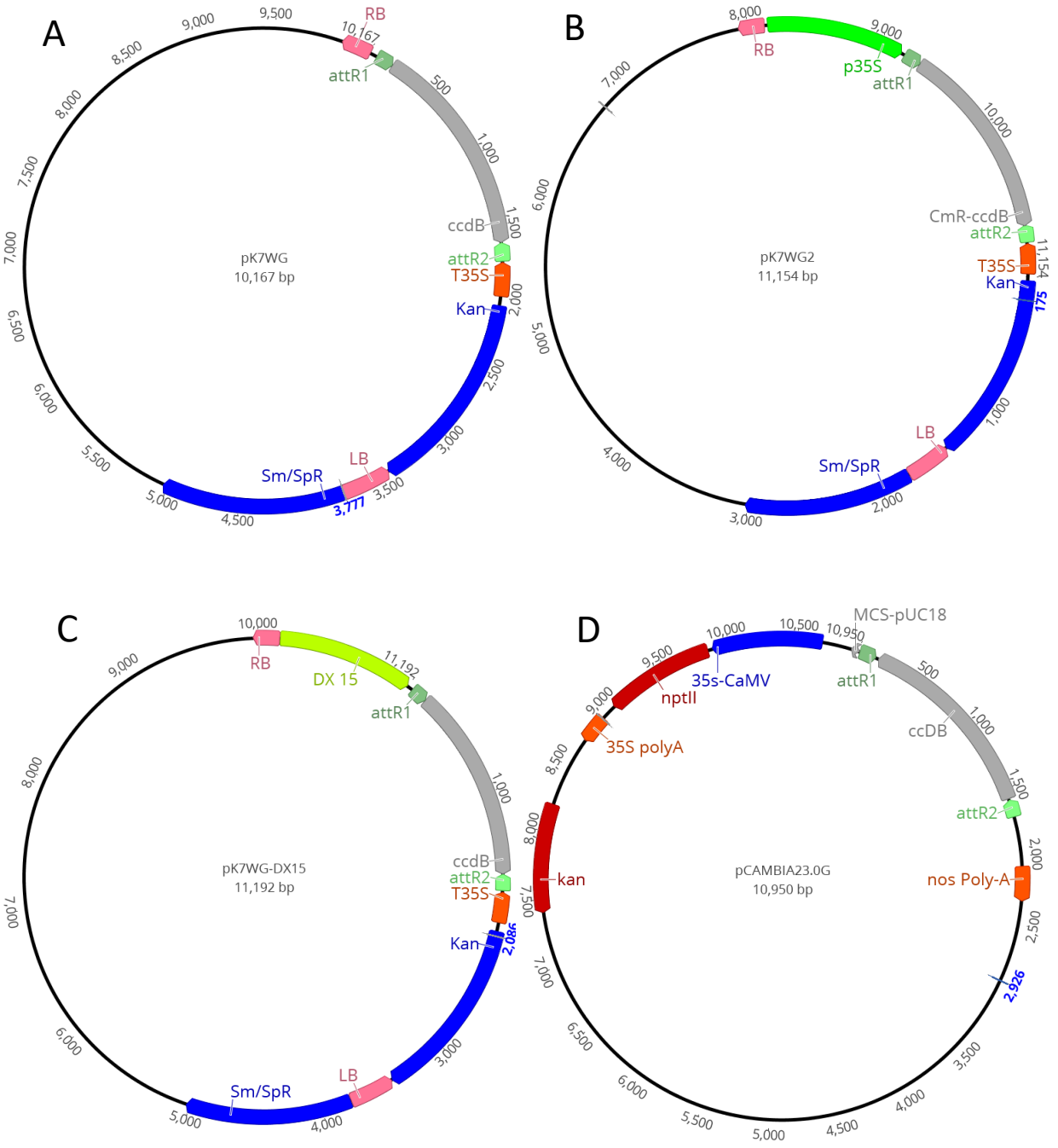

Figure 10: Binary vectors used for single (A.: pK7WG, B.: pK7WG2, C.: pK7WG-DX15) **and multiple gene transformation** (D.: pCAMBIA 23.0G).

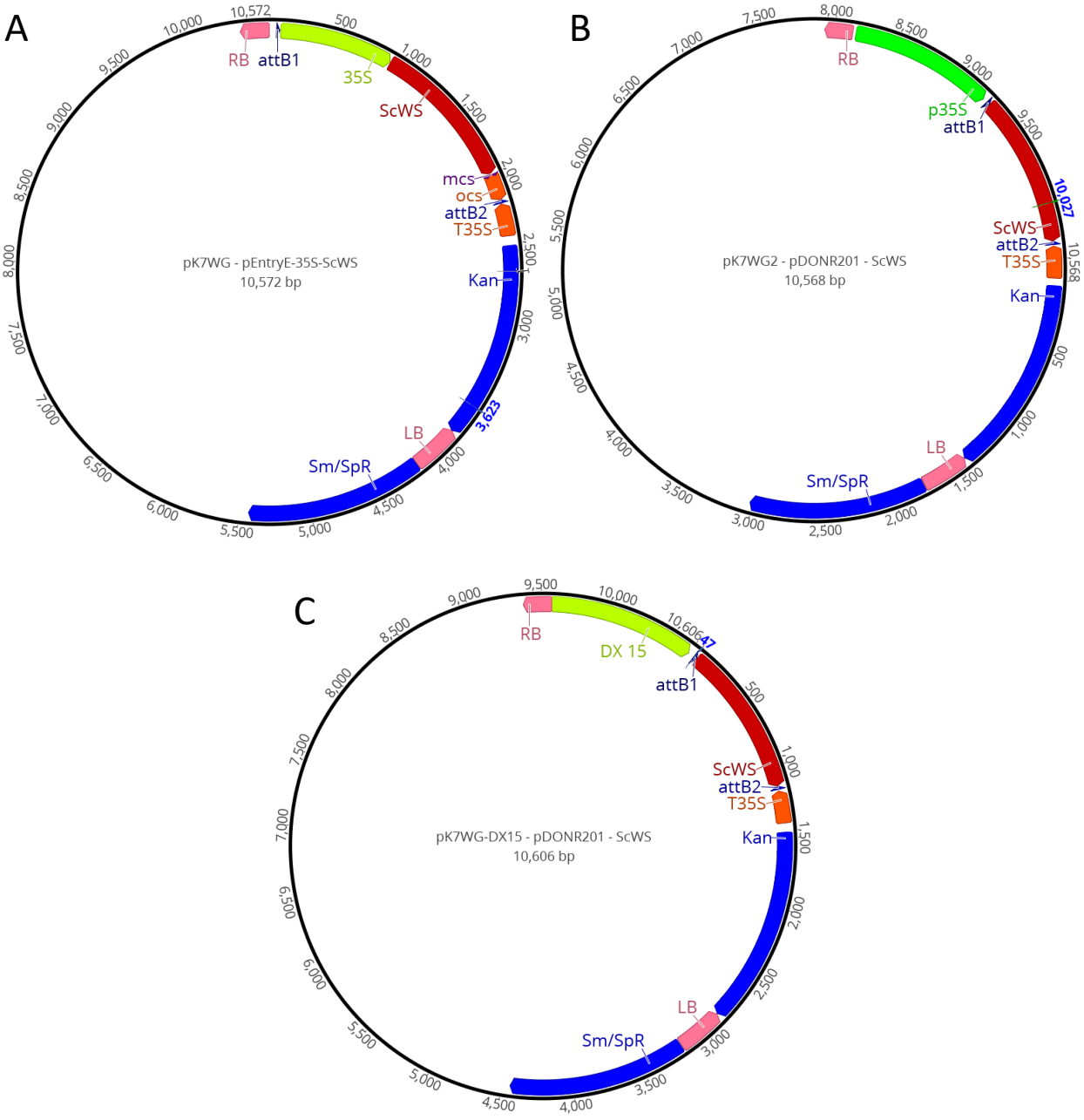

Figure 11: Exemplary *ScWS* binary expression vector pK7WG. A.: pK7WG with promoter 35S from pENTRYE, B.: pK7WG2 with internally promoter p35S, C.: pK7WG with promoter DX15.

2.2. Schematic Overview on the Production of transgenic *P.* x *canescens* lines

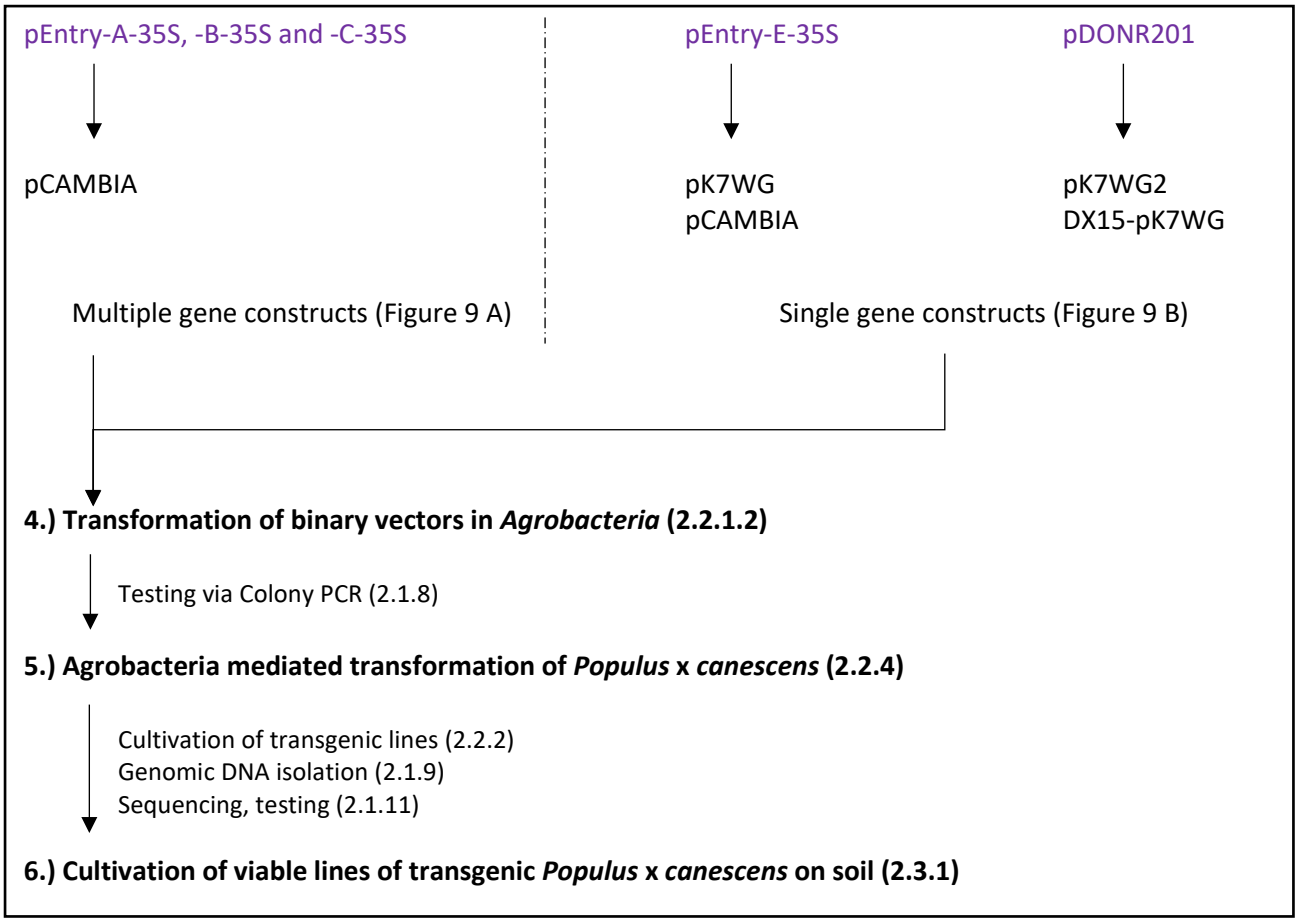

Figure 12: Schematic overview on the production of transgenic poplar lines. Each single step is described in detail in the later chapters, as indicated in brackets (). Main steps are shown in bold and refer to the transformation of binary vectors in *Agrobacteria* (4), the *Agrobacteria* mediated transformation of poplar plants (5) and cultivation of viable lines of transgenic poplar plants (6).

2.2.1. *Agrobacterium tumefaciens* (*Agrobacteria*)

Agrobacteria strain GV3101 pMP90 was utilized for transformation of poplar plants. This strain contains a chromosomal rifampicin resistance and a gentamycin resistance on its Ti-plasmid and can thus, be selected by adding gentamycin (25 mg/L) and rifampicin (20 mg/L) to the cultivation medium.

YEB–medium adjusted to a pH of 7.2 was used for *Agrobacteria* cultivation (Table 14). Petri dishes contained additionally 20 g/L micro agar (Beckton, Dickinson and company, Sparks, MD, U.S.A.).

Table 14: Ingredients for 1 L YEB-media.

Ingredients	Amount [g/l]
Beef extract	5
Yeast extract	1
Peptone	5
Sucrose	5
$MgSO_4$	0.3
Agar	20

2.2.1.1. *Generation of chemically competent Agrobacteria*

Two ml of *Agrobacteria* overnight cultures including antibiotics were incubated at 28°C on a shaker and used as the starter culture. The starter culture was used to inoculate a 50 ml vial containing YEB media (Table 14), without antibiotics. After inoculation, the culture was incubated up to 4 h at 28°C in a shaker at 100 rpm (Sanyo Gallenkamp PLC, Loughborough, UK) until the solution reached an OD_{600} of approximately 0.5. Cells were then precipitated by centrifugation at 4000 rpm and at 4°C (J2-HS, Beckman Coulter, Brea, USA) for 5 min. The supernatant was discarded; precipitated cells were re-suspended in 10 ml of precooled 0.15 M NaCl solution and centrifuged again at 4000 rpm, at 4°C for 5 min. After being re-suspended in 1 ml precooled 75 mM $CaCl_2$, competent cells were aliquoted (200 µl) in reaction tubes and stored at -80°C.

2.2.1.2. *Transformation of chemically competent Agrobacteria*

Aliquots of competent *Agrobacteria* (200 µl) were thawed in an ice bath. One µl containing approximately 100 to 1000 ng binary vector DNA was added and the cells were then kept on ice for 5 min while being stirred occasionally. Aliquots were then transferred to liquid N_2 for 3 min and were then thawed in a water bath at 37°C. Further incubation occurred at 37°C for 5 min. 800 µl of YEB medium without antibiotics was added to the cell suspension. The cells were then incubated at 28°C on a shaker (Eppendorf, Köln, Germany) for 2 hours. After centrifugation for 2 min at 5000 rpm at RT, the cells were re-suspended and plated on two Petri dishes containing YEB agar with the required antibiotic (Table 2).

2.2.2. Sterile plant cultures

P. x *canescens* (*P. alba* x *tremula*, clone INRA 717-1B4) microcuttings were cultivated in sterile conditions in long day (16 h photoperiod) conditions (fluorescent lamps L18W/840, Osram, Munich, Germany) at 22°C in an air-conditioned breeding room utilizing glass jars (Weck® GmbH & Co. KG, Germany) on different cultivation media (Table 15). Jars were sealed with gas permeable fleece rings (Paramoll N260/200, Mank® GmbH, Germany). Cover and sealing were fixed with gas permeable tape (Leucopor®, BSN Medical, Germany). Plantlets were grown for approximately 4 to 6 weeks before propagation or transformation.

Plants from sterile cultures were cut and leaves were discarded. The remaining stem was cut into 6 to 7 segments, each about one to two cm length with one or two internodes. Up to six segments were transferred into one new cultivation jar.

2.2.3. Media for plant cultivation and transformation

Half strength Murashige & Skoog (Murashige and Skoog, 1962) (½ MS including Vitamins, Duchefa, Haarlem, Netherlands) with 2% sucrose (Roth, Karlsruhe, Germany) was used as basic medium for cultivation and transformation of the plants. For stock cultures, Kobe agar was used (Roth, Karlsruhe, Germany).

For the transformation process, plant agar (Duchefa, Haarlem, Netherlands) was used. The pH was adjusted to 5.8 prior autoclaving. Thermo-sensitive agents, such as the cell membrane stabilizer Pluronic® F-68 (AppliChem, Darmstadt, Germany), the growth regulator Thidiazuron and antibiotics (Table 2) were sterile filtered with syringe sterile filter (Sarstedt, Nürnbrecht, Germany) and added after autoclaving.

Table 15: Media used for poplar cultivation and transformation.

Media / Ingredients	Culture (CM)	Co-incubation (K)	Regeneration (Reg)	Selection (Sel)	Selection (Sel-M)
MS mixture ½ [g/L]	2.2	2.2	2.2	2.2	2.2
Sucrose [%]	2	2	2	2	2
pH	5.8	5.8	5.8	5.8	5.8
Kobe agar [g/L]	7	-	-	-	-
Plant agar [g/L]	-	7	7	7	7
Pluronic F-68 [%]	-	-	0.01	0.01	-
Thidiazuron [mg/L]	-	-	0.022	0.022	-
Cefotaxim [mg/L]	-	-	150	150	-
Timentin [mg/L]	-	-	200	200	-
Kanamycin [mg/L]	-	-	-	50	50

2.2.4. *Agrobacteria* mediated transformation of *Populus* x *canescens*

Agrobacteria mediated transformation of poplar plants was done according to the protocol by (Bruegmann et al., 2019) and optimized by (Muhr et al., 2016). Further optimization is described below. A schematic overview of the transformation process is shown in Figure 13.

Agrobacteria transformed with the binary vector of choice were grown in 4 ml YEB medium containing the appropriate antibiotics (Table 2), at 28°C in darkness and were shaken at 90 rpm. Two ml of this starter culture were used to inoculate 100 ml YEB medium, pre-warmed to 28°C and without antibiotics. Incubation of the bacteria occurred in darkness at 28°C on a shaker at 90 rpm for about 3 to 5 hours. When an OD_{600} of 0.3 to 0.5 was reached, 20 µM of 3´,5´-dimethoxy-4´-hydroxyacetophenone (Sigma Aldrich, Darmstadt, Germany) was added to the cell suspension and the incubation was continued for another 30 min.

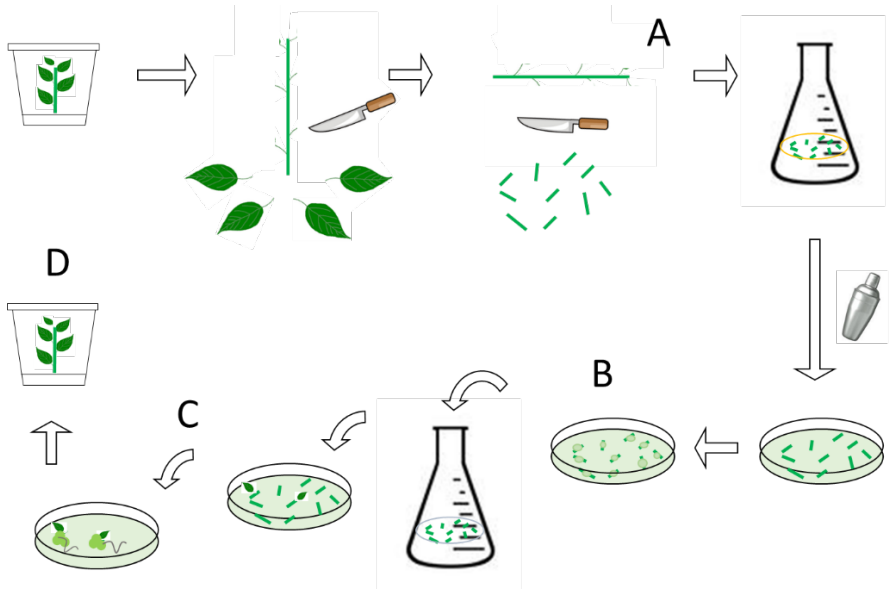

Figure 13: Schematic representation of poplar transformation. A.: Plant stems from sterile culture are cut into parts of 3-5 mm and transferred into *Agrobacteria* solution. **B.:** Stem sections are placed on Petri dishes containing co-incubation medium and *Agrobaceria* overgrow stem parts. **C.:** *Agrobacteria* are removed by several washing steps and positively transformed plantlets start to shoot from calli. **D.:** Plant lines are distinguished depending on the origin of the callus and transferred onto culture media in cultivation jars.

Poplar plantlets were sterile-cultivated for a maximum of four to five weeks prior transformation. Leaves were removed and stem sections without petioles were cut into parts of 4 – 6 mm length. Stem sections were temporarily stored in sterile tap water before transferred into the *Agrobacteria* suspension. Incubation occurred under dark conditions at 120 rpm and 28°C for 30 min. The stem sections were then drained with sterile filter paper and transferred on Petri dishes containing co-incubation medium (K, Table 15). Co-incubation occurred in dark conditions at 25°C for four to five days until stem sections were overgrown with *Agrobacteria*.

The overgrown stem sections were washed with 150 ml sterile tap water in an Erlenmeyer flask for 3 to 4 min by manually shaking the flask. Stem sections were drained on sterile filter paper. These washing steps were repeated three times, 2 to 3 min each, with 400 µg/ml ticarcillin clavulanate (Duchefa, Haarlem, Netherlands) in 150 ml sterile tap water. Sterile tap water without ticarcillin clavulanate was used for the last washing step.

Stem sections were then transferred to Petri dishes containing selection medium. One reference dish with regeneration medium (Reg) was used as regeneration control (Table 15). Further cultivation occurred for four to six weeks at 22°C in long day conditions with 16 h of light, but at a low light intensity of approximately 10 µE m^{-2} s^{-1} (fluorescent lamps L18W/840, Osram, Munich, Germany) and approximately 20 to 40 % air humidity.

When shoots were observed, stem sections were placed in 370ml Weck jars with selection medium (Sel, Table 15) and cultivated at a low light intensity of approximately 20 µE m^{-2} s^{-1}. Rooting plants could be observed after five to eight weeks, indicating a successful transformation. These plants were grouped in lines, cut, and transferred to Weck jars (580 ml) with selection media (Sel-M). When stable growth and rooting of the plantlets was observed after four to eight weeks, positive transformation was tested via Sanger sequencing (Microsynth Seqlab, Göttingen, Germany) by utilizing DNA extracted from one leaf per line. Further cultivation was done on culture medium (CM) without antibiotics.

2.3. Overview on the phenotyping of transgenic plants

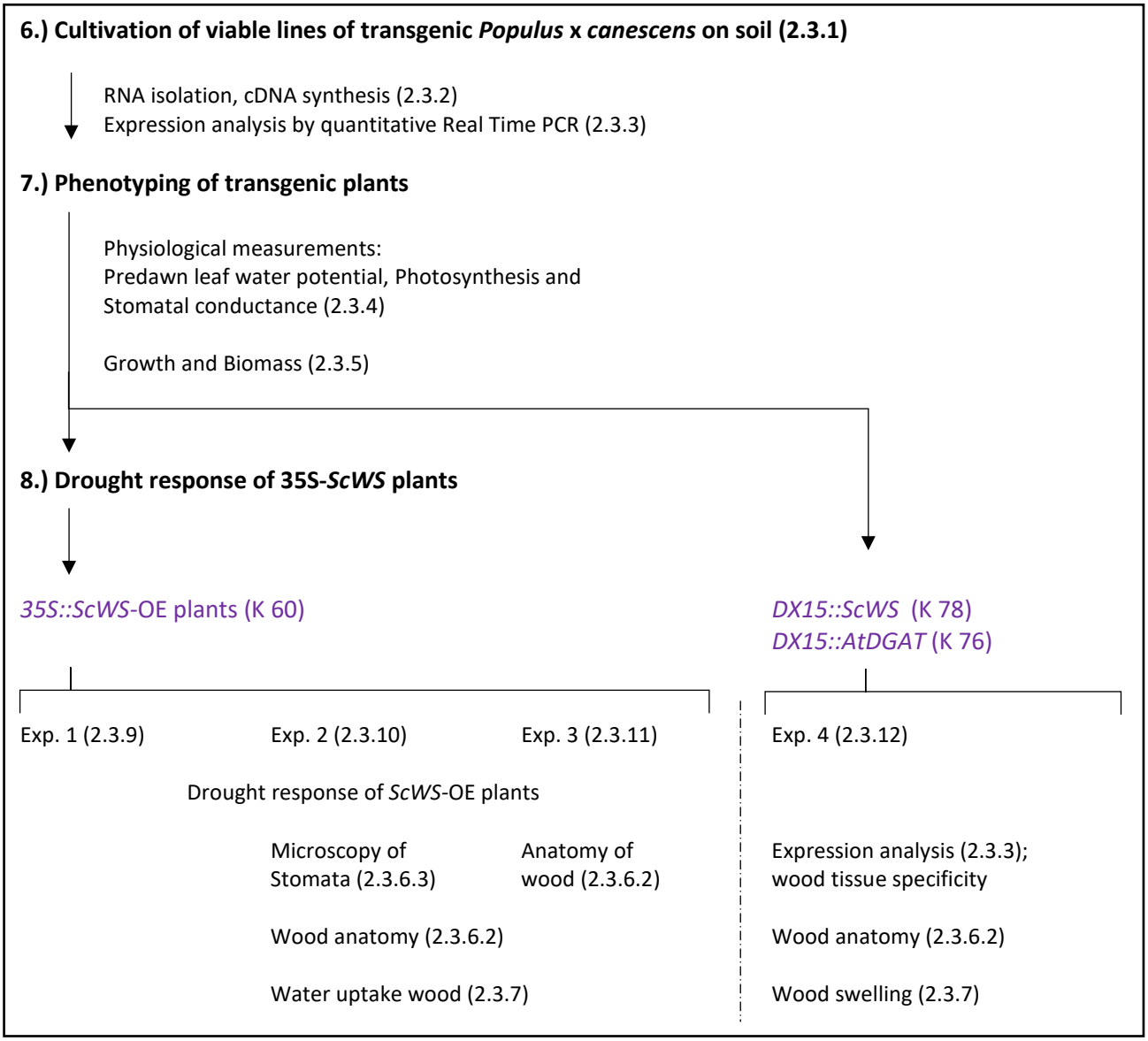

Figure 14: Schematic overview on the phenotyping of transgenic poplar lines. Every single step is described in detail in the later chapters, as indicated in brackets (). Main steps are shown in bold and refer to the cultivation of viable lines (6), the general phenotyping of all transgenic plants (7) and drought stress experiments of *35S::ScWS*-OE plants in the different experiments 1 - 3 (8).

Figure 15: Schematic overview on the phenotyping of transgenic poplar lines. Every single step is described in detail in the later chapters, as indicated in brackets (). Main steps are shown in bold and refer to the cultivation of viable lines (6), the general phenotyping of all transgenic plants (7) and drought stress experiments of *35S::ScWS*-OE plants in the different experiments 1 - 3 (8).

2.3.1. Plant cultivation on soil

Six to eight weeks old plants from sterile culture were potted in peat containing soil (Frühstorfer Erde Type N, HAWITA® Gruppe GmbH, Vechta, Germany). Plants were adapted to greenhouse conditions by a small transparent beaker or plastic bag slipped over each plant. After two weeks, the beaker or plastic bag was gradually uncovered (Figure 19) for one additional week until the plants were exposed without cover. No additional artificial light was applied during the acclimation process. After acclimation, plants were grown at temperatures from 18 °C to 27 °C (summer period) at an air humidity of 50 to 80 % with additional light (PAR of 150 µmol photons m^{-2} s^{-1}) of either fluorescent lamps (3071/400 HI-I, Schuch GmbH, Worms) or LED lights (Schuch GmbH, Worms) at a 16 h photoperiod.

2.3.2. RNA isolation and cDNA synthesis

Frozen samples of leaf (L), developmental xylem (DX) and bark (B) were ground with a steel ball mill (MM 200, Retsch GmbH, Haan, Germany). A maximum of 150 mg material per sample was used. Milling occurred two times for 30 s for L material and three times for B and DX materials at maximum speed. The container holding the samples and the steel ball were cooled down in liquid N_2 to keep the samples frozen during milling.

RNA isolation was done according to the method of Chang et al. (1993). The concentration and purity of isolated RNA was determined with a spectrophotometer (NanoDrop 2000, Thermo Fisher Scientific, Braunschweig, Germany) at A_{260} and A_{280}. An A260/A280 ratio of ≥ 2.0 was considered as a sufficiently pure sample.

For cDNA synthesis, RNA samples were aliquoted (2 µg) and treated with the Ambion® Turbo DNAfree™ kit (Life Technologies, Carlsbad, CA, USA) according to the manufacturer's instructions. Aliquots were then transcribed to cDNA with the RevertAid First Strand cDNA Synthesis Kit (Thermo Fisher Scientific, Braunschweig, Germany), using oligo(dT)-primers, following the instructions of the manufacturer.

2.3.3. Quantitative Real Time PCR (qRT PCR)

Gene-specific primers (Table 17) were designed using PerlPrimer version 1.1.21 (http://perlprimer.sourceforge.net/) and Geneious®, version 11.0.3 (https://www.geneious.com/, Auckland, New Zealand) and were checked *in silico* with the BLAST–tool of the URGI database (https://urgi.versailles.inra.fr/blast/) on the *P.* x *canescens* genome. Several primer pairs were tested at different concentrations by RT-PCR to ensure primer specificity and the primer efficiency. One appropriate primer pair per gene was chosen for the analyses.

QRT PCRs were performed with three technical replicates per sample. Plate setup, primer efficiency and C_t–values were designed and calculated with "qPCRsoft", version 3.4.6 (Analytik Jena, Jena, Germany).

QRT PCR was conducted in a Real-time Thermal Cycler (qTOWER^3 G touch, Analytik Jena, Jena, Germany) in a reaction volume of 20 µl. One reaction contained 10 µl SYBR Green (Roche Diagnostics, Mannheim, Germany), 2 µl of forward and reverse primer (Table 17) at a concentration of 10 µM each, 1 µl nucleic free water and 5 µl cDNA-solution in a dilution of 1:30 or 1:40. After each PCR, a melting curve was measured with an increment of ΔT = 1°C from 65 °C to 95°C (Table 16).

Table 16: qRT PCR conditions.

Temp [°C]	T [sec]	Remarks	Cycles
95	120	Initial incubation	
95	10		45 X
55	10		
72	20	Scan	
60 - 95	15 s, Δ T 1°C	Melting curve	

Table 17: Primers used for qRT PCR.

Purpose	Designation	Gene	Sequence
Reference	A_Ref2_FW	Potri.012G141400 / *Ptr**PPR_2***	ATCGTTCCAAGTCAAGTATGTG
	A_Ref2_RW		TCAAGGGAGCAACTTTACAG
Reference	C_Ref1_FW	Potri.015G001600 / *Ptr**Rpp14***	GCAATGTGAGGAGTTTAGGG
	C_Ref1_RV		TATTAAATGTCTGTGCTGTAGTGTG
Expression	68_WS_860F	*ScWS*	TGAAGAAGGCGGTTTCAGGC
	69_WS_942R		TCCAGTCACCATCACGAACC
Expression	76_DGAT_249F	*AtDGAT1*	TGGTGGCGATAATAACGGTGG
	77_DGAT_344R		CGATGAGCTGGAACCGACG

2.3.4. Predawn leaf water potential, photosynthesis and soil moisture measurements

Prior predawn leaf water potential and photosynthesis measurements, leaves were numbered starting from the top of the plant. On each plant, the same leaf position was taken for the measurements to ensure a consistent position and age. Furthermore, plants were clustered in a series of four to five plants in total, consisting of one or two wildtype plants and three to four different lines of transgenic plants. This pattern was repeated with different plants to minimize positional effects. Up to five groups and therefore up to five biological replicates per measurement were included. Daytime measurements were conducted from 08:30 am to 01:00 pm, measurements at night from 03:00 am to approximately 30 min before sunrise.

The predawn leaf water potential was measured according to the method of Scholander et al. (1964) with the SKPM 1400/40 pressure chamber (UP GmbH, Ibbenbüren, Germany). For this purpose, the leaf was inserted in the pressure chamber with the petiole outside. Pressure was applied with compressed air until liquid appeared at the surface of petiole. The applied pressure was recorded with a manometer.

Photosynthesis (Figure 16) and stomatal conductance were measured with a multiphase Flash™ Fluorometer (LI-6800, LI-COR, Lincoln, U.S.A.). After attachment of the chamber to the leaf, a short acclimation phase of about 30 to 40 sec was conducted. Afterwards, three replicate measurements were taken within three minutes. The light intensity was set to 800 µE m^{-2} s^{-1} for day measurements and for night measurements (respiratory measurements, stomatal conductance) the light source was switched off.

The water use efficiency ($WUE_{instantaneous}$) was calculated according to equation (2)(1):

$$WUE_{(inst)} = \frac{A_{Net\ photosynthesis}}{E_{Transpiration}} \quad \textbf{(1)}$$

Soil moisture (m^3/m^3) was measured by determining the soil resistivity with the HH2 device quipped with the ML2x sensor (Delta-T Devices Ltd., Cambridge, U.K.).

Figure 16: Photosynthesis measurement with the LI-6800 (LI-COR) system of a defined leaf from the top.

2.3.5. Growth and Biomass

The stem diameter was measured in intervals of five to eight days at approximately 1 cm above the soil surface with a digital calliper (Tchibo GmbH, Hamburg, Germany). The stem height from the bottom to the apex was measured with a folding ruler in intervals of two to three days.

At the harvest, the fresh weight of each plant tissue (leaves, stem, roots) was measured with a balance (Sartorius AG, Göttingen, Germany). Aliquots of plant tissues were frozen directly in liquid N_2 and other aliquots were dried at 60°C in a drying oven (Memmert GmbH + Co. KG, Schwabach, Germany) to determine dry weight.

The total leaf area was calculated on the basis of three leaves per plant collected at upper, middle and bottom position. Leaves were scanned and the area measured with ImageJ (https://imagej.nih.gov/ij/, National Institute of Health, U.S.A.). The leaf area per plant was calculated according to equation (2).

$$Leaf\ area\ per\ plant\ (cm^2) = \frac{dry\ weight\ leaf\ (g)_{total} * \frac{area\ of\ sampled\ leaves\ (cm^2)_{scanned}}{number\ of\ sampled\ leaves_{scanned}}}{dry\ weight\ of\ sampled\ leaf\ (g)_{scanned}} \quad (2)$$

2.3.6. Microscopy

Microscopy was conducted with a Zeiss axio observer z1 inverted microscope (Carl Zeiss Jena GmbH, Jena, Germany) connected with a Zeiss AxioCam MRc camera (Carl Zeiss Jena GmbH, Jena, Germany).

For picture processing, the manufacturer's program was used (AxioVision 40, version 4.8.2.0, Carl Zeiss MicroImaging GmbH, Jena, Germany).

2.3.6.1. *Staining solutions*

Staining was done with Sudan III, Fuchsin-Chryosidine-Astra blue (FCA) or Nile red staining solution. For an overview of different staining on poplar stem cross sections, see Figure 17.

Sudan III

6 g Sudan III was dissolved in 100 ml of 96% EtOH and exposed in an ultrasonic bath for 10 min. After filtration through filter paper, 50 ml of 100 % glycerol was added. Staining occurred for 45 to 90 sec directly on the slide. Then the samples were washed with a solution of 50% glycerol in EtOH 6 times for approximately 5 s.

Fuchsin-Chryosidine-Astra blue (FCA)

Ingredients (Table 18) were added to 100 ml of H_2O (bidest). After the ingredients were solved, 2 ml acetic acid was added to the solution. Staining occurred for 45 to 90 sec directly on the slide. Samples were washed afterwards 3 to 5 times for approximately 5 s with tap water.

Table 18: Ingredients of Fuchsin-Chryosidine-Astra blue (FCA) staining solution.

Ingredients	amount [g]
New fuchsin (C.I. 42520)	0.01
Chryosidine (C.I. 11270)	0.015
Astra blue (C.I. 48048)	0.125
H2O (bidest)	100 ml
Acetic acid	2 ml

Nile red

25 mg Nile red was solved in 50 ml of 2 % sulfuric acid solution and boiled for 5 min while being stirred. The solution was cooled before being filtered through filter paper. Staining occurred for 45 to 90 sec directly on the slide. The samples were washed with a solution of 70% glycerol in H_2O 1-2 times for approximately 5 s.

2.3.6.2. *Wood preparation*

Wood from a defined stem height (5 cm above root collar) was either fixed in FAE fixative (2% formaldehyde, 5% acetic acid, 60% EtOH solution) or frozen in liquid N_2 and stored at -20°C. Cuttings of fresh material (25 µm thickness) were made in a freezing microtome (2800 FrigoCut N, Reichert-Jung, Schalksmühle, Germany) and the sections were directly transferred on a microscopic slide. Staining was done immediately afterwards on the slide.

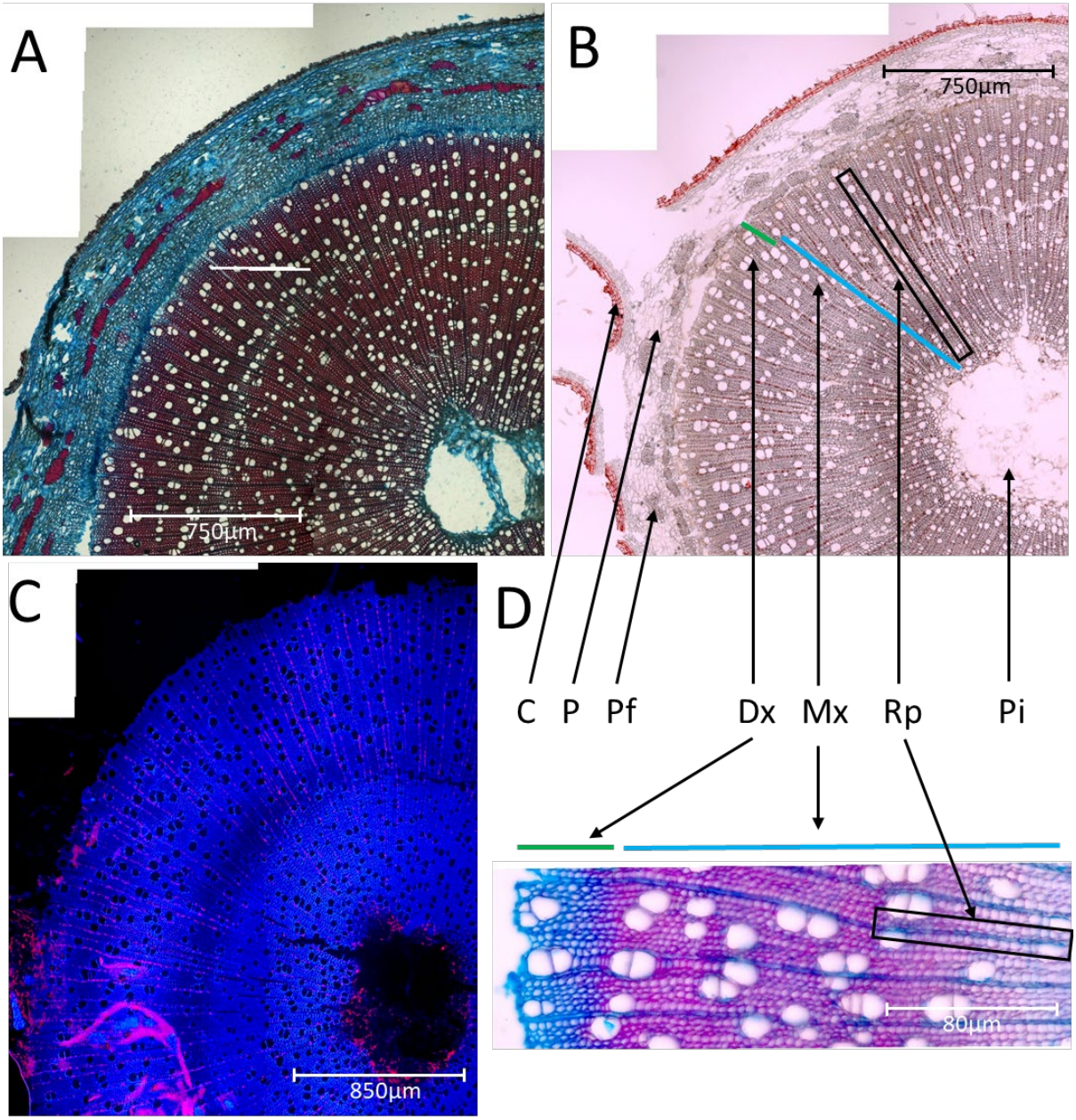

Figure 17: Exemples of cross sections of a poplar stem with different stainings. A.: FCA. **B.:** Sudan III. **C.:** Nile red. **D.:** Wood anatomy of poplar plants. C: cortex, P: phloem, Pf: phloem fibers, vC: vascular cambium, Dx: developing xylem, Mx: mature xylem, Rp: ray parenchyma, Pi: pith.

2.3.6.3. *Leaf preparation, stomata*

Leaves were sampled and processed freshly. Leaf hairs at the bottom side were removed carefully with a sticky tape (tesakrepp®, tesa SE, Norderstedt, Germany) and leaf disks were punched out. Leaf disks were transferred onto a slide and covered with tap water and immediately examined microscopically.

2.3.7. Wood swelling

Defined stem parts of 4 cm length were debarked and freeze-dried (Piatkowski Forschungsgeräte-Vertrieb, München, Germany) for 5 days. The weight of dry stems was measured. Water uptake occurred in a sealed reaction vessel (Falcon™, Fisher Scientific GmbH, Schwerte, Germany), filled with

3 ml of tap water. After 24 h at 22°C in darkness in a cultivator (Memmert GmbH + Co. KG, Schwabach, Germany), the weight of the stems was measured. Water uptake was calculated according to equation (3).

$$Uptake_{\Delta 24h} = \left(\frac{\left(weight_{wet}\ (g) - weight_{dry}\ (g) \right)}{weight_{dry}\ (g)} \right) \quad \textbf{(3)}$$

2.3.8. Plant surface lipid analysis

Lipids of the surface of fresh leaves and bark were extracted by chloroform (Roth, Karlsruhe, Germany). Three defined leaves of each plant were selected (leaf no. 7 representative for the top, leaf no. 15 for the middle and leaf no. 25 for the lower leaves). From each leaf, two disks of defined area (Ø 14 mm, 1.54 cm²) were punched out (Figure 18). All six disks per plant were transferred for 30 sec into the same glass vessel (Kimble®, Rockwood, TN, U.S.A.) containing 5 ml chloroform.

Bark was collected at the stem bottom using the first 5 cm above the root collar. The bark was cut into strips of approximately 50 x 5 mm and exposed to chloroform in a reaction vessel for 30 sec. Prior extraction, a photo of the bark and a standard (Figure 18) was taken to determine the area of the bark.

Processing of the chloroform extracts and lipid analysis was done with a GC/MS (Agilent, Santa Clara, CA, U.S.A.) by Milena Lewandowska (Department for Plant Biochemistry, Albrecht-von-Haller-Institute for Plant Sciences, University of Goettingen). Data were normalized to leaf or bark area.

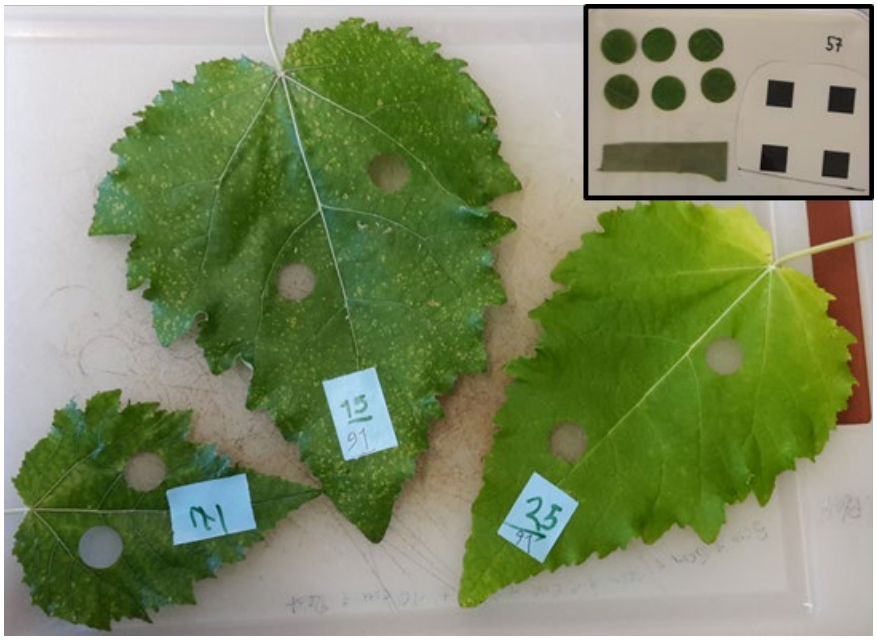

Figure 18: Lipid extraction of leaf and stem surface. Three defined leaves of each plant were taken for sampling. Two disks were taken per leaf and used for lipid extraction. The removed bark section and a standard (upper right, one black square equals 1 cm²) was photographed to determine the area from which the compounds were extracted.

2.3.9. Experiment 1: Severe drought stress

In Exp.1, five lines of 35S-*ScWS* overexpressing plants (K 60) were examined. Two lines could not be investigated further due to a loss of plants. Plants were potted on 17th, January 2018 into soil, adapted to greenhouse conditions (2.3.1) and grown at long day conditions at 22°C and an air humidity of approximately 60% in a greenhouse (Department of Forest Botany and Tree Physiology, University of Goettingen, Germany). 2.5 l pots were utilized.

Figure 19: Plants of Exp.1 are adapted to greenhouse conditions by removing transparent beaker or plastic bags gradually as described (2.3.1).

Plants were grown for 12 weeks in soil in the greenhouse. Photosynthesis and stomatal conductance were examined (2.3.4) before the drought treatments started. The lines G1L5 II, G1L4 and G1L3 II were investigated in detail and therefore clustered into three different groups of plants with similar height and appearance (Table 19). Drought treated plants (d) were not watered anymore at T=0 and underwent a decrease in soil moisture over time (Figure 20). Control plants (w) were held at a soil moisture level of approx. 0.65 $m^3 m^{-3}$. Soil moisture was measured every 24 h, the pre-dawn leaf water potential and photosynthesis (2.3.4) were measured after 4 d of stress treatment (12.04.). The experiment was completed after six days of drought treatment and the plants were harvested.

Table 19: Plant numbers in three different groups in Experiment 1. Groups of plants with similar height and appearance were chosen to undergo drought treatment (d). Watered control plants are indicated as (w).

	Group 1		Group 2		Group 3	
Treatment Line	(d)	(w)	(d)	(w)	(d)	(w)
WT	WT 2	WT 7	WT 8	WT 6	WT 3	WT 1
G1l5II	TG 28	TG 25	TG 27	TG 23	TG 21	TG 24
G1l4	TG 17	TG 16	TG 14	TG 13	TG 12	TG 11
G1l3II	TG 31	TG 32	TG 34	TG 35	TG 38	TG 36

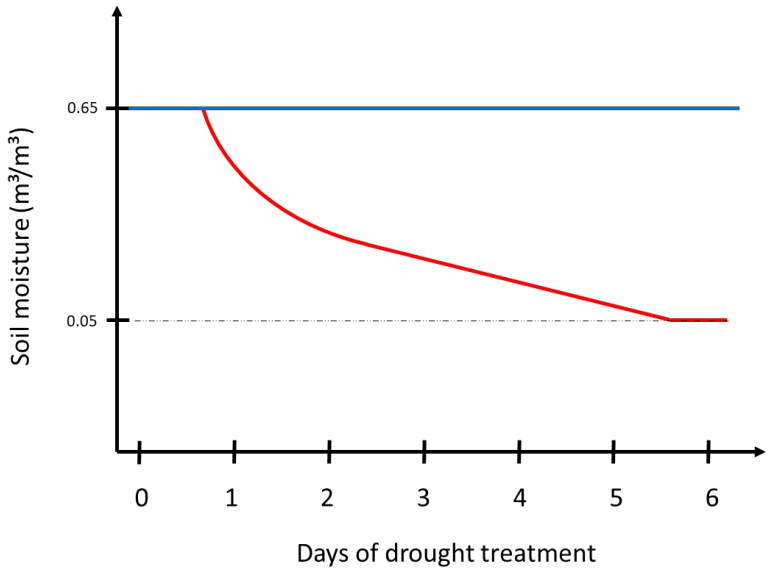

Figure 20: Schematic overview on the decline in soil moisture in Exp.1. Watered plants growing on soil with soil moisture of approx. 0.65 were no longer watered at TP=0. Over time, soil moisture decreased (red line). Control plants were grown at a soil moisture level of 0.65 m^3/m^3 (blue line).

2.3.10. Experiment 2: Mild stress adaptation, followed by severe stress

In experiment 2, 11 lines of 35S-*ScWS* overexpressing plants (K 60) with 118 plants in total were examined. Three lines were not investigated further due to a loss of all plants (Table 20). Plants were potted on 26th, March 2018, adapted to greenhouse conditions (2.3.1) and grown under long day conditions at 22°C to 27°C and air humidity of approximately 50% to 80% in a greenhouse. After 7 weeks, the plants were transferred to another greenhouse with active climate control by air conditioning (Department of Forest Botany and Tree Physiology, University of Goettingen, Germany) and grown at 21°C to 23°C and air humidity levels of 55% to 65%.

Table 20: Plants and lines grown for Exp.2. 11 different lines of *35S::ScWS*-OE plants were used. Three lines indicated with an asterisk (*) were lost. All plants in total (n_{total}) were utilized for general phenotyping and mild drought stress examination (Exp.2.1.) in watered (w) and drought (d) conditions. Plants were divided then into two groups; plants harvested after mild stress ($N_{harvest(2.1.)}$) and plants harvested after severe stress conditions ($n_{harvest\ (2.2.)}$).

	N_{total} =		$N_{harvest\ (2.1.)}$ =		$N_{harvest\ (2.2.)}$ =	
Line	(w)	(d)	(w)	(d)	(w)	(d)
WT	16	15	8	9	8	6
K 60 G1L3	5	6	4	4	1	2
K 60 G1L3 II	8	9	4	6	4	3
K 60 G1L4	8	4	5	4	3	-
K 60 G1L5 I	3	3	3	3	-	-
*K 60 G1L5 II	2	2	-	-	2	2
K 60 G1L6 I	3	4	1	2	2	2
*K 60 G1L6 II	3	2	-	-	3	2
K 60 G1L6 III	3	4	3	3	-	1
K 60 G4L1	3	7	2	2	1	5
K 60 G4L7	4	4	2	3	2	1
*K 60 G4L9	2	-	-	-	2	-

Photosynthesis, stomatal conductance, and the pre-dawn leaf water potential of watered, non-stressed plants were determined (2.3.4). Additionally, the stomatal size and frequency (2.3.6.3) and the stomatal conductance in darkness were analysed. Before a drought treatment was applied, plants were separated into groups of similar height and appearance.

During the treatment, two different levels of drought stress was applied (Figure 21). Control plants were kept in soil with a moisture of approximately 0.5 m^3/m^3. After one week, drought treated plants reached a soil moisture level of 0.17 m^3/m^3 and were kept at this level. The plants were watered every 12 h manually and the amount of water given to each plant was listed to determine the long-term water usage. During this mild-stress period, further referred to as Exp. 2.1, the pre-dawn leaf water potential was measured when all plants in the mild-stress treatment acquired a similar, low soil moisture content. Dead leaves, fallen down as a result of drought stress application, were collected and weighed (Sartorius AG, Göttingen, Germany). After 23 d, plants were divided into two groups: Plants of the first group (Exp. 2.1) were harvested and the surface lipid composition of watered plants was analysed (2.3.8). Plants of the second group (Exp. 2.2) were not watered anymore to achieve severe stress conditions. After 12 d of withholding water, the pre-dawn leaf potential of plants of Exp. 2.2 was determined, before harvest occurred.

Biomass parameters (2.3.5), wood anatomy of frozen stems of both groups (Exp.2.1 and 2.2) and the water uptake of dried wood (2.3.7) were examined after the harvests.

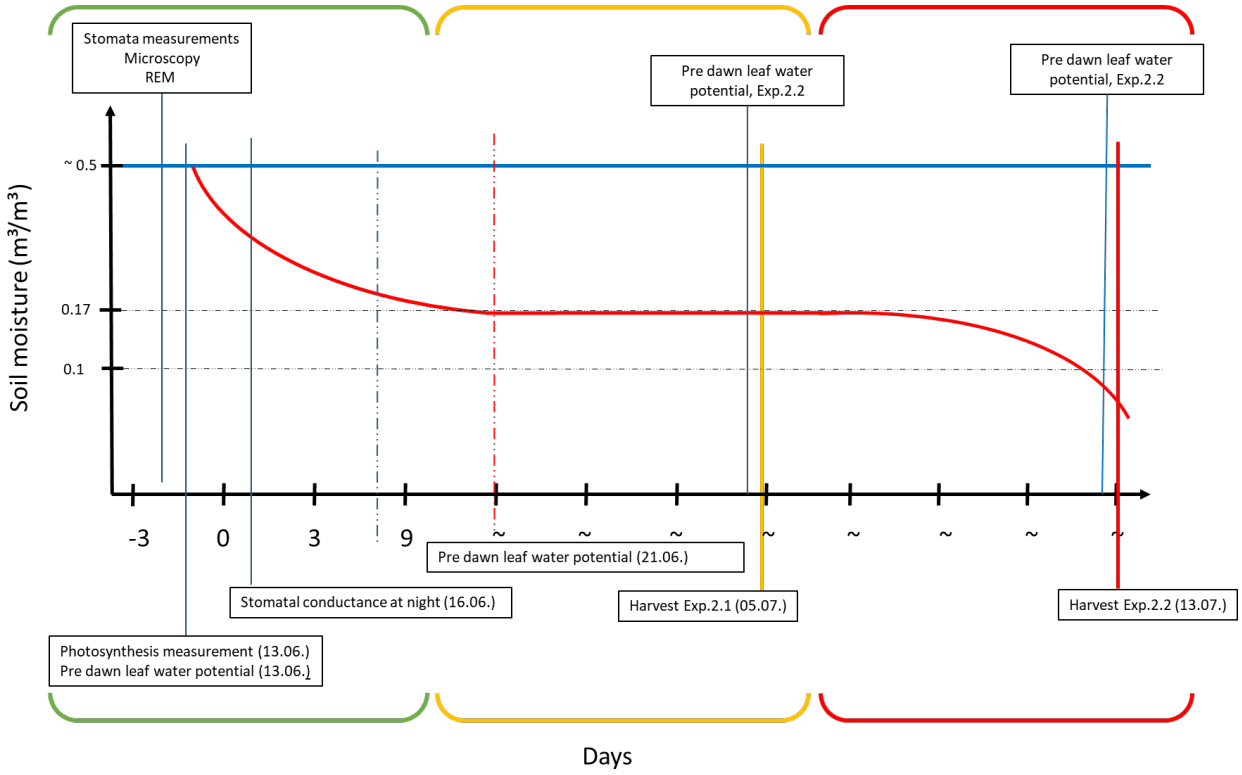

Figure 21: Schematic overview on drought exposure and measurements in Exp 2. Plants growing on soil with a soil moisture level of approx. 0.5 m^3/m^3 were no longer watered (blue line) at TP=0. Soil moisture was adjusted to approx. 0.17 m^3/m^3 for 14 d (green brackets) to apply a mild drought stress (yellow brackets, further referred to as Exp2.1), before a severe drought stress was applied (red brackets, further referred to as Exp.2.2). Plants were then left to dry until harvest. Control plants were grown on a soil moisture level of 0.5 m^3/m^3 (blue line).

2.3.11. Experiment 3: Mild stress

In experiment 3, four lines of 35S-*ScWS* overexpressing plants (K 60) with 56 plants in total were examined. Plants were potted on 23rd, August 2018, adapted to greenhouse conditions (2.3.1) and grown at long day conditions at 22°C and air humidity of approximately 60% in a greenhouse (Department of Forest Botany and Tree Physiology, University of Goettingen, Germany). Plants were transferred into bigger pots (3L) after 11 weeks. Photosynthesis and the stomatal conductance (2.3.4) were measured after 13 weeks.

After 14 weeks, plants were divided into groups of same height and appearance and a stress treatment was applied to half of the plants in each group (Figure 22). Treated plants were not watered anymore at T = 0. Soil moisture was measured every 24 h.

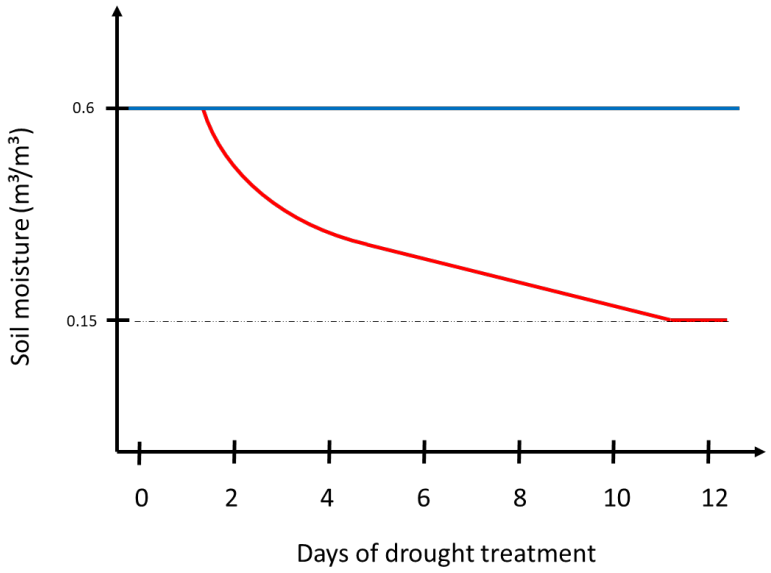

Figure 22: Schematic presentation of Exp. 3. Watered plants were growing in soil with a moisture of approximately 0.6 m^3 m^{-3}. Half of the plants were no longer watered at TP = 0. Over time, soil moisture decreased (red line). Control plants were kept at a soil moisture of 0.6 m^3/m^3 (blue line).

2.3.12. Experiment 4: Effects of the DX15 - promoter

In experiment 4, five lines of *DX15::AtDGAT1* and one line of *DX15::ScWS* expressing plants were examined (Table 21). Due to loss in sterile culture, only one *DX15::ScWS* was available for the greenhouse experiment. Plants were potted on 23rd, August 2018, adapted to greenhouse conditions (2.3.1) and grown at long day conditions at 22°C and an air humidity of approximately 60% in a greenhouse (Department of Forest Botany and Tree Physiology, University of Goettingen, Germany). Plants were transferred into bigger pots (3L) after 11 weeks. Photosynthesis and the stomatal conductance (2.3.4) were measured after 13 weeks. The plants were used to determine growth and biomass (2.3.5), the anatomy of wood (2.3.6.2) and the water uptake of dried wood (2.3.7). To examine wood specificity of the DX15 promoter, expression analysis was conducted with leaf, bark and DX tissue (2.3.3) on *AtDGAT1* and *ScWS*.

Table 21: Overview of plants grown for experiment 4. Plant lines with two different gene setups under the DX15 promoter, *DX15::AtDGAT1* (5 lines) and *DX15::ScWS* (1 line) were grown.

Gene / Construct	n (gene/construct) =	Line	n (line) =
DX15::AtDGAT1 (K 76)	37	K 76 I	12
		K 76 II	11
		K 76 V	6
		K 76 VII	6
		K 76 X	2
DX15::ScWS (K 78)	12	K 78 III	12
WT	17		17

2.4. Statistical analyses and data processing

For statistical analyses, R (Version 3.5.3, © 2019, The R foundation for Statistical Computing, www.r-project.org) was used. Normal distribution and homogeneity of variance were checked by visual inspection of the residuals and data was transformed logarithmically if necessary. A One-Way-ANOVA and Tukey's HSD test were performed to check for significance. If the p-value was < 0.05, the differences between groups were considered to be significant.

Data were processed with Excel 2013 (Microsoft, Redmond, WA, U.S.A.). Bar charts were drawn with Origin® (OriginLab®, Northampton, MA, U.S.A.). Vector maps and *in silico* cloning were prepared with Geneious®, version 11.0.3 (https://www.geneious.com/, Auckland, New Zealand). Picture processing was performed using ImageJ 1.52a (https://imagej.nih.gov/ij/, National Institute of Health, U.S.A.).

3. Results

3.1. Production of transgenic *P.* x *canescens* lines

Several different multiple gene-promoter and gene-binary vector combinations were produced and employed for the transformation of *P.* x *canescens*. Vectors using the pCAMBIA backbone could not be transformed successfully into poplar plants, whereas single gene vectors composed with the pK7WG backbone were positively transformed in several cases. Transformation with multiple gene vectors was not achieved in this study. Poplar could not be transformed with the genes *AtWRI1* and *AtDGAT1* under a 35S promoter, whereas transgenic plants were obtained with *AtDGAT1* using the DX15 promoter in a pK7WG construct. Transgenic plants including the *MaFAR* gene were only obtained using the construct K 71, which was inserted by the pDONR201-entry vector system. The transformation of this construct was intended as the first stage for a two – step transformation protocol to obtain transgenic plants with the *MaFAR* and the *ScWS* genes. Since the *ScWS* gene constructs could be transformed, the *MaFAR* transformation pipeline was not investigated further *in vivo*. The *ScWS* was transformed successfully under both the 35S (K 60, K 72) and the DX15 promoter (K 78). However, all viable lines of K 72 were lost in cultivation stage due to a failure in the plant breeding room electrical system and thus not available for further studies.

Table 22: Binary vectors transformed into *P. x canescens*. Five constructs of the binary vector were positively transformed as indicated and viable plant lines were cultivated separately. *: This 35S promoter is part of the pK7WG2 system. [1]: K 71 was not used in further experiments. [2]: K 72 was transformed successfully but all lines were lost during further cultivation due to a failure in the plant breeding room electrical system. Transformation experiments are listed in the column "Number of transformation experiments". Since each transformation experiment included a high amount of individual stem material, positive transformation lead to several different lines as indicated by a pound key (#). A list of all individual lines used in different experiments is shown in **Table 23**.

Promoter	Genes	Binary vector	Entry vector	Construct No.	Viability	Lines	Number of transformation experiments	Remarks
35-S	*AtWRI1, AtDGAT1*	pCAMBIA 23.0G	pENTRY	K 30	-	-	2	
	AtWRI1, MaFAR,ScWS	pCAMBIA 23.0G	pENTRY	K 32	-	-	2	
	MaFAR,ScWS	pCAMBIA 23.0G	pENTRY	K 31	-	-	2	
	AtWRI1	pCAMBIA 23.0G	pENTRY	K 61	-	-	2	
	AtDGAT1	pCAMBIA 23.0G	pENTRY	K 62	-	-	2	
	ScWS	pCAMBIA 23.0G	pENTRY	K 64	-	-	3	
	AtWRI1	pK7WG	pENTRY	K 57	-	-	2	No stable lines; marginal rooting
	AtDGAT1	pK7WG	pENTRY	K 58	-	-	4	
	ScWS	pK7WG	pENTRY	K 60#	+	11	4	
35-S*	*AtDGAT1*	pK7WG2	pDONR201	K 70	-	-	2	
	MaFAR	pK7WG2	pDONR201	K 71	+[1]	5	1	intendent for double transformation
	ScWS	pK7WG2	pDONR201	K 72	+[2]	7[2]	2	lost in culturing process
DX15	*AtDGAT1*	pK7WG-DX15	pDONR201	K 76#	+	14	2	
	MaFAR	pK7WG-DX15	pDONR201	K 77	-	-	1	
	ScWS	pK7WG-DX15	pDONR201	K 78#	+	3	2	

Table 23: Overview of all viable lines cultured and examined in greenhouse experiments. Three constructs transformed into polar plants led to various viable lines. A subset of these lines was grown and examined in greenhouse conditions. Expression analysis was done either with leaf material ([1]) or more detailed with bark, leaf and developmental xylem material ([2]) as indicated.

Promoter	Gene	Construct	Line	Experiment
35S	*ScWS*	K 60	G1L3	2
			G1L3I	3
			G1L3II[1,2]	2,1
			G1L4[1,2]	3,2,1
			G1L5I[2]	3,2
			G1L5II[1]	1
			G1L6I[1]	2,1
			G1L6II	2,1
			G1L6III[1]	2
			G4L1	2
			G4L7	2
			G4L9	3,2
DX15	*AtDGAT1*	K 76	K76I	4
			K76II[2]	4
			K76III	-
			K76IV	-
			K76V[2]	4
			K76VI	-
			K76VII	4
			K76VIII	-
			K76IX	-
			K76X	4
			K76XI	-
			K76XII	-
DX15	*ScWS*	K 78	78I	-
			78II	-
			78III[2]	4

3.1.1. Verification of constructs

Entry vectors containing the gene of interest were tested by Sanger sequencing for the correct sequence of the gene and promoter before being inserted into the binary vector system. Since multiple constructs contained multiple copies of the same promoter (2.1.16), Sanger sequencing of the binary vectors was not useful and the correct insertion of previously sequenced genes was tested via PCR (Figure 23). Transformed *Agrobacteria* were screened prior poplar transformation by colony PCR (Figure 24). Positive colonies were used for transformation of poplar plants as described in 2.2.4.

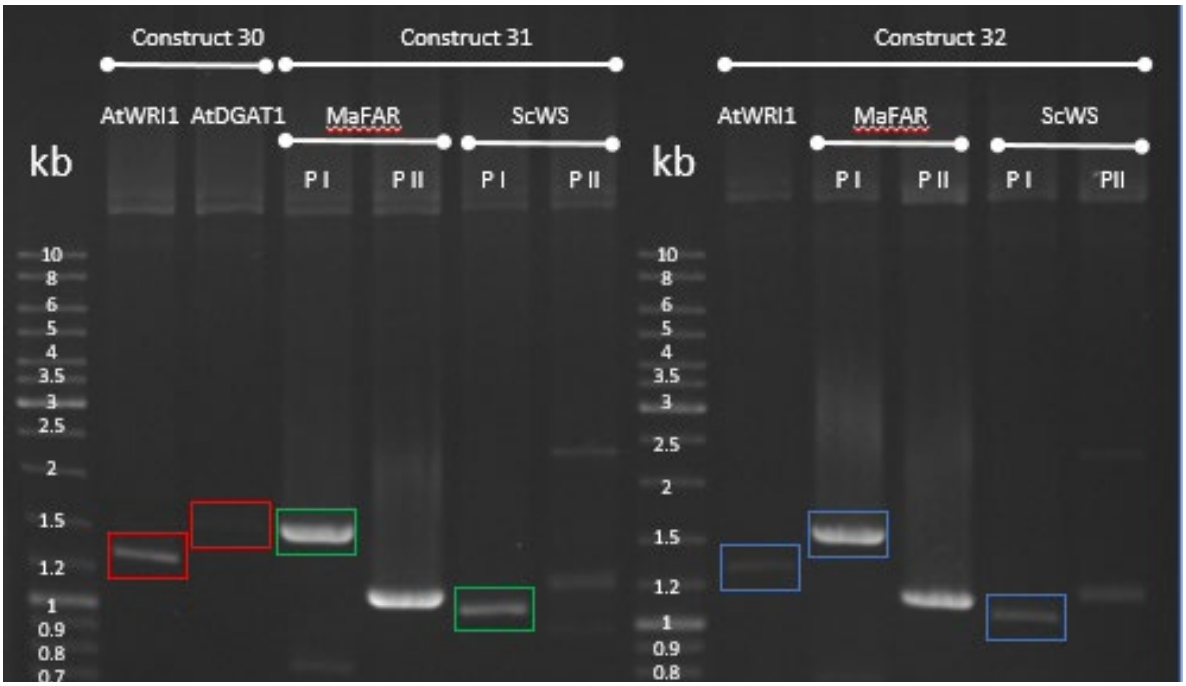

Figure 23: Representative agarose gel electrophoresis of a PCR of multiple gene constructs K 30, 31 and 32. K 30 contained *AtWRI1* and *AtDGAT1* (red boxes), K 31 contained *MaFAR* and *ScWS* (green boxes) and K 32 contained *AtWRI1*, *MaFAR* and *ScWS*. Two different primer pairs were tested (P I: Cloning primers, **Table 9**; P II: Sequencing primers, **Table 10**).

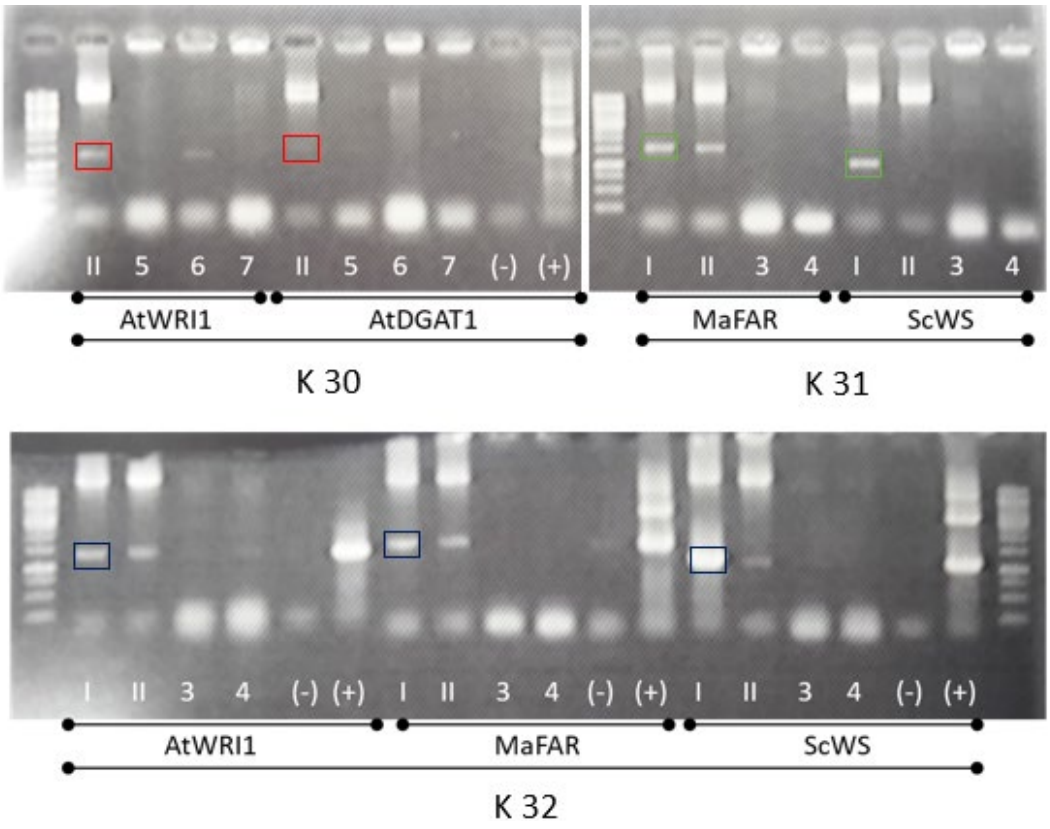

Figure 24: Representative colony PCR of multiple gene constructs K 30, 31 and 32. Single colonies of transformed *Agrobacteria* (I, II, 3, 4) were screened for positive insertion of the indicate gene in the binary vector. (-): negative control; (+): positive control. Colonies with a positive insertion are highlighted.

3.1.2. Verification of positively transformed plants

After transformation of stem pieces (2.2), regenerated plantlets from each stem piece were considered to form an individual line, which then was cultured further. Plants were screened as described in 2.1.10. Sanger sequencing was performed afterwards. Each line screened positively was further tested for correct insertion of the gene by Sanger sequencing (Figure 28). All lines showed correct insertion of the gene of interest.

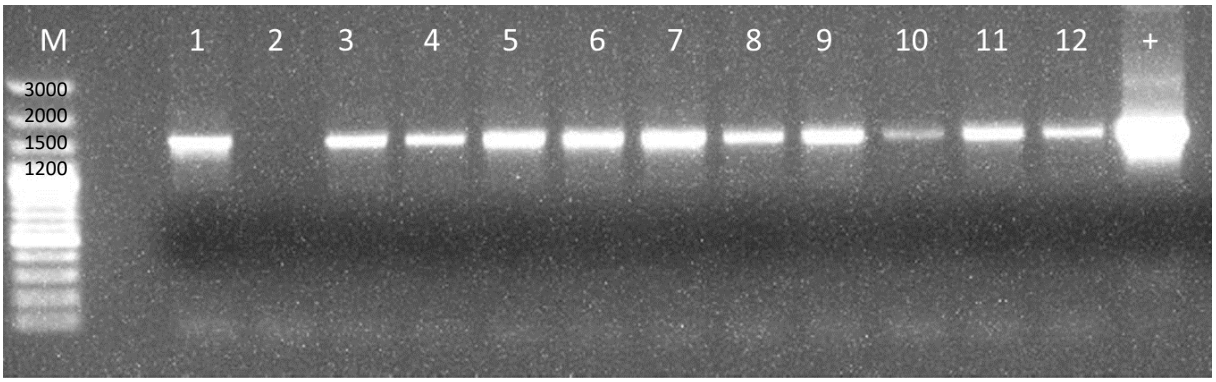

Figure 25: PCR screening of *35S::ScWS* transformed plants with construct 60 (K60). M: Marker; 1: G4L1, 2: G4L7 (tested positive in further test, not shown here), 3: G4L9, 4: G1L3, 5: G1L3I; 6: G1L3II; 7: G1L4; 8: G1L5I; 9: G1L5II; 10: G1L6I; 11: G1L6II; 12: G1L6III; +: positive control.

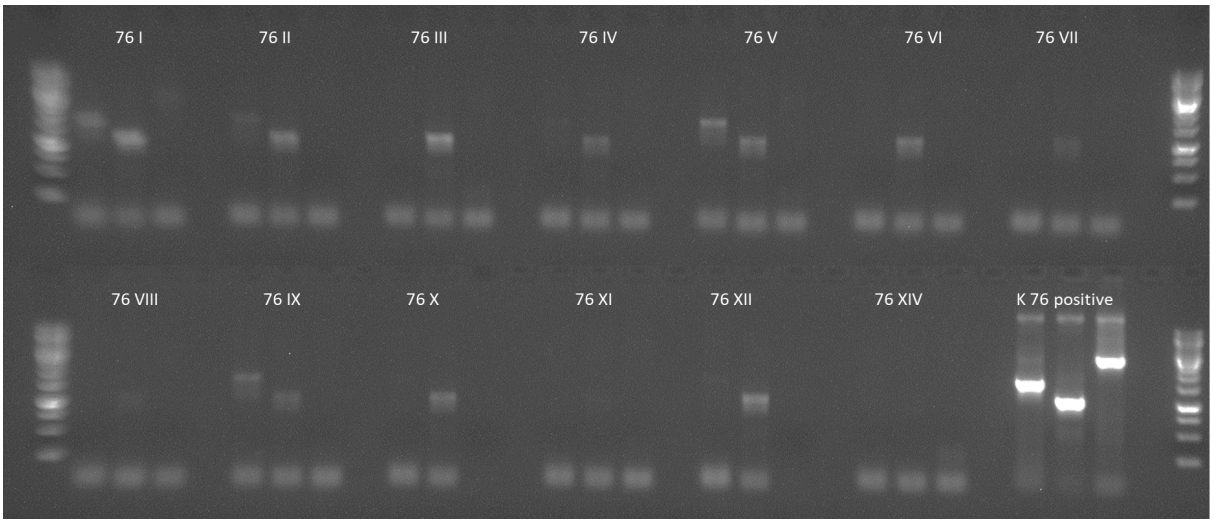

Figure 26: PCR screening of *DX15::AtDGAT1* transformed plants with construct 76 (K76). Each line was tested as described in 2.1.10. Each triplet of lanes shows screening for *AtDGAT1* (1st lane), promoter DX15 (2nd lane) and sequence from right border to left border of pK7WG construct (3rd lane) of the different lines.

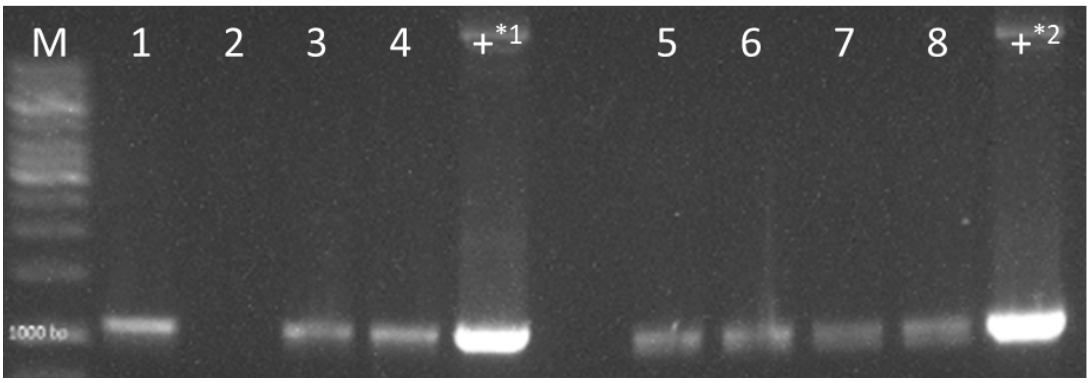

Figure 27: PCR screening of *DX15::ScWS* transformed plants with construct 78 (K78). Plants were screened (2.1.10) for *ScWS* (lanes 1-4) and for DX15 promoter (5-8). M: Marker, 1: K78I; 2: tested negative, line was expelled from further experiments, 3: K78II; 4: K78III.; +*1: positive control *ScWS*; 5: K78I; 6: expelled line, 7: K78II; 8: K78III.; +*2: positive control DX15.

Figure 28: Representative alignment of sequence data of plant line K60 G1L5 I. Sequence data, derived from sequenced plant genomic DNA, was aligned to the sequence of the *ScWS* (top line). To get sufficient data of genes longer than 750 kB, two sequences were amplified, one in 5'-3' direction (middle line) and one in 3'-5' direction (bottom line). For a magnification of this graph, please see the attached CD.

3.2. Characterisation of transgenic *P.* x *canescens*

3.2.1. Characterisation of *35S::ScWS* transgenic plants

The effects of the overexpression of *ScWS* on the plant's performance were tested in three different greenhouse experiments. General parameters (e.g. growth rates, biomass accumulation, etc.) are shown in this chapter. To further evaluate the effect of overexpressed *ScWS* in drought conditions, different levels of drought stress were applied: Severe drought stress, further referred to as Experiment 1 (2.3.9), mild + severe drought stress, further referred to as Experiment 2 (2.3.10) and mild stress, further referred to as Experiment 3 (2.3.11). To summarize and to compare the effects of drought stress applied in the different experiments, drought - specific parameters (e.g. photosynthesis, predawn leaf water potential, etc.) and their impact on the performance are shown in chapter **Fehler! Verweisquelle konnte nicht gefunden werden.**.

The effects of the DX15 - promoter were tested in one greenhouse experiment, further referred to as Experiment 4 (2.3.12).

3.2.1.1. *Expression of ScWS under the 35S promoter*

Expression of *ScWS* under the 35S promoter was tested with qRT PCR (2.3.3). Expression was confirmed in leaf tissue (Exp.1, Figure 29, A), in roots and DX (Exp.2, Figure 29, B). A basal expression of a wax ester synthase was observed in WT leaf and DX.

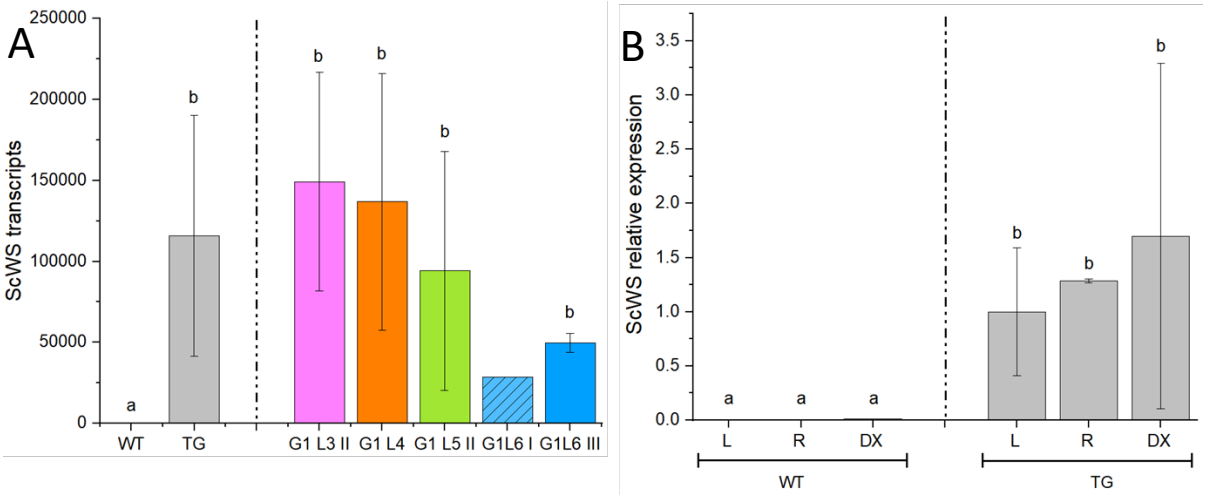

Figure 29: Expression analysis of *35S::ScWS* plant lines. A.: Expression of *ScWS* in leaves from Exp.1. N_{WT} = 3, N_{TG} =13, N_{lines} = 3, except line G1L6I (n =1, no mean ± SE). Basal expression was found in WT leaf (mean = 1.01 ± 0.01). Expression was normalized to WT – expression level. **B.:** Expression of *ScWS* in leaves (L), root (R) and developing xylem (DX). N_{WT} = 1, N_{TG} = 3. The sample of WT contained basal expression of *WS* in root ($3.3*10^3 \pm 0.2*10^3$) and DX ($10.2*10^{-3} \pm 1.3*10^{-3}$), but no expression was detected in leaf. Different letters indicate significant differences among lines at $P \leq 0.05$ (ANOVA). Values are means ± SD.

3.2.1.2. *Growth rates and biomass of ScWS-OE plants*

Growth rates and biomass of *ScWS*-OE plants and the WT were examined. For a schematic overview of the experimental parameters, see 2.3.9 (Exp.1), 2.3.10 (Exp.2) and 2.3.11 (Exp.3).

Growth rates of *ScWS*-OE plants were not affected compared to the WT under the short -term drought treatment of Exp.1 (Figure 30 A) and Exp.3 (Figure 30 B). Under long term mild drought conditions after a growing period of 100 d in Exp.2 (Figure 30 C), transgenic plants were shorter in height than the WT and had a thinner stem diameter (Figure 31 B).

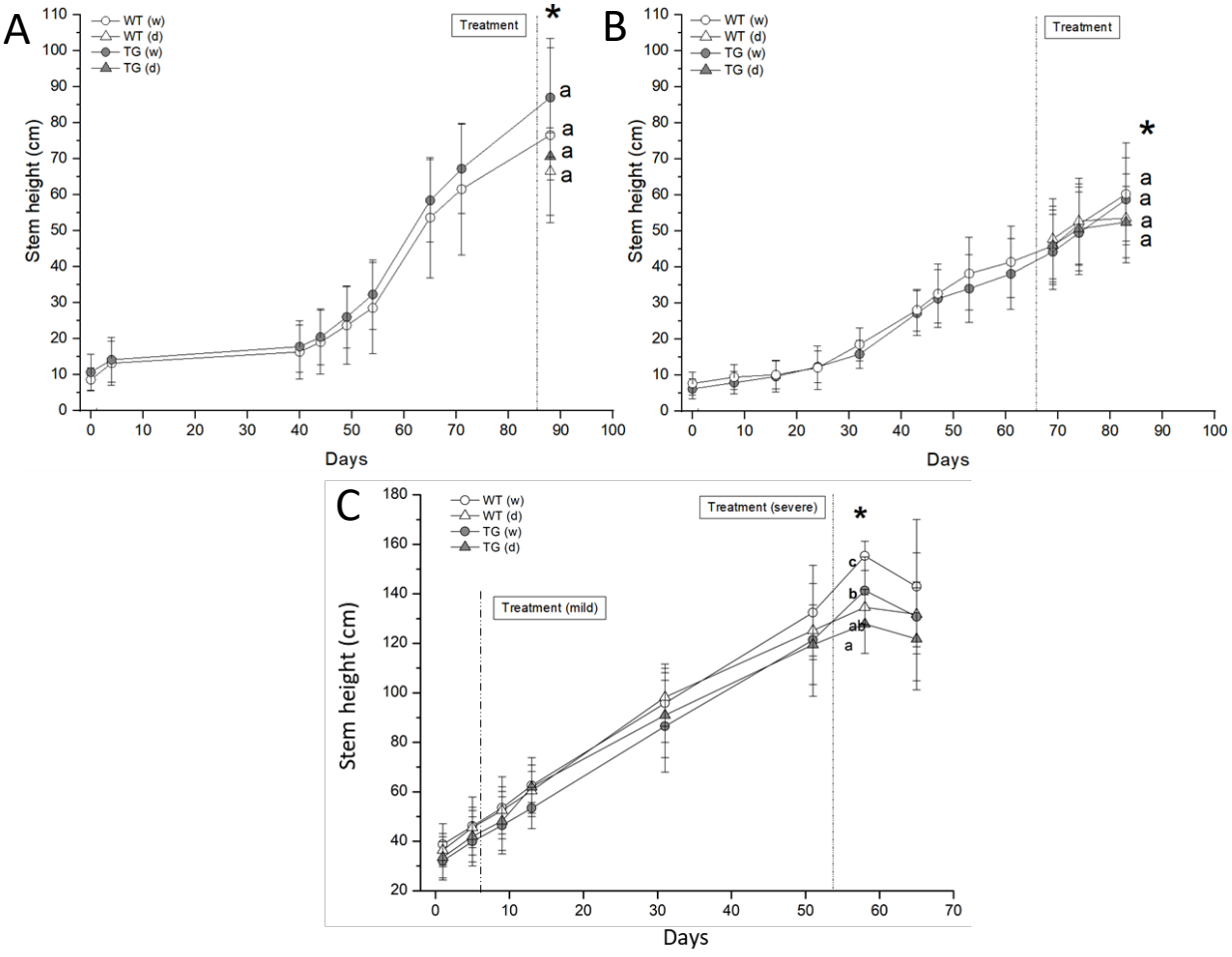

Figure 30: Height growth of *ScWS*–OE poplar plants. Plant groups are indicated as following: Transgenic: grey, wildtype: white. Treatment: triangle, control: circle. Harvests are indicated with an asterisk. Start of treatments are indicated with a dotted line. Data shows mean ± SE. **A.:** Growth of plants of Exp.1. $N_{WT(w)} = 5$, $N_{WT(d)} = 3$, $N_{TG(w)} = 14$, $N_{TG(d)} = 9$. **B.:** Growth of plants of Exp.3. $N_{WT(w)} = 9$, $N_{WT(d)} = 11$, $N_{TG(w)} = 15$, $N_{TG(d)} = 22$. **C.:** Growth of plants of Exp.2. $N_{WT(w)} = 15$, $N_{WT(d)} = 13$, $N_{TG(w)} = 50$, $N_{TG(d)} = 40$. Different letters indicate significant differences among the WT and the transgenic plants at $P \leq 0.05$ (ANOVA). Values are means ± SD.

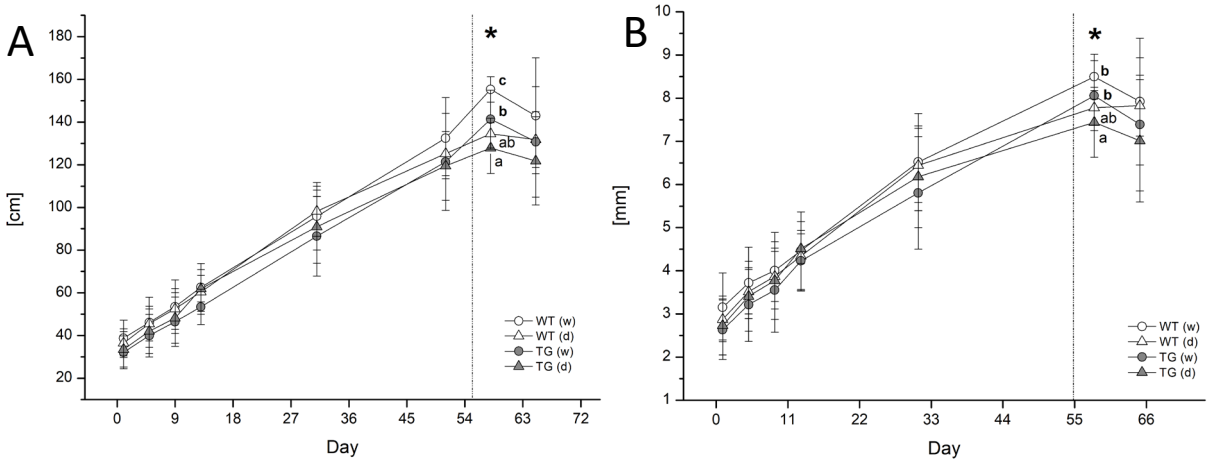

Figure 31: Height g (A) and diameter growth (B) of stems of *ScWS*–OE and WT plants in Exp.2. Significant differences are indicated with an asterisk. $N_{WT(w)}$ = 15, $N_{WT(d)}$ =13, $N_{TG(w)}$ = 50, $N_{TG(d)}$ = 40. Different letters indicate significant differences at P ≤ 0.05 (ANOVA). Values are means ± SD.

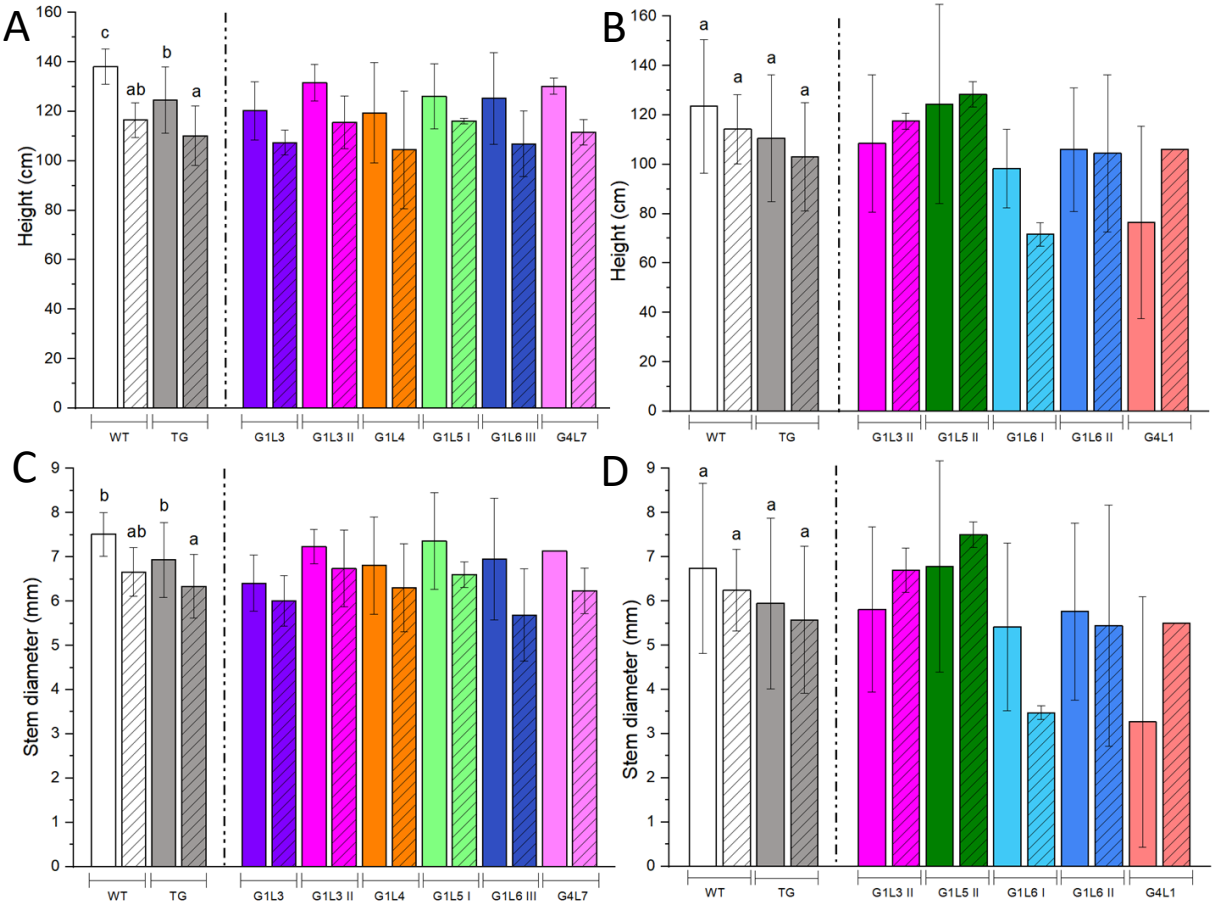

Figure 32: Height (A, B) and stem diameter (C, D) of *ScWS*-OE lines and the WT in Exp.2 (2.3.10) at the harvest. Drought treated groups are indicated by hatched bars. The TG group, indicated in grey, is the mean of all transgenic lines tested. Several representative lines are shown, for a complete list of tested lines and plants see **Table 20**. Data show height (**A**) and stem diameter (**B**) of plants after 23 d of mild drought stress and of controls. $N_{WT(w)}$ = 7, $N_{WT(d)}$ =7, $N_{TG(w)}$ = 23, $N_{TG(d)}$ = 26. After 12 d of further severe stress, height (**C**) and stem diameter (**D**) were measured. $N_{WT(w)}$ = 8, $N_{WT(d)}$ = 6, $N_{TG(w)}$ = 25, $N_{TG(d)}$ = 14. Different letters indicate significant differences among lines at P ≤ 0.05 (ANOVA). Values are means ± SD.

The total plant leaf area of the transgenic lines tended to be lower than that of the WT, but the effect was only significant in Exp. 2 (Fig. 32 B). Under drought stress, plant leaf area of drought treated TG plants decreased significantly compared to the WT (Figure 33 B). In short term experiments, no significant differences were found (Figure 33 A, C).

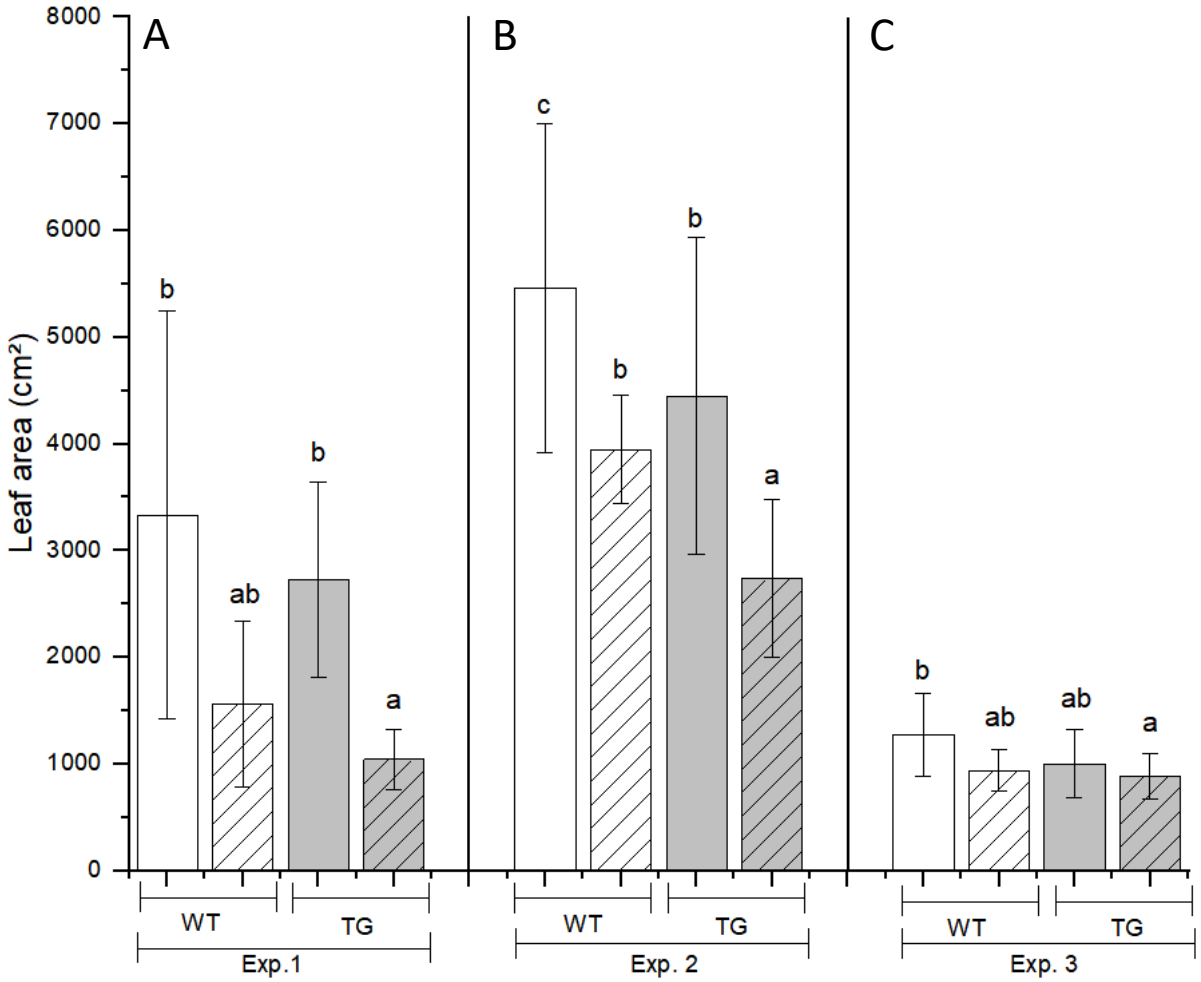

Figure 33: Total leaf area (plant) of *ScWS*-OE and WT poplar plants. Comparison of the leaf area of experiment 1 (**A**), 2 (**B**) and 3 (**C**). Drought treated plants are indicated by hatched bars. **A.:** Leaf area of plants from **Exp.1**. $N_{WT(w)} = 5$, $N_{WT(d)} = 3$, $N_{TG(w)} = 16$, $N_{TG(d)} = 10$. **B.:** Leaf area of plants from **Exp.2**. $N_{WT(w)} = 15$, $N_{WT(d)} = 13$, $N_{TG(w)} = 48$, $N_{TG(d)} = 40$. **C.:** Leaf area of plants from **Exp.3**. $N_{WT(w)} = 9$, $N_{WT(d)} = 8$, $N_{TG(w)} = 15$, $N_{TG(d)} = 16$. Different letters indicate significant differences among lines at $P \leq 0.05$ (ANOVA, Tukey). Values are means ± SD.

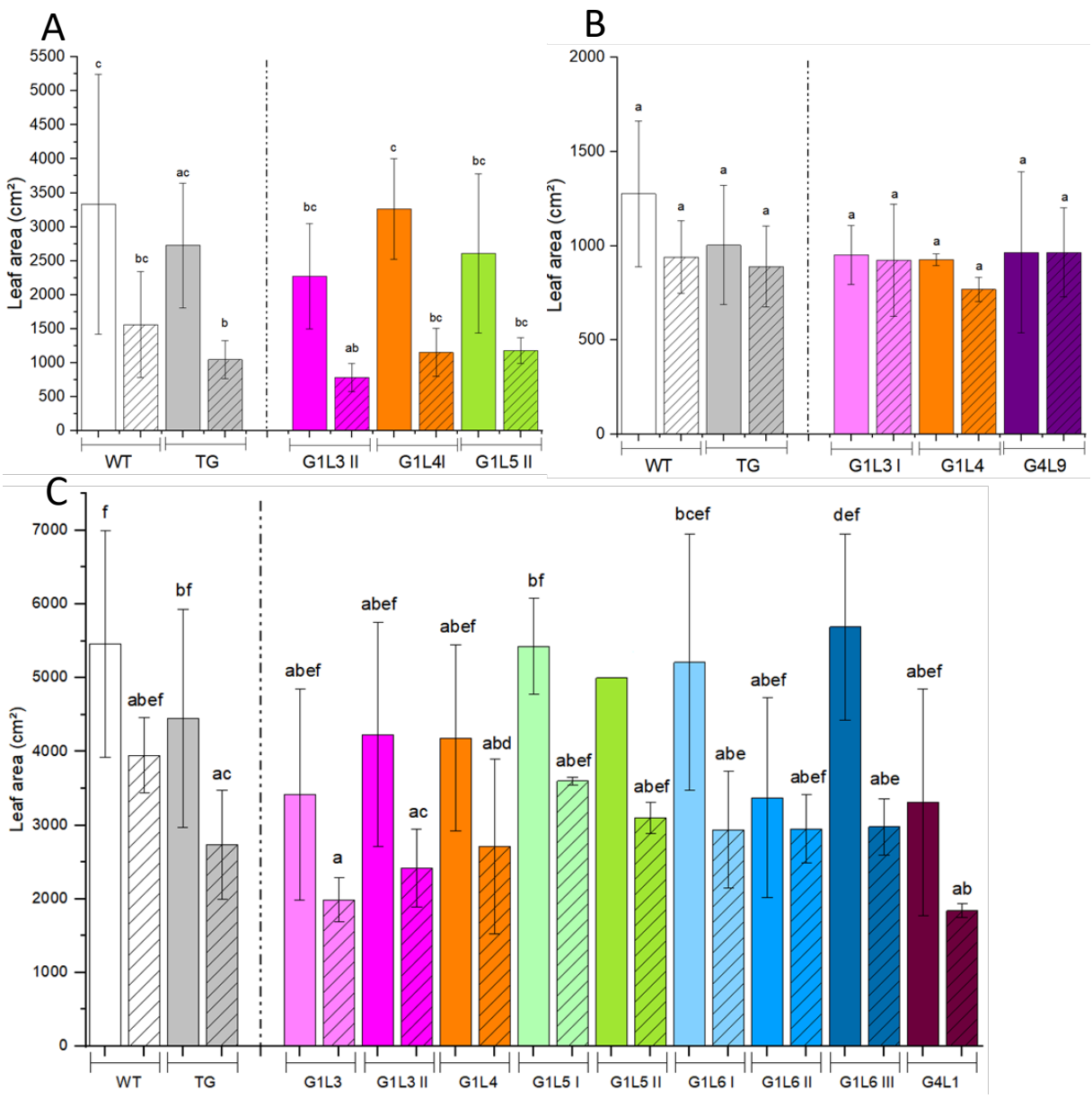

Figure 34: Leaf area (per plant) of *ScWS*-OE lines and the WT. Representative lines are shown if N ≥ 2. The TG group indicated in grey is the mean of all transgenic plants tested, including representative lines. Drought treated plants are indicated by hatched bars. **A.:** Leaf area of lines from **Exp.1**. $N_{WT(w)}$ = 5, $N_{WT(d)}$ = 3, $N_{TG(w)}$ = 16, $N_{TG(d)}$ = 10, $N_{G1L3II\ (W)}$ = 5, $N_{G1L3II\ (d)}$ = 3, $N_{G1L4\ (W)}$ = 4, $N_{G1L4\ (D)}$ = 3, $N_{G1L5II\ (W)}$ = 5, $N_{G1L5II\ (D)}$ = 3. **B.:** Leaf area of plants from **Exp.3**. $N_{WT(w)}$ = 9, $N_{WT(d)}$ = 8, $N_{TG(w)}$ = 15, $N_{TG(d)}$ = 16, $N_{G1L3I\ (W)}$ = 3, $N_{G1L3I\ (d)}$ = 4, $N_{G1L4\ (W)}$ = 3, $N_{G1L4\ (D)}$ = 4, $N_{G4L9\ (W)}$ = 3, $N_{G4L9\ (D)}$ = 5. **C.:** Leaf area of plants from **Exp.2**. Line G1L5II control (n = 1) is shown for completion. $N_{WT(w)}$ = 15, $N_{WT(d)}$ = 13, $N_{TG(w)}$ = 48, $N_{TG(d)}$ = 40, $N_{G1L3\ (W)}$ = 4, $N_{G1L3\ (d)}$ = 5, $N_{G1L3II\ (W)}$ = 4, $N_{G1L3II\ (d)}$ = 7, $N_{G1L4\ (W)}$ = 8, $N_{G1L4\ (D)}$ = 4, $N_{G1L5I\ (W)}$ = 3, $N_{G1L5I\ (D)}$ = 3, $N_{G1L5II\ (W)}$ = 1, $N_{G1L5II\ (D)}$ = 2, $N_{G1L6I\ (W)}$ = 3, $N_{G1L6I\ (d)}$ = 4, $N_{G1L6II\ (W)}$ = 3, $N_{G1L6II\ (d)}$ = 2, $N_{G1L6III\ (W)}$ = 3, $N_{G1L6III\ (d)}$ = 4, $N_{G4L1\ (W)}$ = 7, $N_{G4L1\ (d)}$ = 3. Different letters indicate significant differences among lines at P ≤ 0.05 (ANOVA, Tukey). Values are means ± SD.

The root-to-shoot ratio was not affected by overexpression of *ScWS* either in severe stress conditions of experiment 1 (Figure 35 A) or in long mild stress conditions of experiment 2 (Figure 35 B). In experiment 3 (Figure 35 C), significant differences were observed due to the treatment. No differences were found among the lines tested (Figure 36 A, B, C).

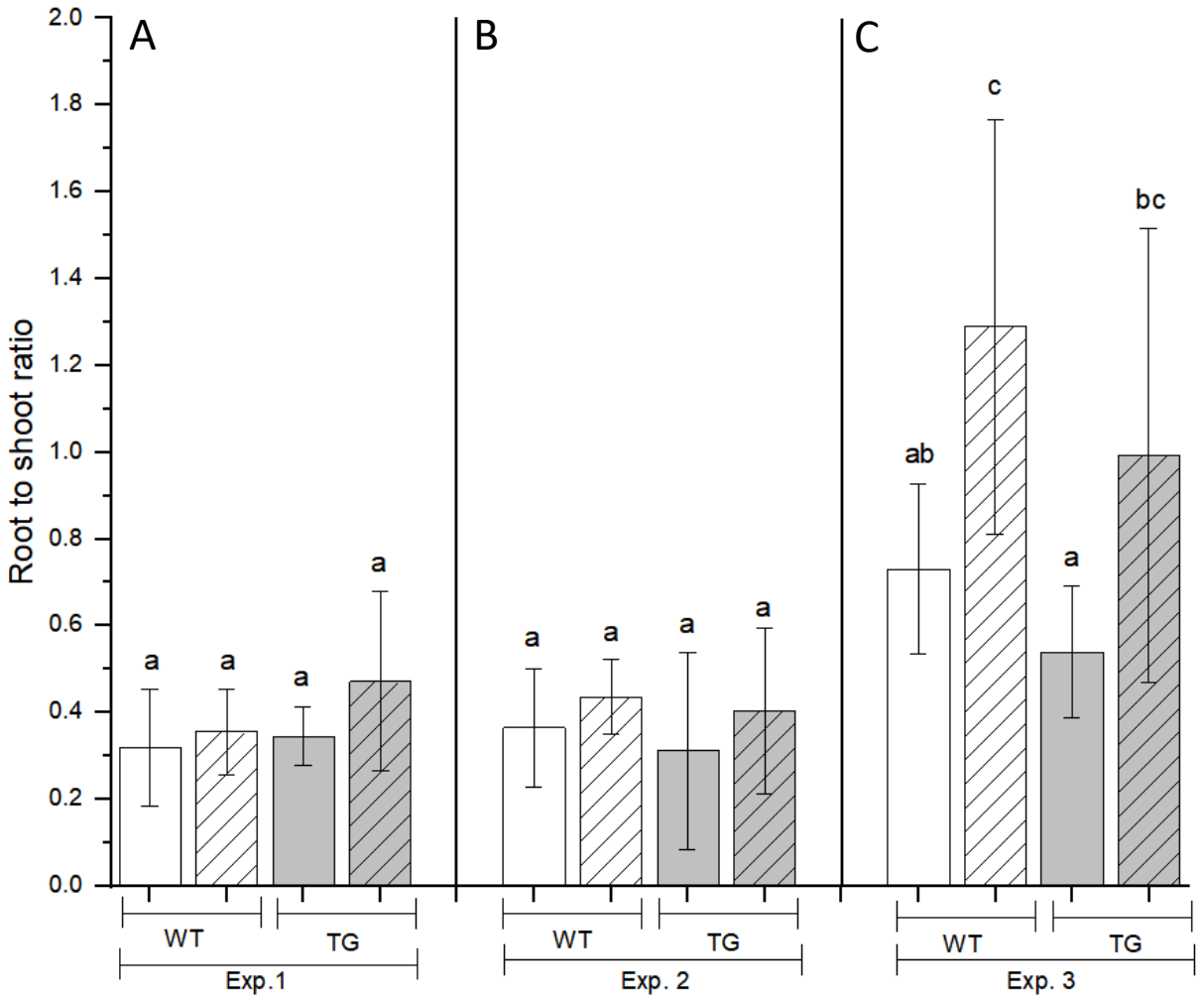

Figure 35: Root-to-shoot ratio of *ScWS*-OE and WT poplar plants. Comparison of the root-to-shoot ratio of experiment 1 (**A**), 2 (**B**) and 3 (**C**). Drought treated plants are indicated by hatched bars. **A.:** Root-to-shoot ratio of plants from **Exp.1**. $N_{WT(w)}$ = 5, $N_{WT(d)}$ = 3, $N_{TG(w)}$ = 16, $N_{TG(d)}$ = 10. **B.:** Root-to-shoot ratio of plants from **Exp.2**. $N_{WT(w)}$ = 13, $N_{WT(d)}$ =19, $N_{TG(w)}$ = 38, $N_{TG(d)}$ = 33. **C.:** Root-to-shoot ratio of plants from **Exp.3**. $N_{WT(w)}$ = 9, $N_{WT(d)}$ =8, $N_{TG(w)}$ = 12, $N_{TG(d)}$ = 16. Different letters indicate significant differences among lines at $P \leq 0.05$ (ANOVA, Tukey). Values are means ± SD.

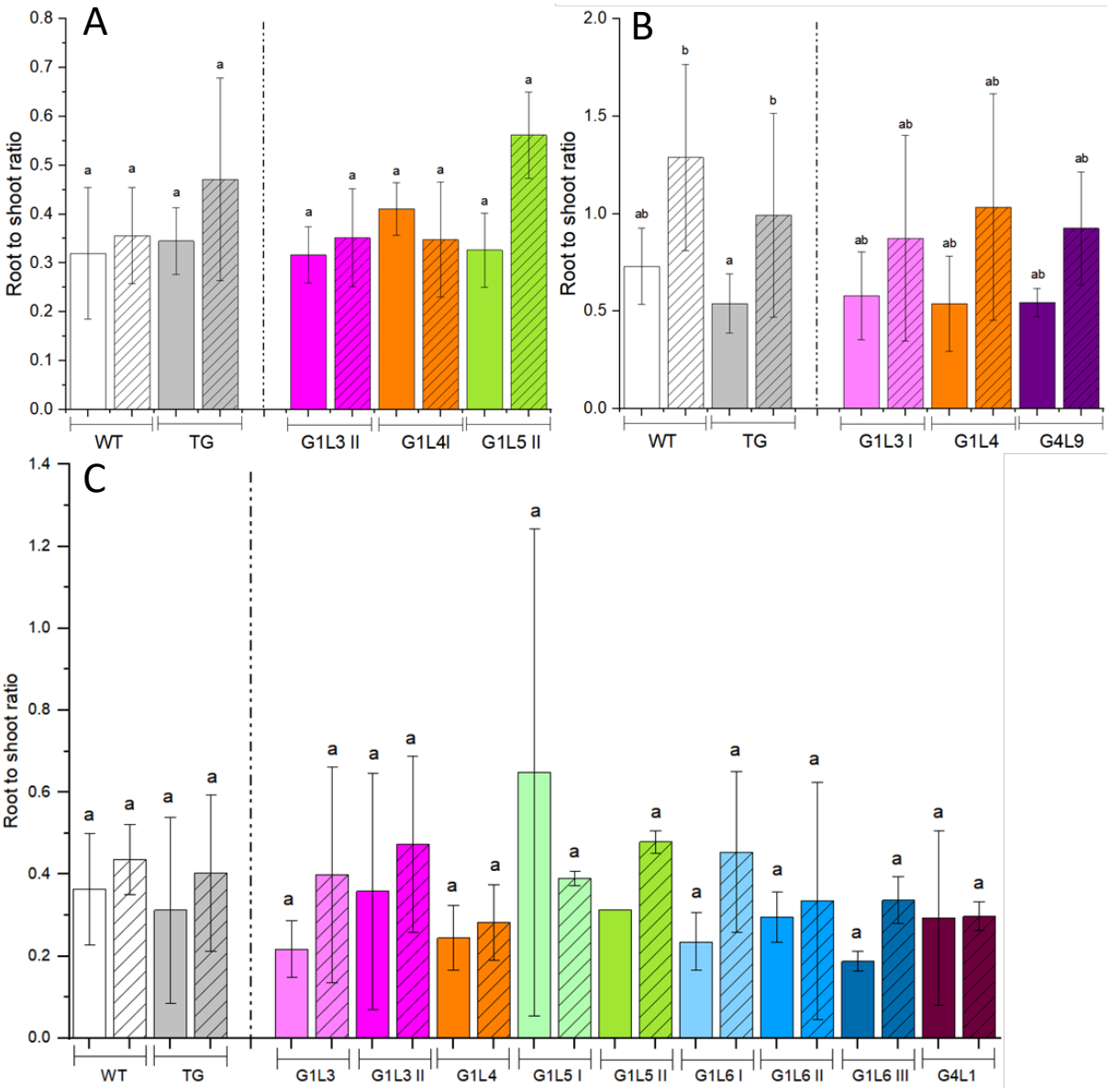

Figure 36: Root-to-Shoot ratio of *ScWS*-OE lines and the WT. Representative lines are shown if N ≥ 2. The TG group indicated in grey is the mean of all transgenic plants tested, including representative lines. Drought treated plants are indicated with hatched bars. **A.:** Root-to-shoot ratio of lines from **Exp.1**. $N_{WT(w)}$ = 5, $N_{WT(d)}$ = 3, $N_{TG(w)}$ = 16, $N_{TG(d)}$ = 10, $N_{G1L3II\ (W)}$ = 5, $N_{G1L3II\ (d)}$ = 3, $N_{G1L4\ (W)}$ = 4, $N_{G1L4\ (D)}$ = 3, $N_{G1L5II\ (W)}$ = 5, $N_{G1L5II\ (D)}$ = 3. **B.:** Root-to-shoot ratio of plants from **Exp.3**. $N_{WT(w)}$ = 9, $N_{WT(d)}$ = 8, $N_{TG(w)}$ = 11, $N_{TG(d)}$ = 14, $N_{G1L3I\ (W)}$ = 3, $N_{G1L3I\ (d)}$ = 4, $N_{G1L4\ (W)}$ = 4, $N_{G1L4\ (D)}$ = 5, $N_{G4L9\ (W)}$ = 4, $N_{G4L9\ (D)}$ = 4. **C.:** Root-to-shoot ratio of plants from **Exp.2**. Line G1L5II control (n = 1) is shown for completion. $N_{WT(w)}$ = 15, $N_{WT(d)}$ =13, $N_{TG(w)}$ = 48, $N_{TG(d)}$ = 40, $N_{G1L3\ (W)}$ = 5, $N_{G1L3\ (d)}$ = 6, $N_{G1L3II\ (W)}$ = 7, $N_{G1L3II\ (d)}$ = 8, $N_{G1L4\ (W)}$ = 8, $N_{G1L4\ (D)}$ = 4, $N_{G1L5I\ (W)}$ = 4, $N_{G1L5I\ (D)}$ = 3, $N_{G1L5II\ (W)}$ = 2, $N_{G1L5II\ (D)}$ = 2, $N_{G1L6I\ (W)}$ = 3, $N_{G1L6I\ (d)}$ = 4, $N_{G1L6II\ (W)}$ = 3, $N_{G1L6II\ (d)}$ = 2, $N_{G1L6III\ (W)}$ = 3, $N_{G1L6III\ (d)}$ = 4, $N_{G4L1\ (W)}$ = 7, $N_{G4L1\ (d)}$ = 3. Different letters indicate significant differences among lines at P ≤ 0.05 (ANOVA, Tukey). Values are given as means ± SD.

In short-time experiments (Figure 37 A, C), no significant differences were found in the dry biomass of leaves, stems and roots. Exclusively in Exp.1 (Figure 37 A), drought treated WT and TG plants both demonstrated significant lower stem biomass. In long-time Exp.2 (Figure 37 B), significant differences between watered WT and TG plants were found in the biomass of leaves and roots, but not in stem. Consequently, the total biomass of watered *ScWS*-OE plants was significantly reduced compared to watered WT plants. No significant differences were observed among the lines in all three experiments (Figure 37 A, B, C).

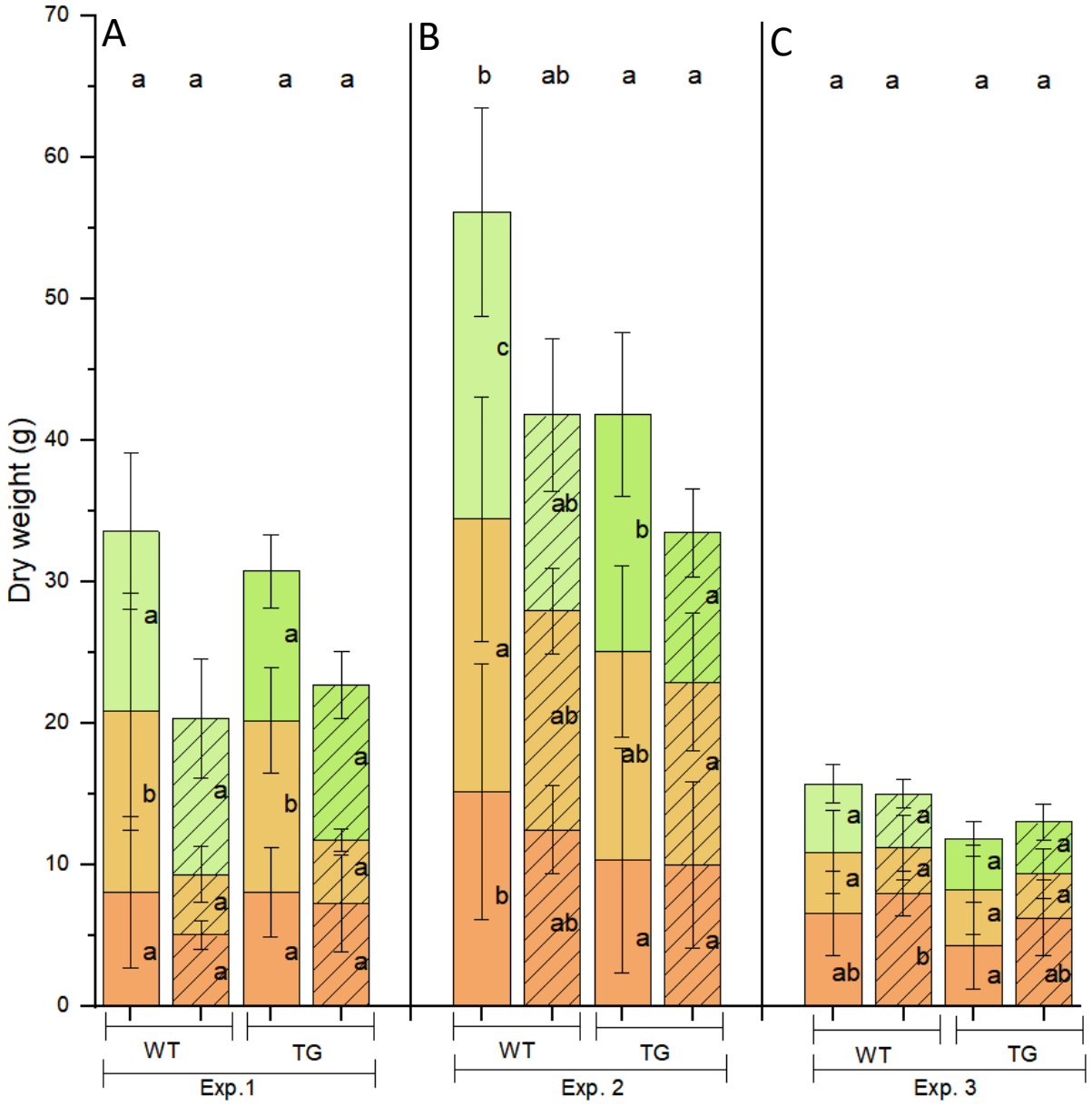

Figure 37: Dry mass of *ScWS*-OE and WT poplar plants. Comparison of the dry mass of experiments 1 (**A**), 2 (**B**) and 3 (**C**), stacking the results of leaves (green), stem (light brown) and roots (brown). Drought treated plants are indicated by hatched bars. Each tissue was compared with each other, significant differences are indicated with different letters at P ≤ 0.05 (ANOVA, Tukey). Significance of the compete dry mass is shown above. **A.:** Dry mass of plants in **Exp.1**. $N_{WT(w)}$ = 5, $N_{WT(d)}$ = 3, $N_{TG(w)}$ = 16, $N_{TG(d)}$ = 10. **B.:** Dry mass of plants in **Exp.2**. $N_{WT(w)}$ = 13, $N_{WT(d)}$ =19, $N_{TG(w)}$ = 38, $N_{TG(d)}$ = 33. **C.:** Dry mass of plants in **Exp.3**. $N_{WT(w)}$ = 9, $N_{WT(d)}$ = 8, $N_{TG(w)}$ = 12, $N_{TG(d)}$ = 16. Values are means ± SD.

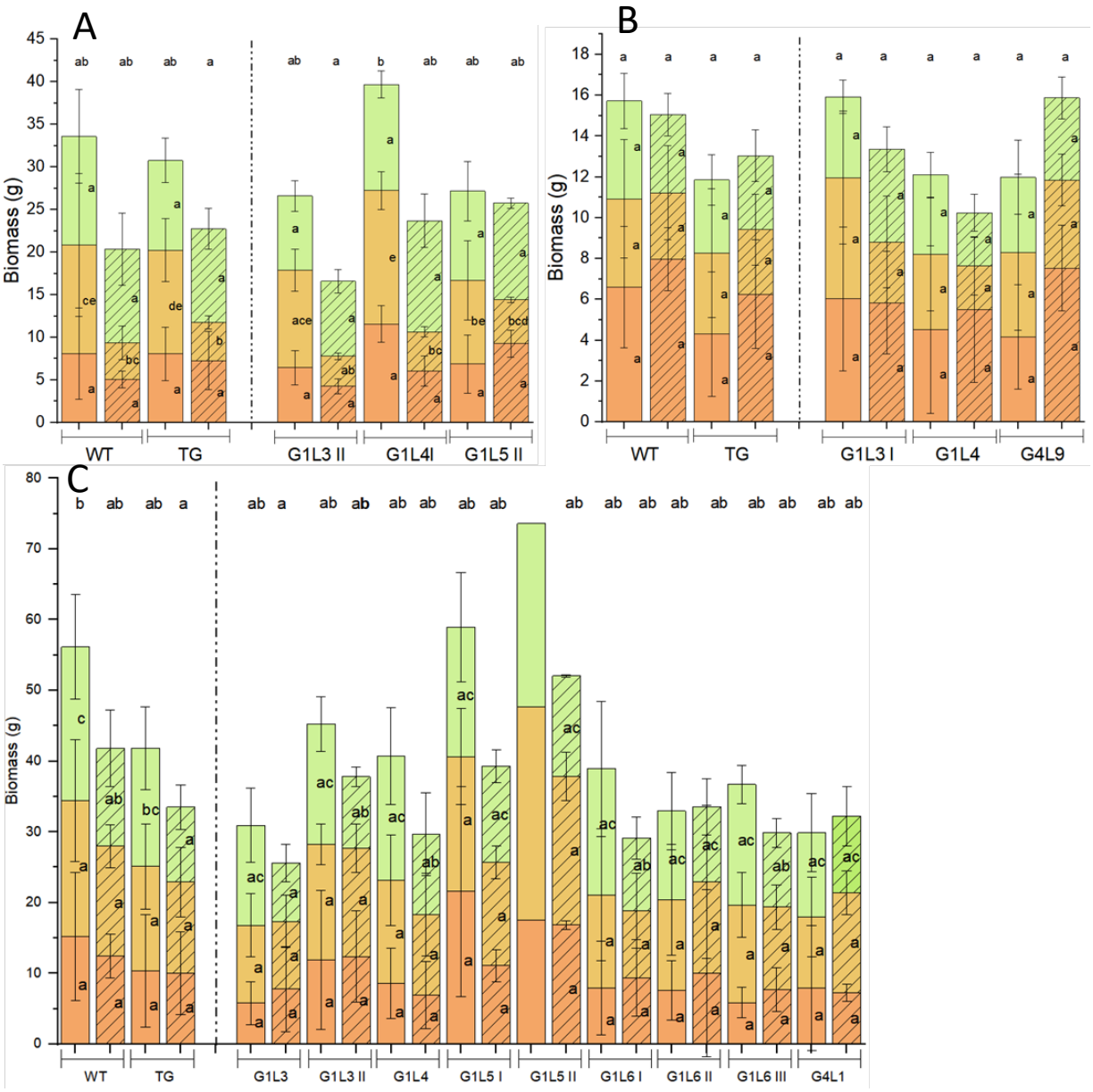

Figure 38: Dry mass of *ScWS*-OE lines and WT poplars. Dry mass of lines of experiment 1 (**A**), Exp.2 (**B**) and Exp.3 (**C**), stacking the masses of leaves (green), stem (light brown) and roots (brown). Each tissue was compared with each other, significant differences are indicated with different letters at $P \leq 0.05$ (ANOVA, Tukey). Representative lines are shown if $N \geq 2$. The TG group is the mean of all transgenic plants tested including representative lines. Drought treated plants are indicated with hatched bars. **A.:** Dry mass of lines from **Exp.1**. $N_{WT(w)} = 5$, $N_{WT(d)} = 3$, $N_{TG(w)} = 16$, $N_{TG(d)} = 10$, $N_{G1L3II\ (W)} = 5$, $N_{G1L3II\ (d)} = 3$, $N_{G1L4\ (W)} = 4$, $N_{G1L4\ (D)} = 3$, $N_{G1L5II\ (W)} = 5$, $N_{G1L5II\ (D)} = 3$. **B.:** Dry mass of lines from **Exp.3**. $N_{WT(w)} = 9$, $N_{WT(d)} = 8$, $N_{TG(w)} = 11$, $N_{TG(d)} = 14$, $N_{G1L3I\ (W)} = 3$, $N_{G1L3I\ (d)} = 4$, $N_{G1L4\ (W)} = 4$, $N_{G1L4\ (D)} = 5$, $N_{G4L9\ (W)} = 4$, $N_{G4L9\ (D)} = 4$. **C.:** Dry mass of lines from **Exp.2**. Line G1L5II control (n = 1) is shown for completion. $N_{WT(w)} = 15$, $N_{WT(d)} = 13$, $N_{TG(w)} = 48$, $N_{TG(d)} = 40$, $N_{G1L3\ (W)} = 5$, $N_{G1L3\ (d)} = 6$, $N_{G1L3II\ (W)} = 7$, $N_{G1L3II\ (d)} = 8$, $N_{G1L4\ (W)} = 8$, $N_{G1L4\ (D)} = 4$, $N_{G1L5I\ (W)} = 4$, $N_{G1L5I\ (D)} = 3$, $N_{G1L5II\ (W)} = 2$, $N_{G1L5II\ (D)} = 2$, $N_{G1L6I\ (W)} = 3$, $N_{G1L6I\ (d)} = 4$, $N_{G1L6II\ (W)} = 3$, $N_{G1L6II\ (d)} = 2$, $N_{G1L6III\ (W)} = 3$, $N_{G1L6III\ (d)} = 4$, $N_{G4L1\ (W)} = 7$, $N_{G4L1\ (d)} = 3$. Values are means ± SD.

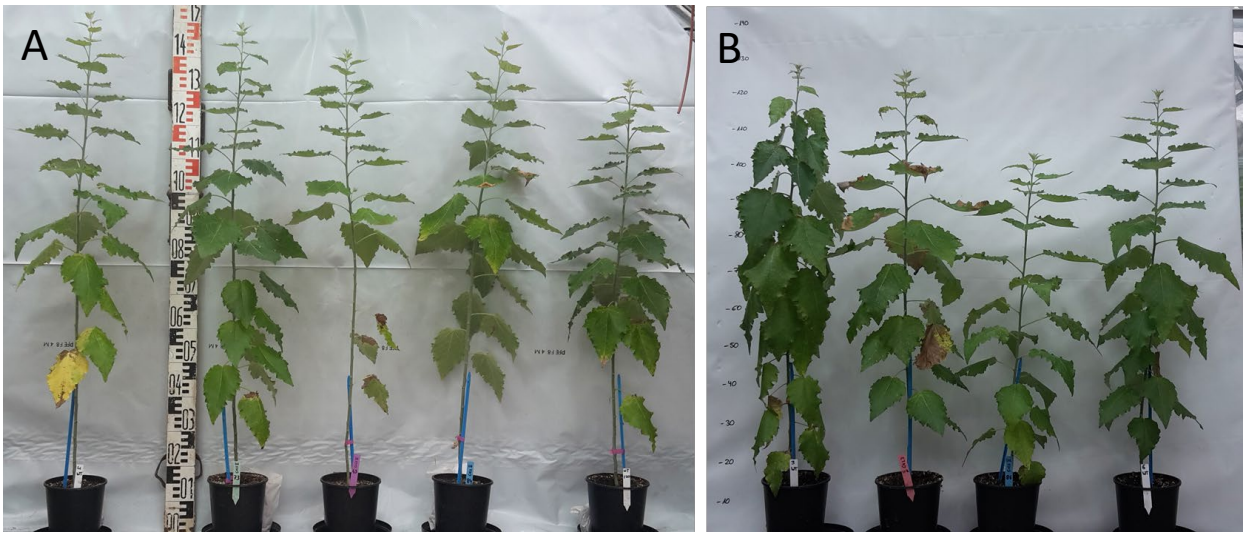

Figure 39: *ScWS*-OE and WT plants of Exp.2. A: Plants of Exp.2.1 (2.3.10) before harvest, after 23 d of mild drought stress. F.l.t.r.: WT, G1L5II, G1L3II, G1L6II, WT. **B:** Plants of Exp.2.2 before harvest. Plants of this group underwent 23 d of mild drought stress and additionally severe drought treatment of 12 d. F.l.t.r.: WT, G1L3II, G1L6II, WT.

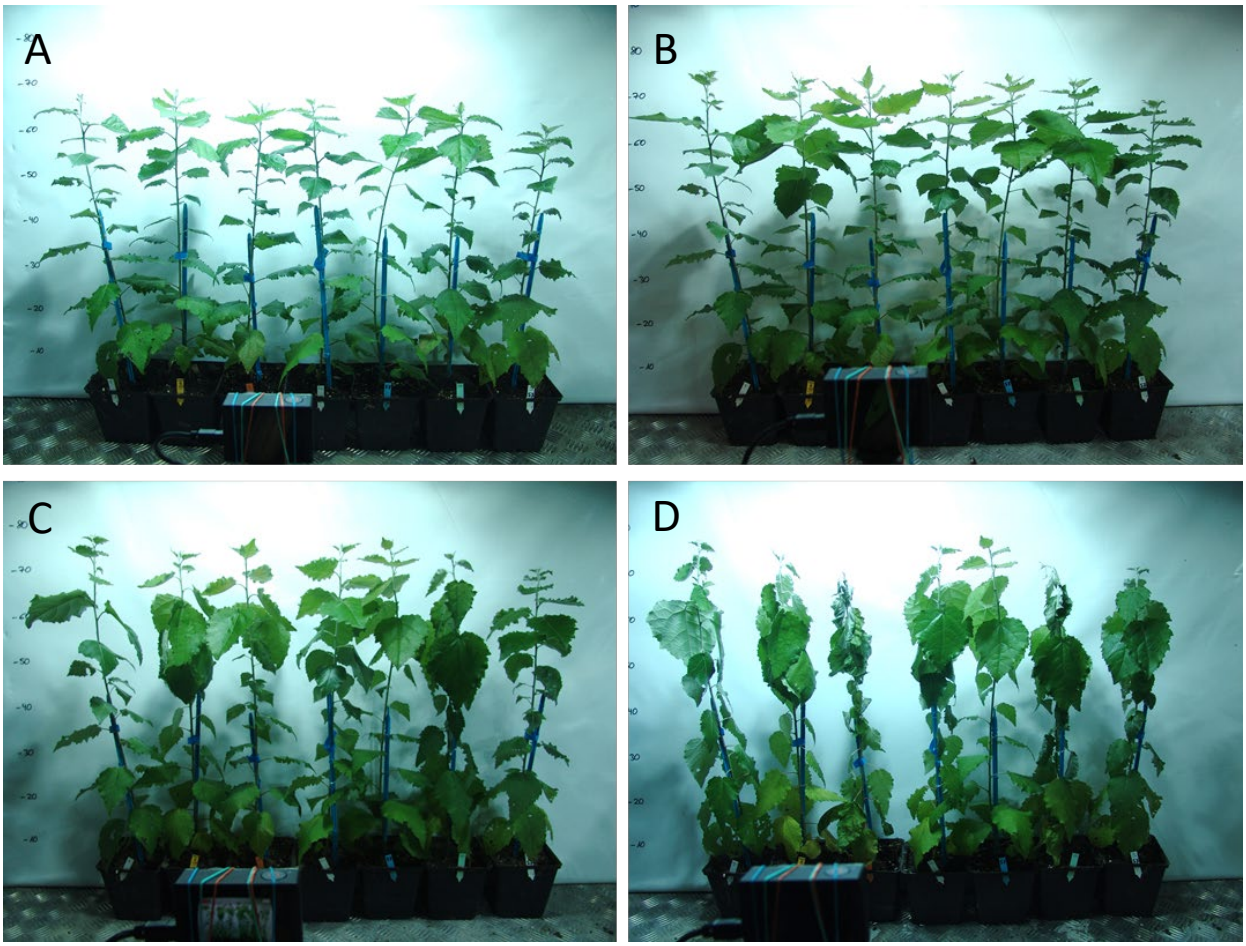

Figure 40: *ScWS*-OE plants and WT in Exp.3 during drought treatment. F.l.t.r.: WT, G4L9, G1L4, G1L5I, G1L6II, G1L5II, WT. **A.:** Start drought treatment. **B.:** Drought treatment, d 4. **C.:** Drought treatment, d 8. **D.:** Drought treatment, d 12.

3.2.1.3. *Stomatal conductance is affected in ScWS-OE lines in the light, but not in darkness*

Photosynthesis and stomatal conductance were measured (2.3.4) on watered plants. To maintain comparability, the seventh or eighth leaf counted from the top was taken for measurements. Photosynthesis measurements in all experiments were conducted with a light intensity of 800 µmol m^{-2} s^{-1}.

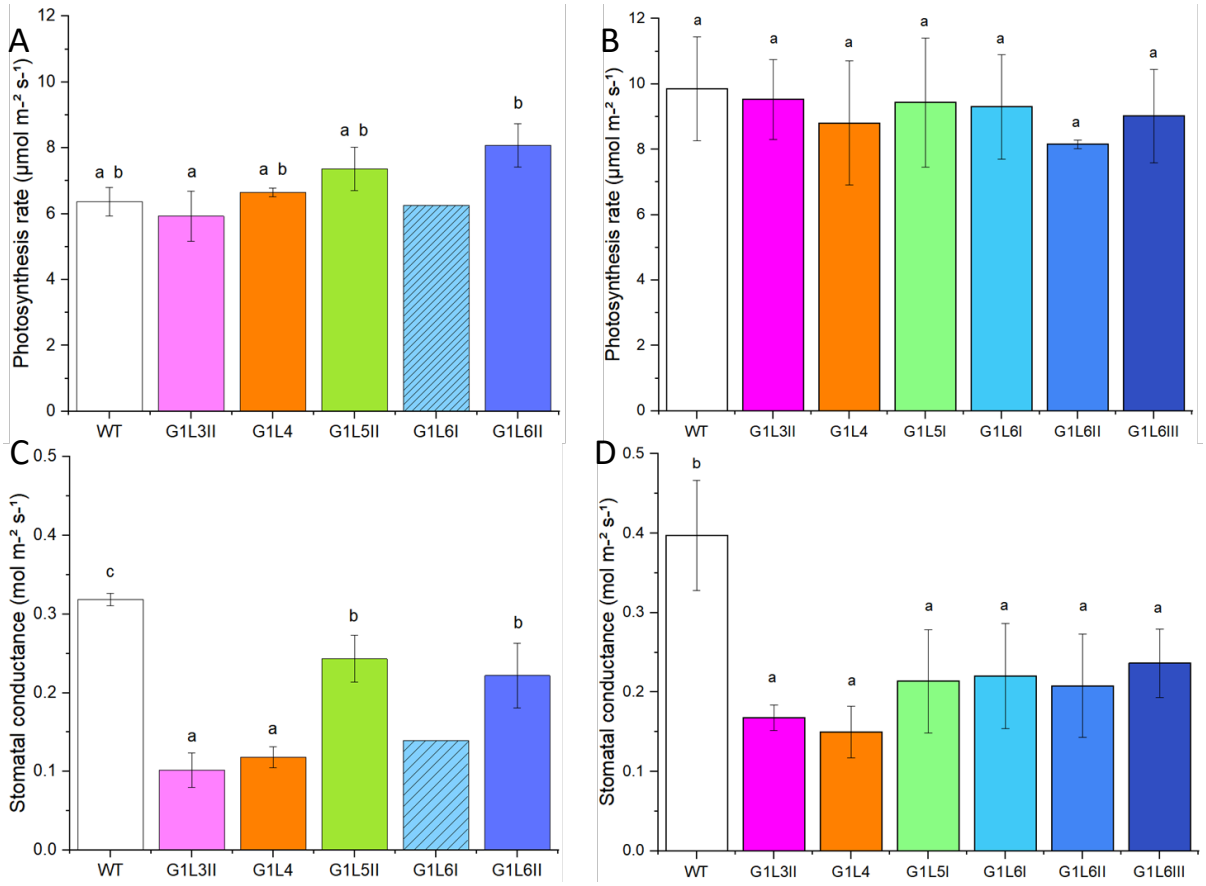

Figure 41: Comparison of photosynthesis (A, B) and stomatal conductance (C, D) of *ScWS*-OE plants and the WT in Exp.1 (A, C) and Exp.2 (B, D). Well-watered plants were measured. The photosynthesis rate (**A**, **B**) was not affected significantly compared to the WT (white bar). No standard deviation is shown for line G1L6I due to lack of plants. The stomatal conductance (**C**, **D**) was significantly decreased in all lines compared to the WT. Measuring conditions: T_{air} = 26.1 – 27.2 °C, RH_{air} = 62-59%, CO_{2air} = 301.5 – 311.8 µmol mol^{-1}. **A, C:** Plants of Exp.1, N_{WT} = 4, $N_{G1L4,\ G1L5\ II,\ G1L3II}$ = 4, N_{G1L6I} = 2, N_{G1L6II} = 1. **B, D:** Plants of Exp.2, N_{WT} = 16, N_{G1L3II} = 10, $N_{G1L4,\ G1L5\ I}$ = 6, N_{G1L6I} = 4, N_{G1L6II} = 2, $N_{G1L6III}$ = 3. Measuring conditions: T_{air} = 25.1-27.8°C, RH_{air} = 62-60%, $CO2_{air}$ = 383 – 393 µmol mol^{-1}. Plants were divided into two groups and grown in two different greenhouses. Different letters indicate significant differences among lines at P ≤ 0.05 (ANOVA). Values are means ± SD.

Photosynthesis measurements revealed no differences of *ScWS*-OE plants compared to the WT in short term Exp.1 (Figure 41 A) and long-term Exp.2 (Figure 41 B). The stomatal conductance of *ScWS*-OE plants were significantly decreased in all lines and experiments when compared to the WT (Figure 41 C, D), but differences among the lines were observed: the lines G1L5II and G1L6II demonstrated significant lower stomatal conductance compared to the WT but significant higher stomatal conductance than the lines G1L3II and G1L4 in Exp.1 (Figure 41 C). In long-term experiment 2, the lines

G1L5II and G1L6II were not significantly different to the other lines, but a similar pattern tendency for higher stomatal conductance levels was observed (Figure 42).

The water use efficiency (instantaneous) of watered plants of Exp.1 was not affected significantly (Figure 42 D), but demonstrated a tendency for higher levels of TG plants. In darkness, the stomatal conductance was not different compared to the WT (Figure 43 B). The respiratory quotient of transgenic plants (Figure 43 A) did not differ significantly from the WT, but small differences among the lines were observed (Figure 43 A).

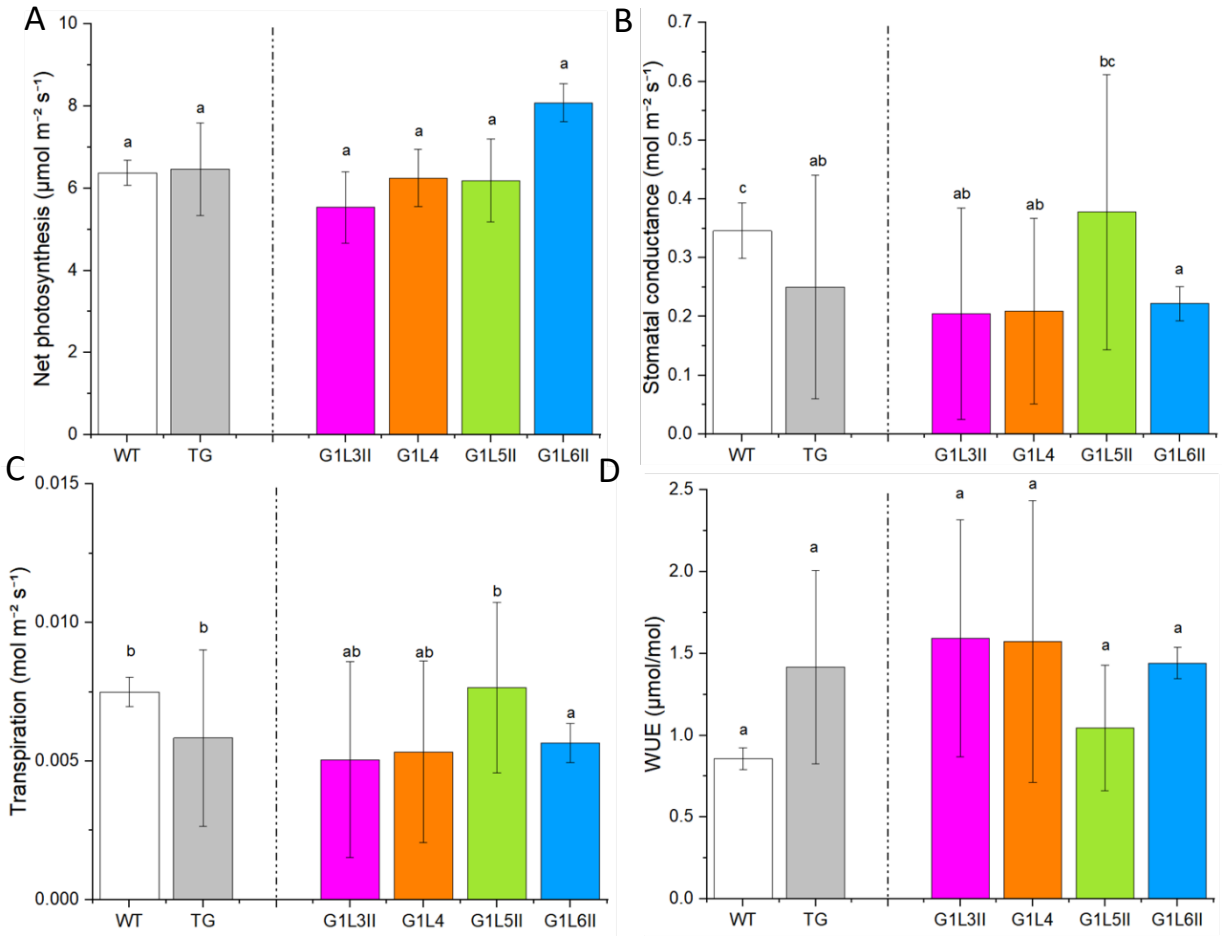

Figure 42: Photosynthesis measurement of watered *ScWS*-OE and WT plants in Exp.1. The TG group indicated in grey is the mean of all transgenic plants tested, including the represented lines. **A.:** Net photosynthesis, **B.:** stomatal conductance, **C.:** transpiration and **D.:** water use efficiency (instantaneous). $N_{WT} = 4$, $N_{G1L4,\ G1L5\ II,\ G1L3II} = 4$, $N_{G1L6I} = 2$. Measuring conditions: $T_{air} = 26.1 – 27.2$ °C, $RH_{air} = 62\text{-}59\%$, $CO_{2air} = 301.5 – 311.8$ µmol mol^{-1}. Different letters indicate significant differences among lines at $P \leq 0.05$ (ANOVA). Values are means ± SD.

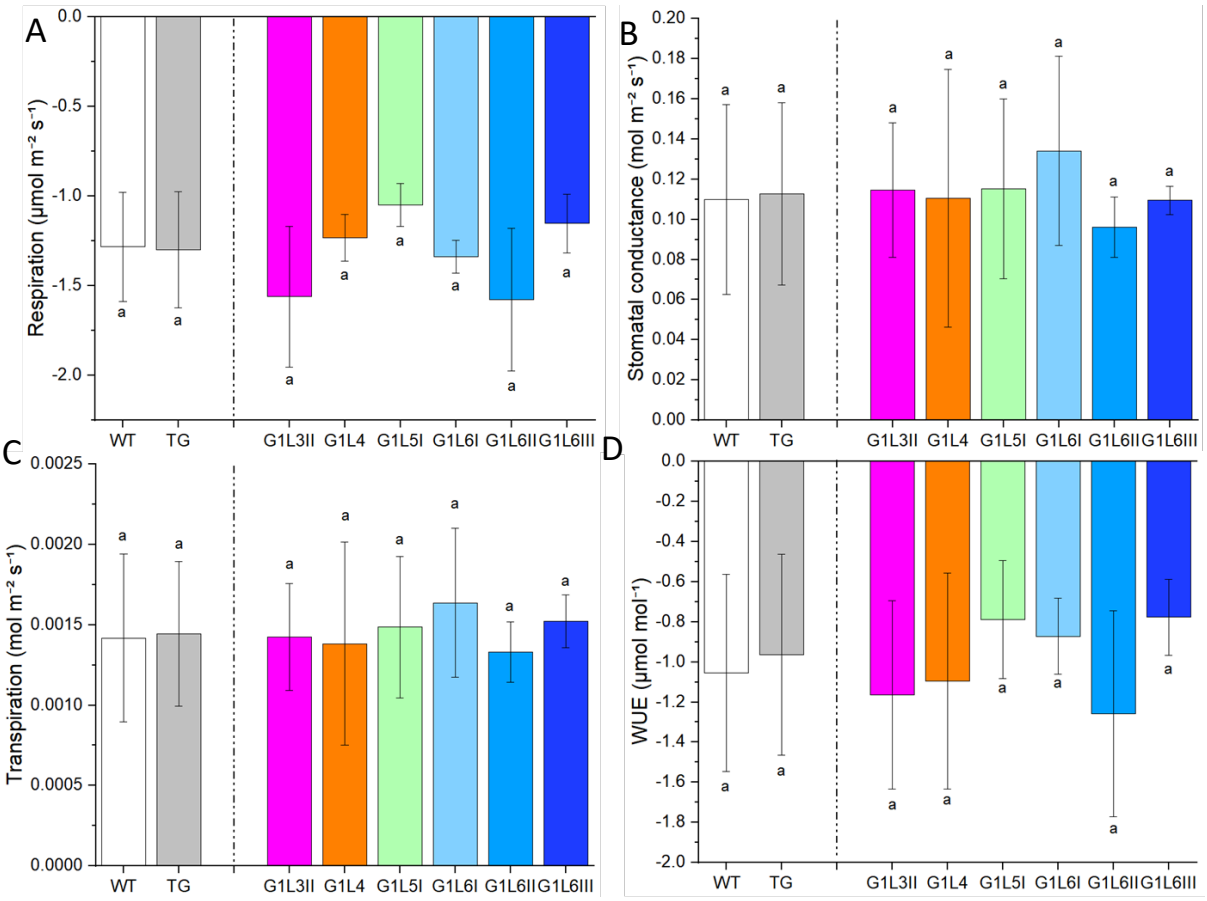

Figure 43: Gas exchange of watered *ScWS*-OE and WT plants of Exp.2 in darkness. The TG group indicated in grey is the mean of all transgenic plants tested. **A.:** Respiration, **B.:** stomatal conductance, **C.:** transpiration and **D.:** water use efficiency (instantaneous). N_{WT} = 13, N_{TG} = 24, N_{G1L3II} = 5, N_{G1L4} = 6, N_{G1L5I} = 6, N_{G1L6I} = 2, N_{G1L6II} = 3, $N_{G1L6III}$ = 2. Measurement parameters: T_{air} = 25.4 – 26.7 °C, RH_{air} = 61-58%, $CO2_{air}$ = 400.05 – 421.5 µmol mol^{-1}. Different letters indicate significant differences among lines at P ≤ 0.05 (ANOVA). Values are means ± SD.

3.2.1.4. *Smaller stomata in ScWS-OE plants*

To examine the reason for decreased stomatal conductance, stomata were inspected under a light microscope (2.3.6.3). In transgenic plants, the stomatal length was significantly smaller than that of the WT (Figure 44 A). The frequency of the stomata was not affected (Figure 44 B). Stomata of *ScWS*-OE plants seemed to accumulate more lipid-like compounds as determined by Sudan III staining (Figure 45 F). Scanning electron microscopy did not reveal significant differences in the morphology of the stomata of TG (Figure 46 D, E, F) and WT (Figure 46 A, B, C) plants. However, the surface of transgenic plants appears more smoothly (Figure 46 H) compared to the WT (Figure 46 G).

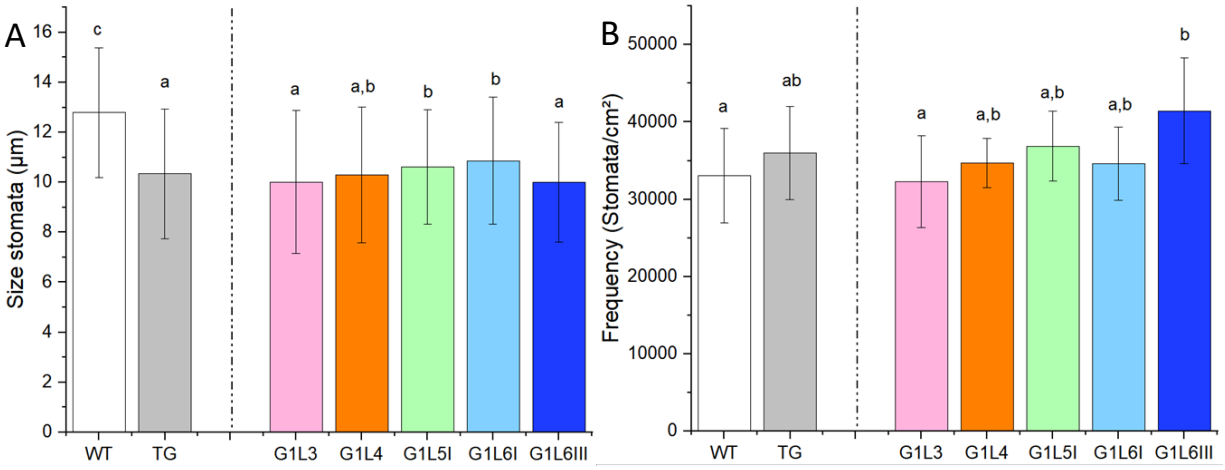

Figure 44: Size of stomata (A) and frequency (B) of *ScWS*-OE and WT poplar plants. The TG group indicated in grey is the mean of all transgenic lines tested. $N_{WT} = 4$, $N_{TG} = 13$, $N_{G1L3} = 3$, $N_{G1L4} = 3$, $N_{G1L5I} = 4$, $N_{G1L6I} = 2$, $N_{G1L6III} = 2$. Different letters indicate significant differences among lines at $P \leq 0.05$ (ANOVA). Values are means ± SD.

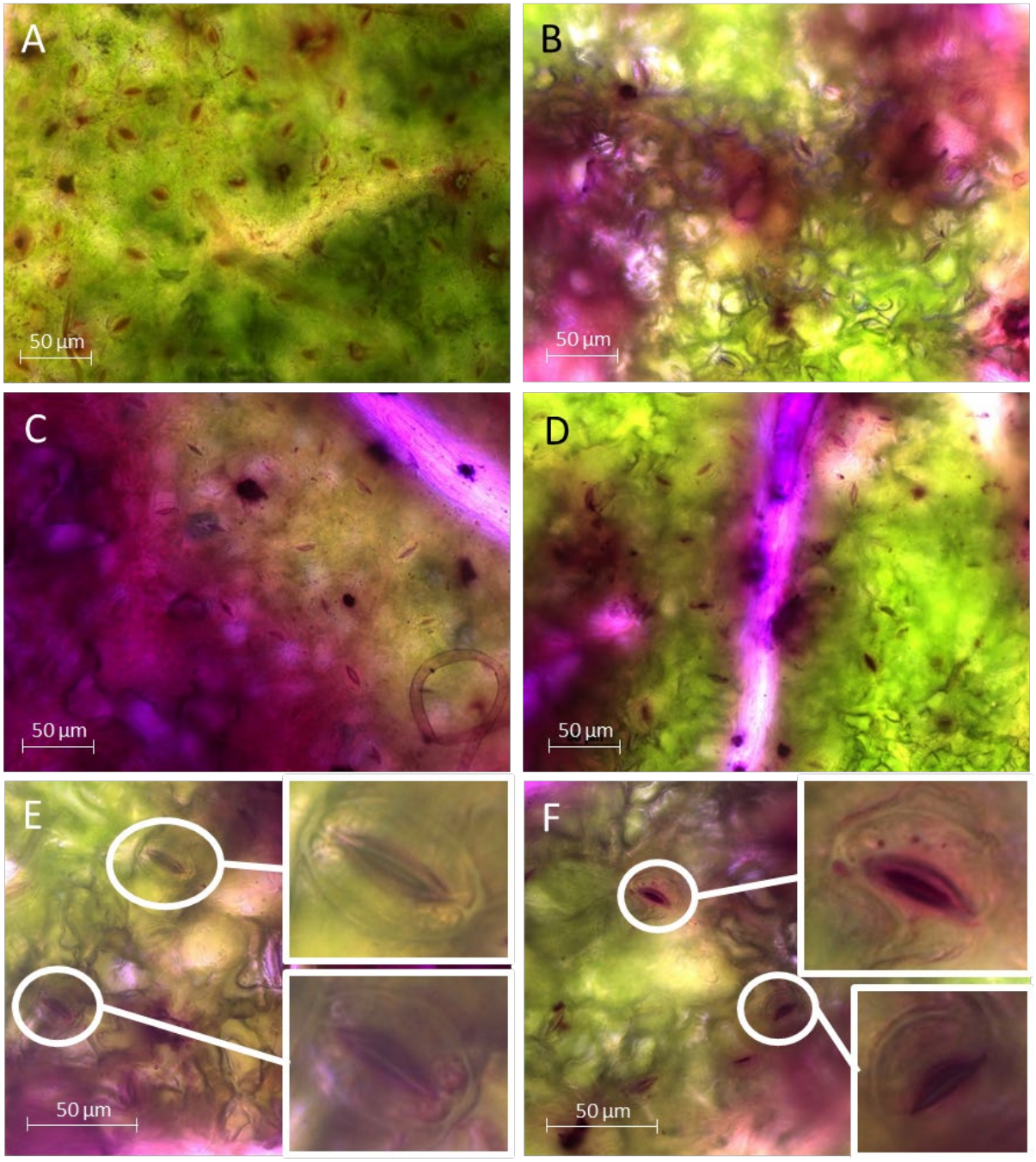

Figure 45: Representative figure of stomata size, frequency and lipid distribution of WT and *35S::ScWS* poplar leaves observed under a light microscope. Stomata were stained with Sudan III. **A, B.:** WT poplar, 400X. **C, D.:** Transgenic poplar overexpressing *ScWS* (line G1L4), 400X. **E.:** WT poplar, 630X**. F.:** Transgenic poplar overexpressing *ScWS*, 630X**.**

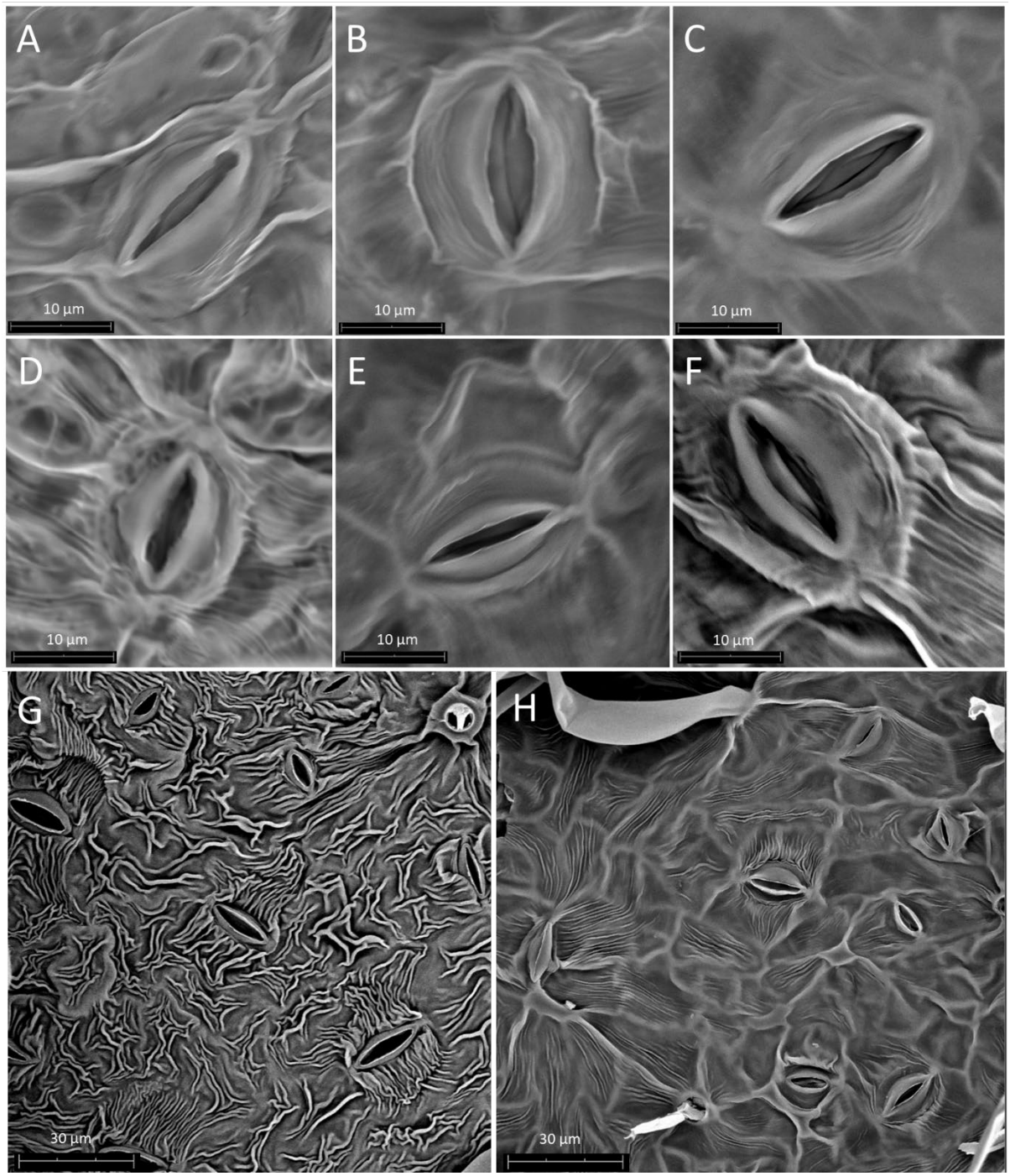

Figure 46: Representative figures of stomatal morphology of WT and *35S::ScWS* plants. REM microscopy of stomata. **A, B, C.:** WT plants, 8000X. **D, E, F.:** Transgenic plants overexpressing *ScWS*, 8000X**. G.:** Leaf surface of a WT plant, 2000X. **H.:** Leaf surface of a TG plant (G1L3), 2000X. Figures courtesy of Dr. U. Lipka and F. Häffner.

3.2.1.5. *Composition of leaf and stem surface of ScWS-*OE *plants are affected*

The impact of overexpressed *ScWS* on the composition of lipid-derived hydrocarbons on the plant's surface was investigated. Therefore, surface extractions of non-stressed plants were examined by GC-MS.

Alkanes with a carbon chain length of 25 to 29 were significantly lower on leaves and on stems of TG plants compared to the WT. Alkanes with a chain length of 27 significantly decreased by approximately 40 % on leaves. Alkanes with a chain longer than 31 carbons were neither affected on leaf nor on the stem surface by overexpression of the *ScWS*. Fatty acids with a carbon chain length of 24 and 26 were found on leaf surface to be significantly decreased but not on the stem surface.

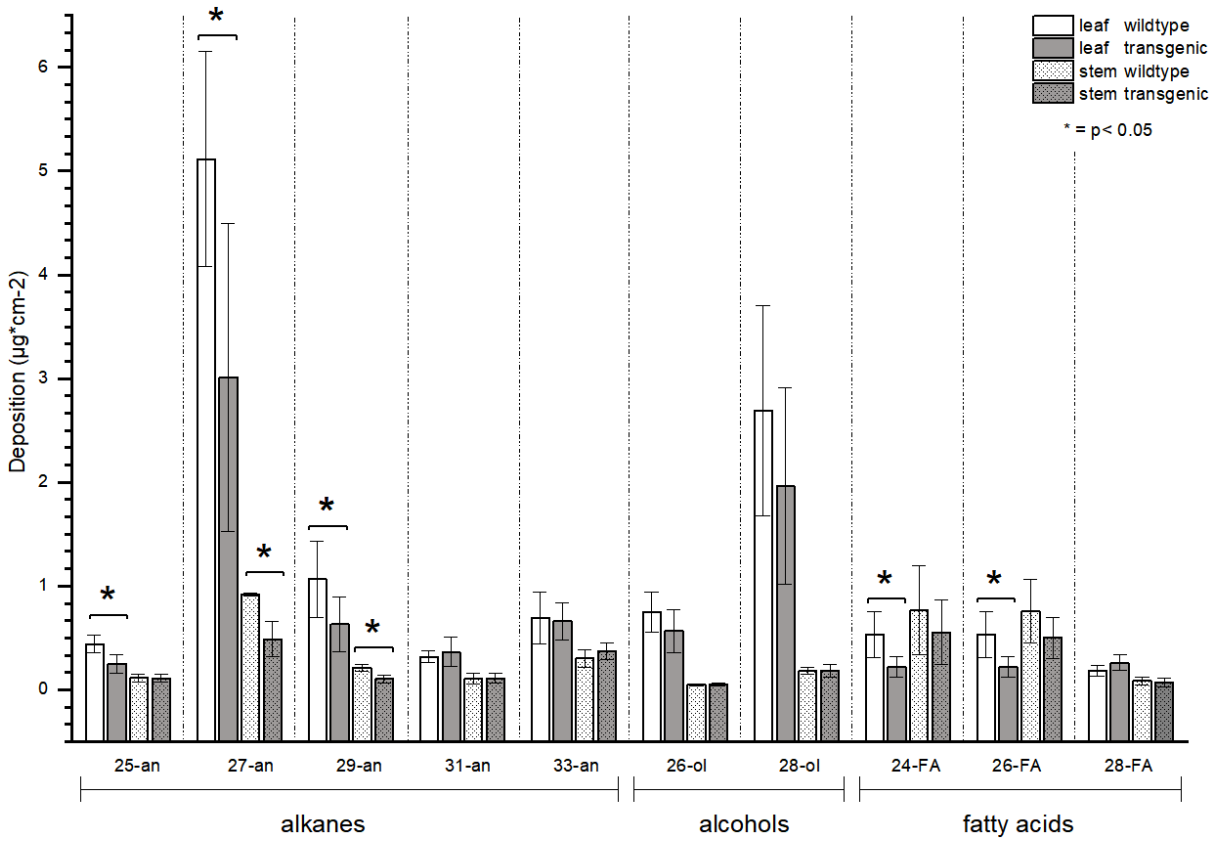

Figure 47: Amount of wax ester precursors on leaf and stem cuticula (µg cm^{-2}). Alkanes, alcohols and fatty acids of different carbon chain length of leaf and stem surfaces (dotted bars) were quantified via GC-MS. Significant differences ($p<0.05$) compared to WT are highlighted with an asterisk. Plants of the lines G1L3, G1L4, G1L6II and G1L6III were pooled in the transgenic group. $N_{WT} = 4$, $N_{TG} = 10$. Values are means ± SD.

3.2.2. Characterisation of *DX15::ScWS* and *DX15::AtDGAT1*: Wood specific expression

Since *ScWS* and *AtDGAT1* could be transformed successfully under the DX15 promoter, plants were multiplied and grown in a greenhouse to investigate the phenotypes under non-stress conditions (Exp. 4, Table 23).

3.2.2.1. *Preparation of pK7WG-DX15*

For wood-specific expression, the promoter of the Fasciclin-like AGP8 was chosen. This promoter, further referred to as DX15 (Figure 69), was demonstrated to have high levels of expression in mature and developing xylem (Ko et al. 2012). A nucleotide BLAST of the published DX15 sequence (Ko et al. 2012) showed 99.1% similarity to Potri.009G012200 of *P. trichocarpa* (www.Popgenie.org).

Three individual *P. trichocarpa* plants were used to amplify the region identified as DX15 promoter. After ligation into the pK7WG binary construct, the three constructs were sequenced to test the correct insertion.

3.2.2.2. *Missing repetitive element*

A missing motive compared to the published sequence of Ko *et al.* (2012) and the sequence of Potri.009G012200 was found in all constructs cloned. Three individual poplar plants were utilized for promoter cloning. At position 733, the motive (3'-TTGATAG-5') was found repeated four times up to position 762 in the published sequence. The sequenced constructs revealed one missing motive, resulting in three repeats instead of four (Figure 48). Construct 74 II was poorly sequenced and thus not further investigated, but the missing motive was confirmed as well. Construct 74 III was used for all further cloning and transformation steps into poplar plants (Figure 70).

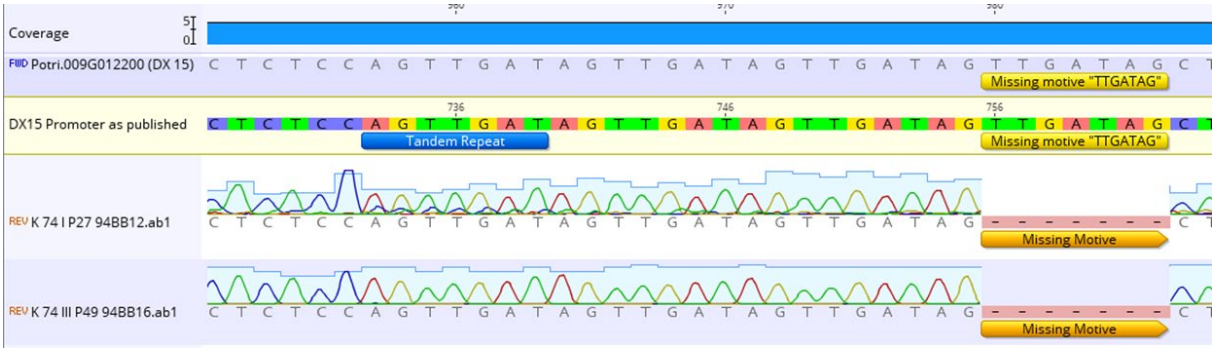

Figure 48: Missing motive "TTGATAG" in the DX15 promoter cloned in this study. Sequencing results of K74 I and in K74 III. The promoter was inserted in the pK7WG binary vector system. Three constructs are showing a missing repetitive element compared to the published sequence and Potri.009G012200 as indicated. Due to poor sequencing results, construct 74 II (not shown in figure) was not used for further steps.

3.2.2.3. *Gene expression by the DX15 promoter*

Since *AtDGAT1* and *ScWS* were positively transformed utilizing the DX15 promoter, the expression and the tissue–specificity were tested by qRT PCR for both genes with the plants from Exp. 4 (2.3.12). When expressed under the DX15 promoter, high expression levels of *AtDGAT1* (Figure 49 A) and *ScWS* (Figure 49 B) were found in DX. No expression of *AtDGAT1* was found in the WT (Figure 49 A, C), but a basal expression of *WS* was found in all tissues of WT plants, measured with the *ScWS* primer (Figure 49 B, D), despite a high primer specificity of the primers that have been used (Table 17). Both genes, *AtDGAT1* (Figure 49 C) and *ScWS* (Figure 49 D) were drastically overexpressed in DX, but basal expression was observed in leaf (L) and bark (B) tissue (Figure 49 C, D).

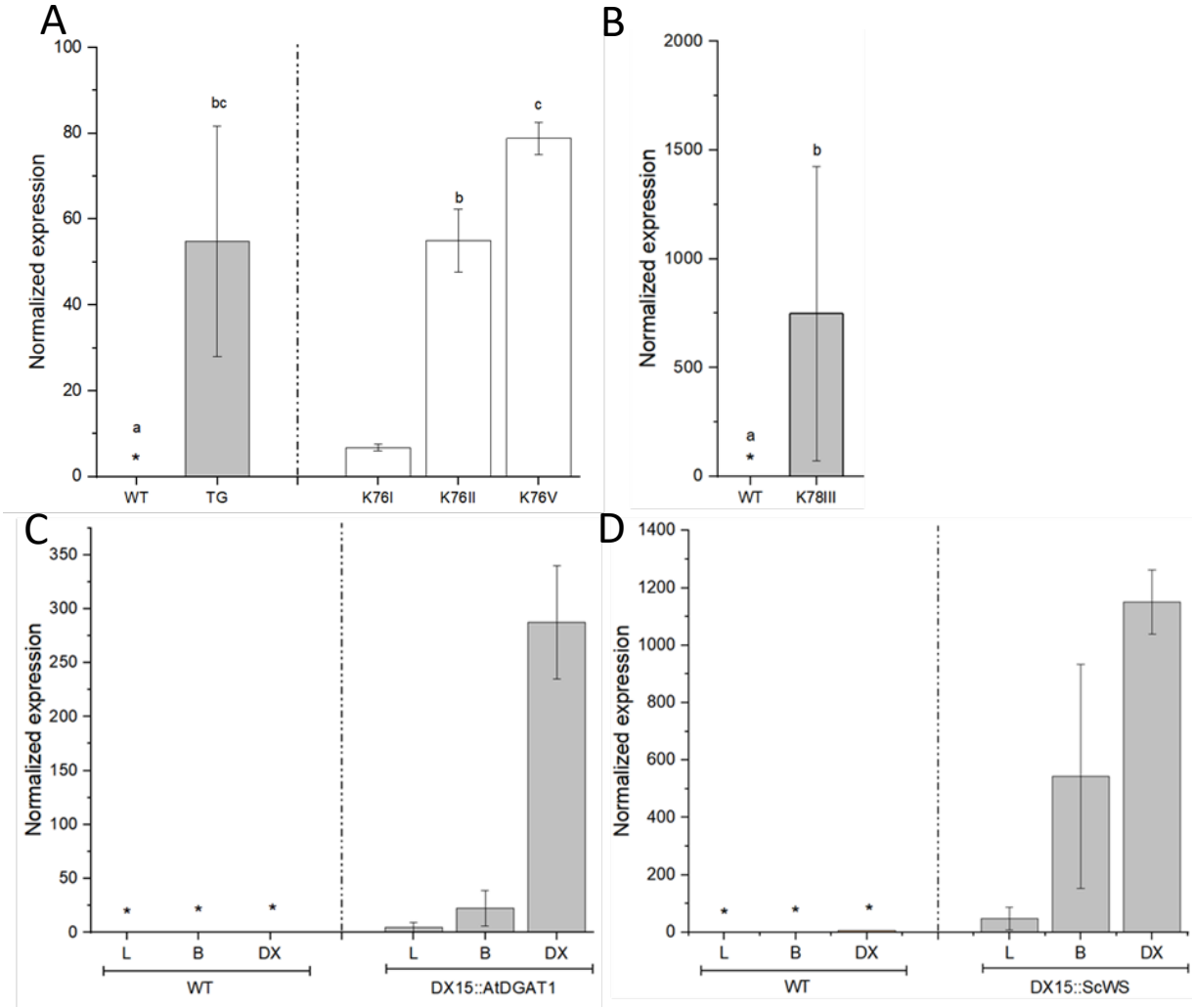

Figure 49: Gene expression of transformed plants with DX15 promoter. A.: Expression of *AtDGAT1* in developing xylem. No expression of *AtDGAT1* was found in WT. Expression was normalized to expression level of Potri.015G001600 (*Cref1*). N_{WT} = 3, N_{TG} = 5, N_{K76I} = 1, N_{K76II} = 2, N_{K76III} = 2. **B.:** Normalized expression of *ScWS* in developing xylem. Expression of *ScWS* was normalized to WT expression levels (0.53 ± 0.36), indicated with an asterisk. N_{WT} = 3, N_{K78III} = 3. **C.:** Normalized expression of *AtDGAT1* in leaf, bark and developing xylem. No expression of *AtDGAT1* was found in all tissues of WT as indicated with an asterisk. Expression was normalized to leaf expression level (Mean 0.16 ± 0.08) of transgenic plants. N_{WT} = 3, $N_{DX15::AtDGAT1}$ = 3, pooled from line K76I, K76II and K76V. **D.:** Normalized expression of *ScWS* in leaf, bark and developing xylem. Expression was normalized to leaf expression level (Mean 0.037 ± 0.005) of wildtype plants. N_{WT} = 2, $N_{DX15::ScWS}$ = 2, line K78III. Different letters indicate significant differences among lines at $P \leq 0.05$ (ANOVA). Values are means ± SD.

3.2.2.4. *Wood anatomy of DX15::AtDGAT1*

Since the DX15 promoter caused enhanced expression of the *AtDGAT1* in developing xylem, but not in bark and leaf tissue, the wood anatomy of poplar plants (2.3.12) was examined. For a schematic picture of cross sections of poplar wood, see Figure 17. To identify changes in wood anatomy, FCA-staining was used on cross-sections to subdivide lignified- (reddish appearance) and non-lignified (blue) sections. No significant differences in the size of lignified area close to the DX (Figure 50) was found.

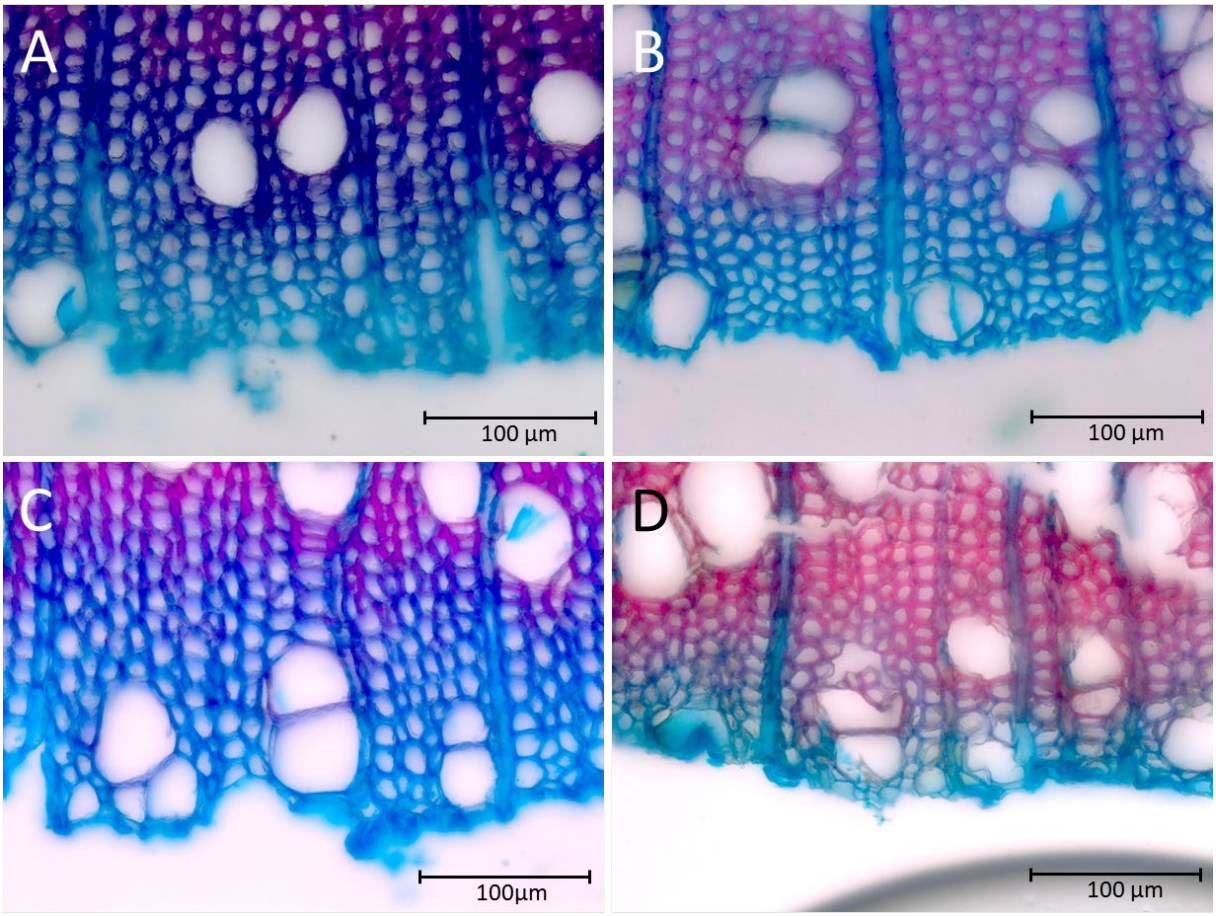

Figure 50: Cross sections in the DX **area and mature wood of WT and *DX15::AtDGAT1* poplar plants, stained with FCA. A.:** WT, plant 38. **B.:** WT, plant 47. **C.:** Line K76II, plant 33. **D.:** Line K76V, plant 39.

To investigate whether lipids were detected in wood of *DX15::AtDGAT1* plants, Nile red staining was used on cross sections (Figure 51). In the xylem, lipid droplets were exclusively found in the ray cells, but not in vessels and DX area of both WT and transgenic plants (Figure 51). Because of poor heterogeneity of the stained samples, no conclusion about the size and quantity of lipid droplets in ray cells could be drawn.

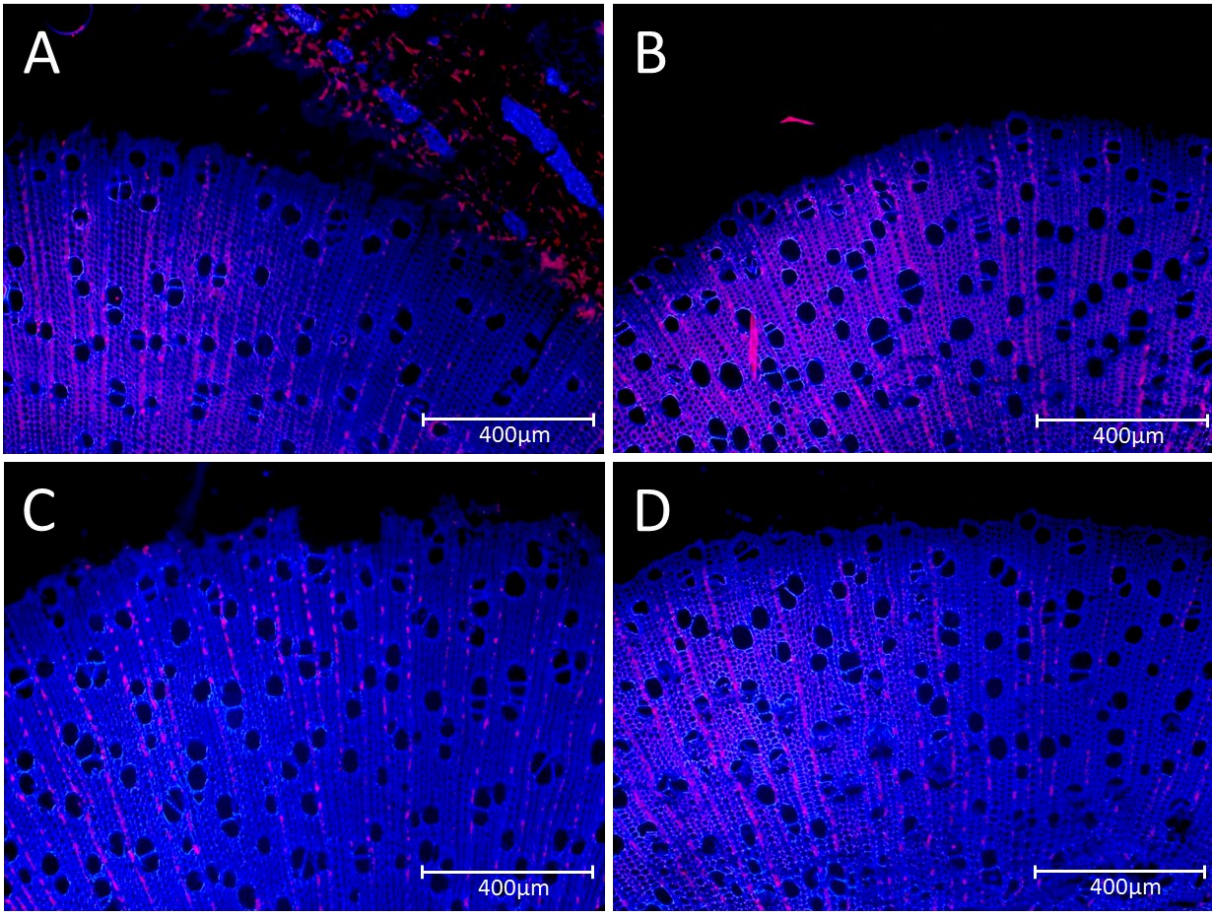

Figure 51: Cross sections of in wood of WT and *DX15::AtDGAT1* poplar plants, stained with Nile red. Lipids were found in ray cells (reddish colour). **A.:** WT, plant 38. **B.:** WT, plant 47. **C.:** Line K76II, plant 33. **D.:** Line K76V, plant 39.

3.2.2.5. *Swelling of wood of DX15::AtDGAT1 poplar plants*

Lipids in wood influence the water balance under drought (Schneider et al., 1999) by covering the inner walls of xylem vessels. Since Nile red staining did not permit conclusions on lipid distribution, the water uptake of dried wood was tested as described in material and methods (2.3.7). The transgenic lines showed a trend towards lower swelling but only line K76I was significantly different from the WT Figure 51.

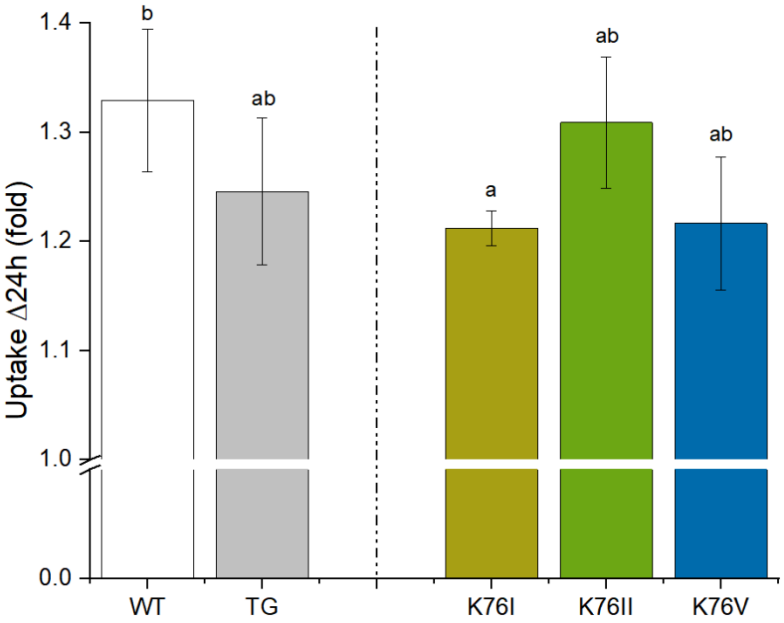

Figure 52: Relative water uptake of poplar wood of WT and *DX15::AtDGAT1* plants in 24 h. The TG group indicated in grey is the mean of all transgenic lines tested. $N_{WT} = 9$, $N_{TG} = 9$, $N_{K76I} = 3$, $N_{K76II} = 3$, $N_{K76V} = 3$. Different letters indicate significant differences among lines at $P \leq 0.05$ (ANOVA). Values are means ± SD.

3.2.2.6. *Wood anatomy of DX15::ScWS*

To identify changes in wood anatomy, FCA-staining was used on cross-sections to subdivide lignified- (reddish appearance) and non-lignified (blue) sections. No significant differences in the size of lignified area close to the DX (Figure 53) was found.

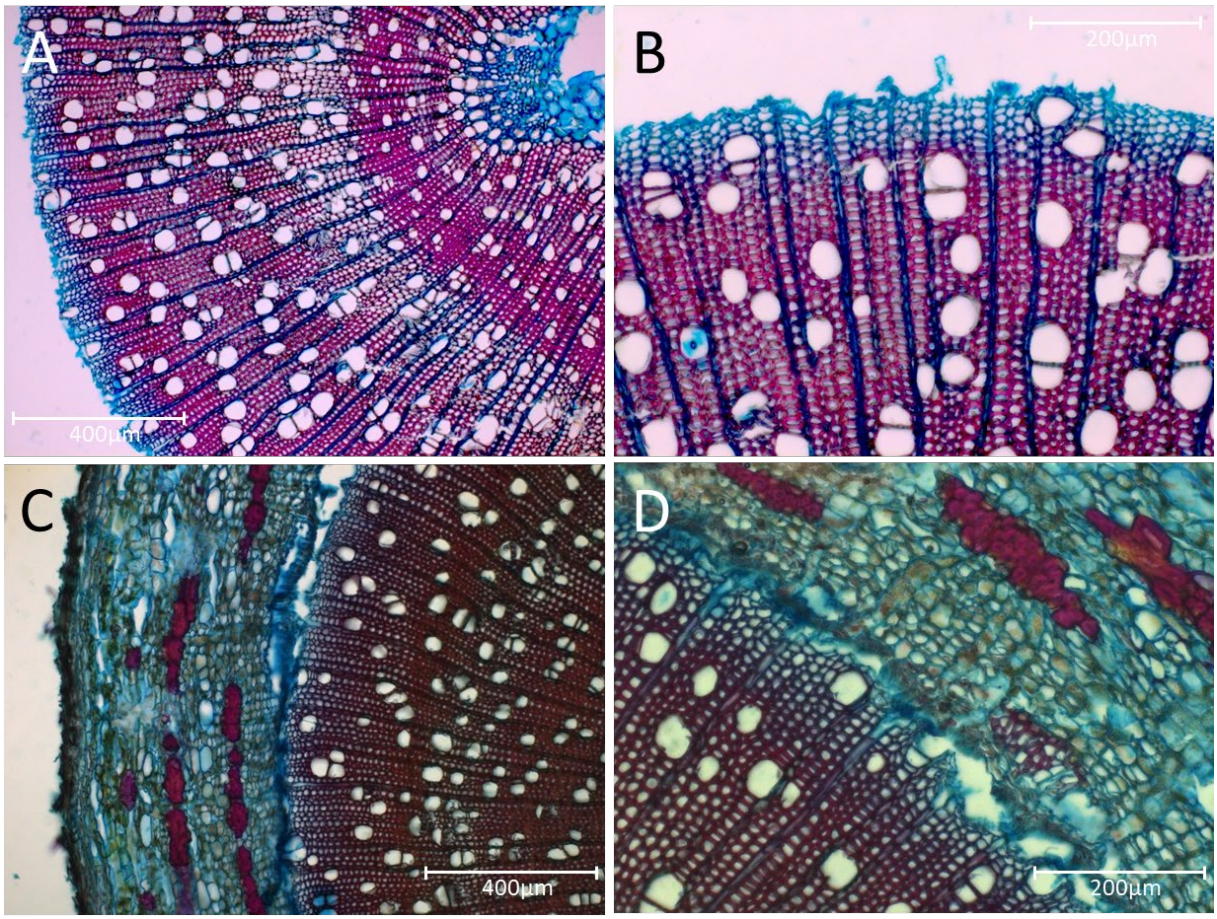

Figure 53: Cross sections of poplar stems with the DX **area in wood of WT and *DX15::ScWS* plants, stained with FCA. A**.: WT, plant 38. **B.:** WT, plant 47. **C.:** Line K78III, plant 33. **D.:** Line K78III, plant 39.

To identify lipids in wood of *DX15::ScWS* and the WT plants, Nile red was used on cross sections (Figure 54). In the xylem, lipid droplets were exclusively found in the ray cells of the stem, but not in vessels and DX area of WT and transgenic plants. The bark also showed staining. No differences between size or quantity of lipid droplets in ray cells of the transgenic compared with the WT plants were found.

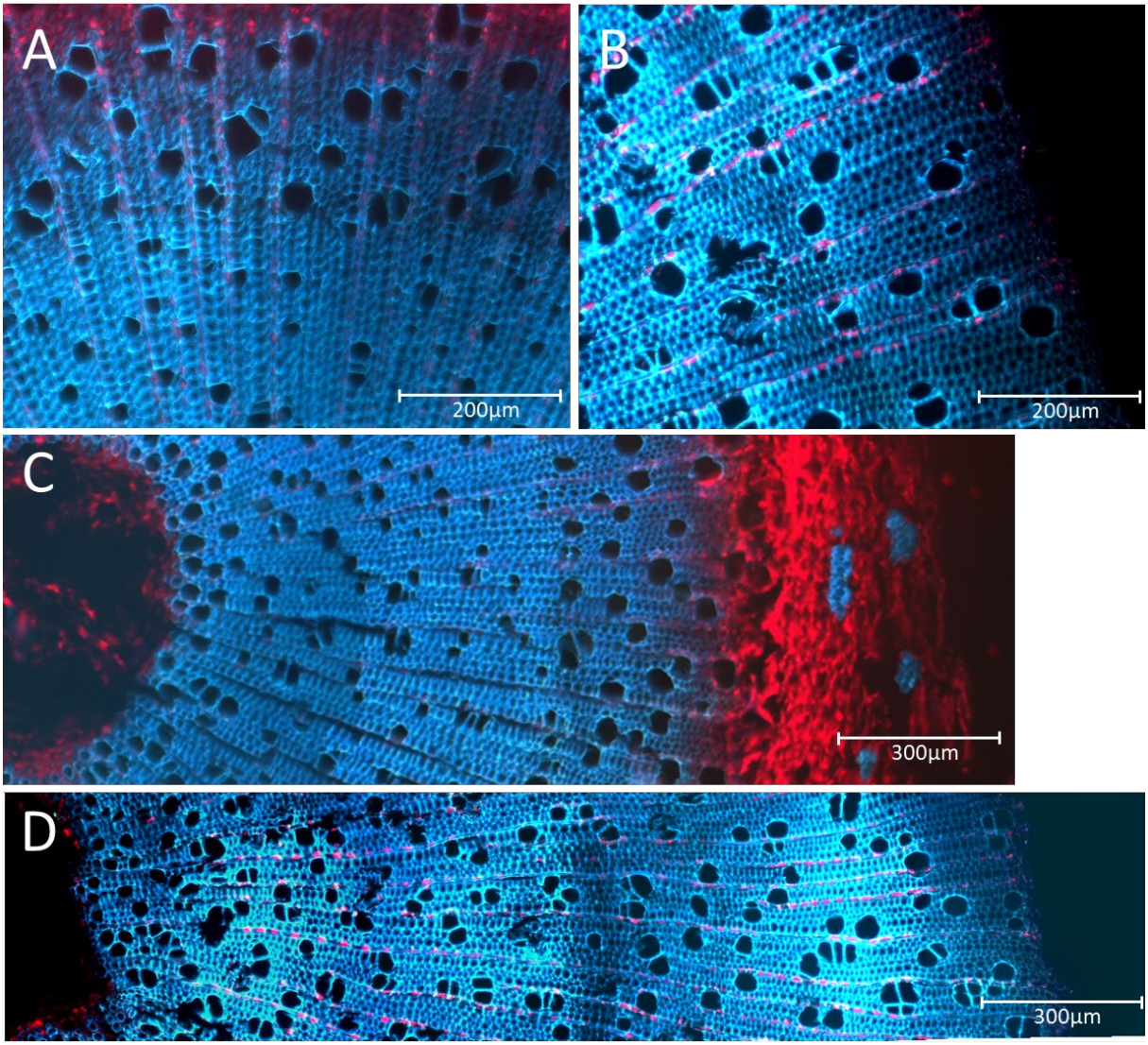

Figure 54: Cross sections of stems of WT and *DX15::ScWS* poplar plants, stained with Nile red. Lipid accumulation was found in ray cells (reddish colour). **A**.: WT, plant 35. **B.:** Line K78III, plant 33. **C.:** Complete cross section from pith to bark of WT, plant 35. **D.:** Cross section from pith (left) to DX (right) of line K78III, plant 33.

3.2.2.7. *Swelling of wood: DX15::ScWS*

Since Nile red staining did not permit conclusions on lipid distribution in *DX15::ScWS* plants, the water uptake of dried wood was tested as described in material and methods (2.3.7). The water uptake of *DX15::ScWS* plants (line K78III) were significantly lower than that of the WT (Figure 55).

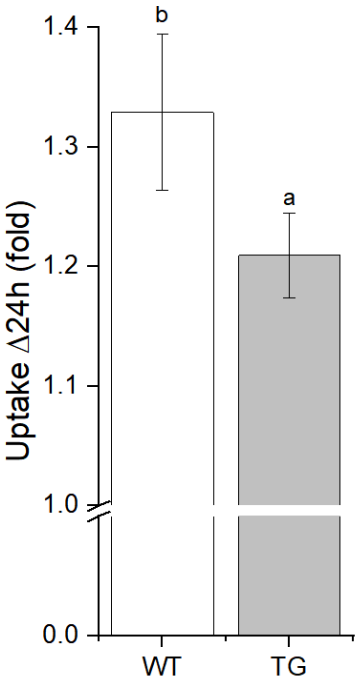

Figure 55: Relative water uptake of poplar wood of *DX15::ScWS* and WT plants in 24 h. The TG group indicated in grey shows the line K78III. $N_{WT} = 9$, $N_{TG} = 7$. Different letters indicate significant differences among lines at $P \leq 0.05$ (ANOVA). Values are means ± SD.

3.3. Drought performance of *ScWS*–OE *P.* x *canescens*

Since the *ScWS* was transformed successfully under 35S promoter into poplar, yield in several different lines and since we demonstrated a significant reduction in stomatal conductance, the plants were investigated in three drought experiments with different experimental designs as explained in material and methods 2.3.9 (Exp.1), 2.3.10 (Exp.2) and 2.3.11 (Exp.3).

3.3.1. Viability under severe drought stress is improved in *ScWS*-OE lines

Since the stomatal conductance was affected in *ScWS*-OE lines, a drought stress experiment (Exp.1) was conducted to examine the plant responses undergoing water shortage. In this experiment, plants did not receive any water at T_0. Soil moisture was controlled daily. WT plants were demonstrated to show symptoms of drought stress (leaves going limp) up to 24 h earlier than the *ScWS*-OE lines (Figure 56 A, B). The soil moisture of WT plants decreased faster in comparison to the *ScWS*-OE plants (Figure 56 C).

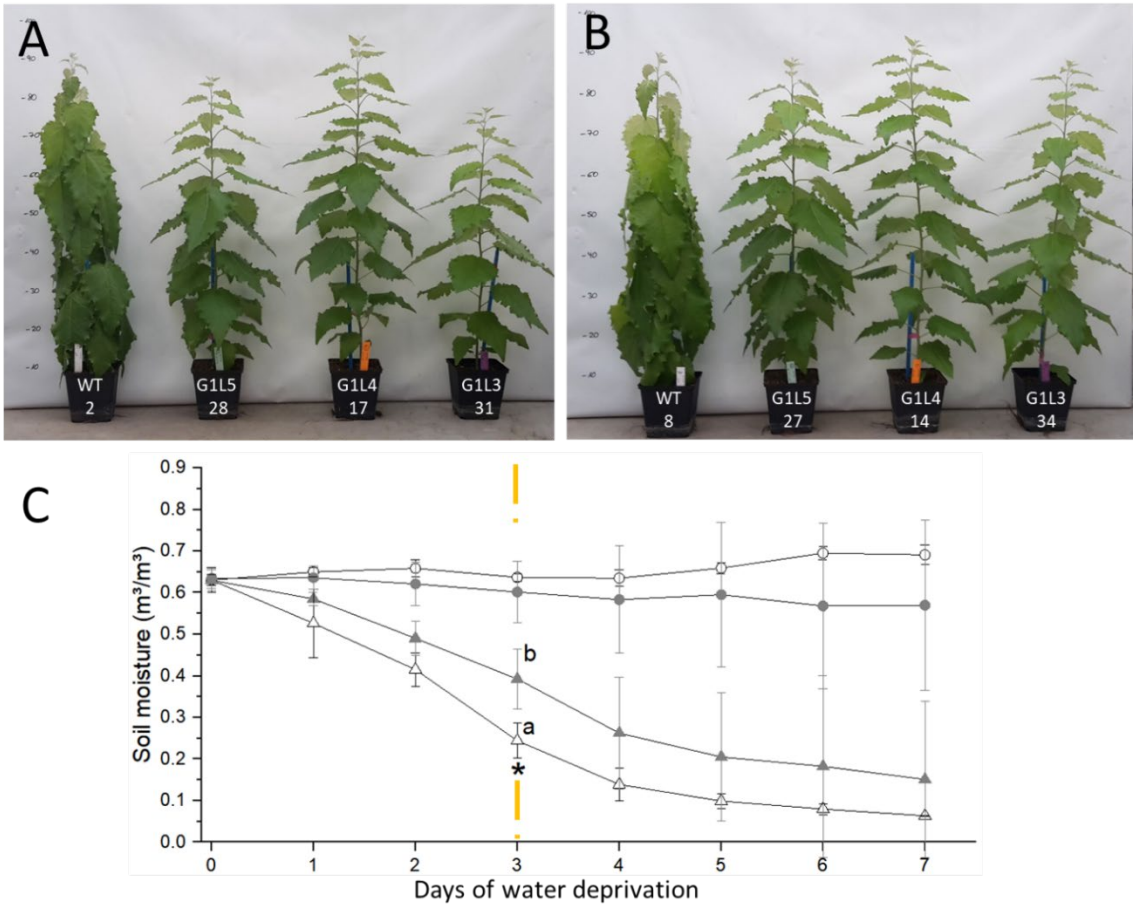

Figure 56: Response of *35S::ScWS* and WT poplar plants to severe drought stress. A. and **B.:** In two different plant groups of same height and appearance, the WT control demonstrated drought stress at TP = 3. **C.:** Soil moisture during the drought treatment. White: WT, grey: TG. Treatment is marked with a triangle, controls with a circle. At Tp = 3, a significant difference between drought treated WT and TG plants was observed, as indicated with an asterisk. $N_{WT} = 3$, $N_{TG} = 9$. Different letters indicate significant differences among lines at $P \leq 0.05$ (ANOVA). Values are means ± SD.

3.3.1.1. *ScWS*-OE *plants: better adaption to stress*

Under severe stress (Figure 57 A), *ScWS*-OE plants showed significantly higher predawn leaf water potentials (Ψ_{PLWP}) levels compared to WT plants. In contrast, mild drought stress did not result in differences between WT and TG plants (Figure 57 B). In Exp.2 (2.3.10), the change from mild drought stress (Figure 57 C) to severe stress (Figure 57 D) led to significant decreased Ψ_{PLWP} levels of WT drought treated plants after 24 h.

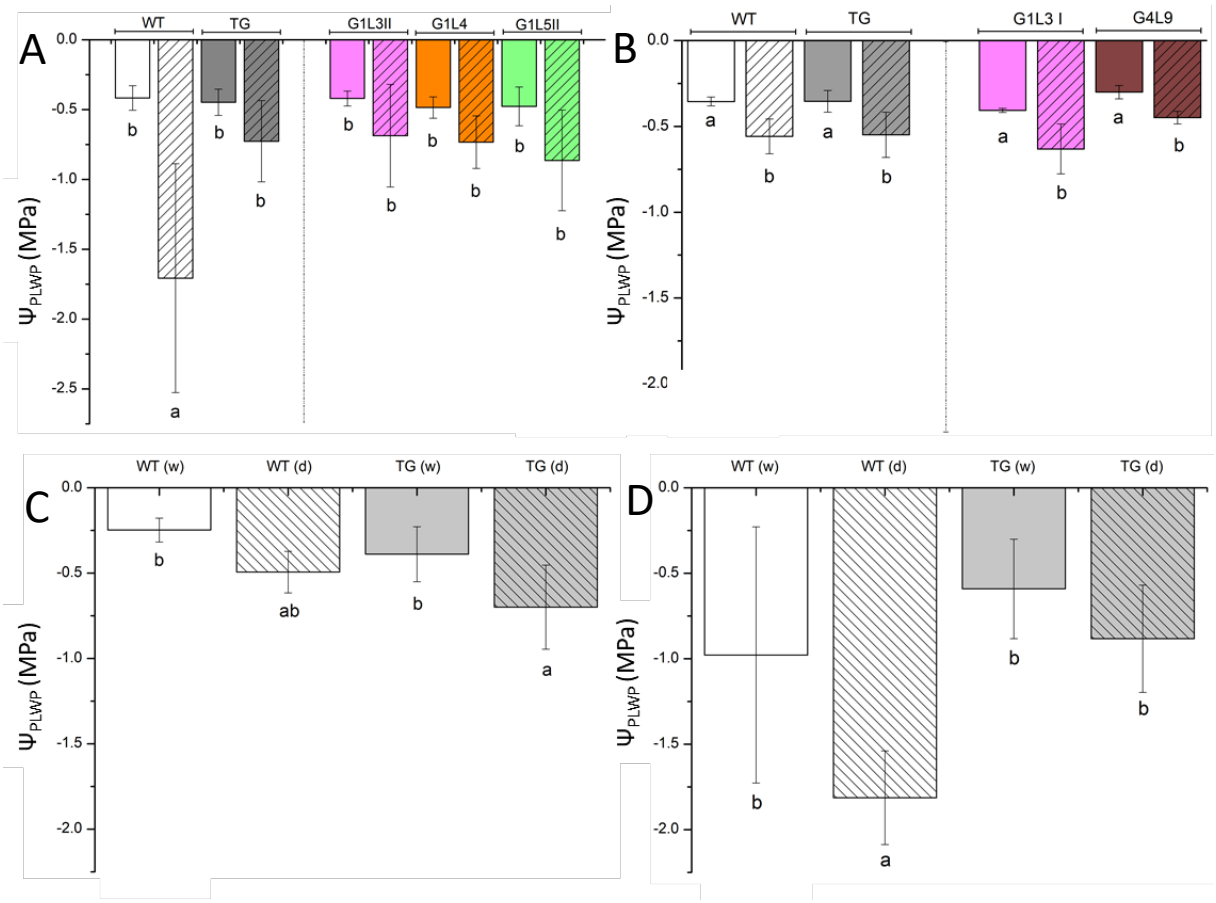

Figure 57: Predawn leaf water potential of drought treated *ScWS*-OE and WT poplar plants. The TG group indicated in grey represents the mean of all transgenic plants tested. Drought treatment is indicated by hatched bars. **A.:** Ψ_{PLWP} after 4 d of severe stress treatment (Exp.1). $N_{WT(w)} = 3$, $N_{WT(d)} = 3$, $N_{TG(w)} = 9$, $N_{TG(d)} = 9$, $N_{Line(w)} = 3$, $N_{Line(d)} = 3$. **B.:** Ψ_{PLWP} after 5 d of mild stress treatment (Exp.3). $N_{WT(w)} = 6$, $N_{WT(d)} = 7$, $N_{TG(w)} = 3$, $N_{TG(d)} = 8$, $N_{Line(w)} = 3$, $N_{Line(d)} = 3$. **C.:** Ψ_{PLWP} after 21 d of mild stress treatment (Exp.2). $N_{WT(w)} = 4$, $N_{WT(d)} = 4$, $N_{TG(w)} = 8$, $N_{TG(d)} = 5$. **D.:** Ψ_{PLWP} of the same plants shown in fig. C after 29 d of severe drought treatment. All measurements were performed with following parameters: $T_{air} = 24.4$ to 27.2 °C, $RH_{air} = 62$ to 56 %. Different letters indicate significant differences among lines at $P \leq 0.05$ (ANOVA). Values are means ± SD.

Under severe stress conditions (Exp.1), the net photosynthesis of drought stressed WT and TG plants declined but did not differ significantly (Figure 58 A). The stomatal conductance was significantly lower in watered TG plants compared to watered WT plants, but no significant effect was observed in the drought-stressed group (Figure 58 B). The transpiration was significantly lower in the watered TG plants compared to the WT control (Figure 58 C), but not in the drought group. The instantaneous water use efficiency (WUE) was significantly increased in watered TG plants when compared to the WT. Both watered and drought stressed TG plants showed significantly higher WUE than watered WT plants (Figure 58 D).

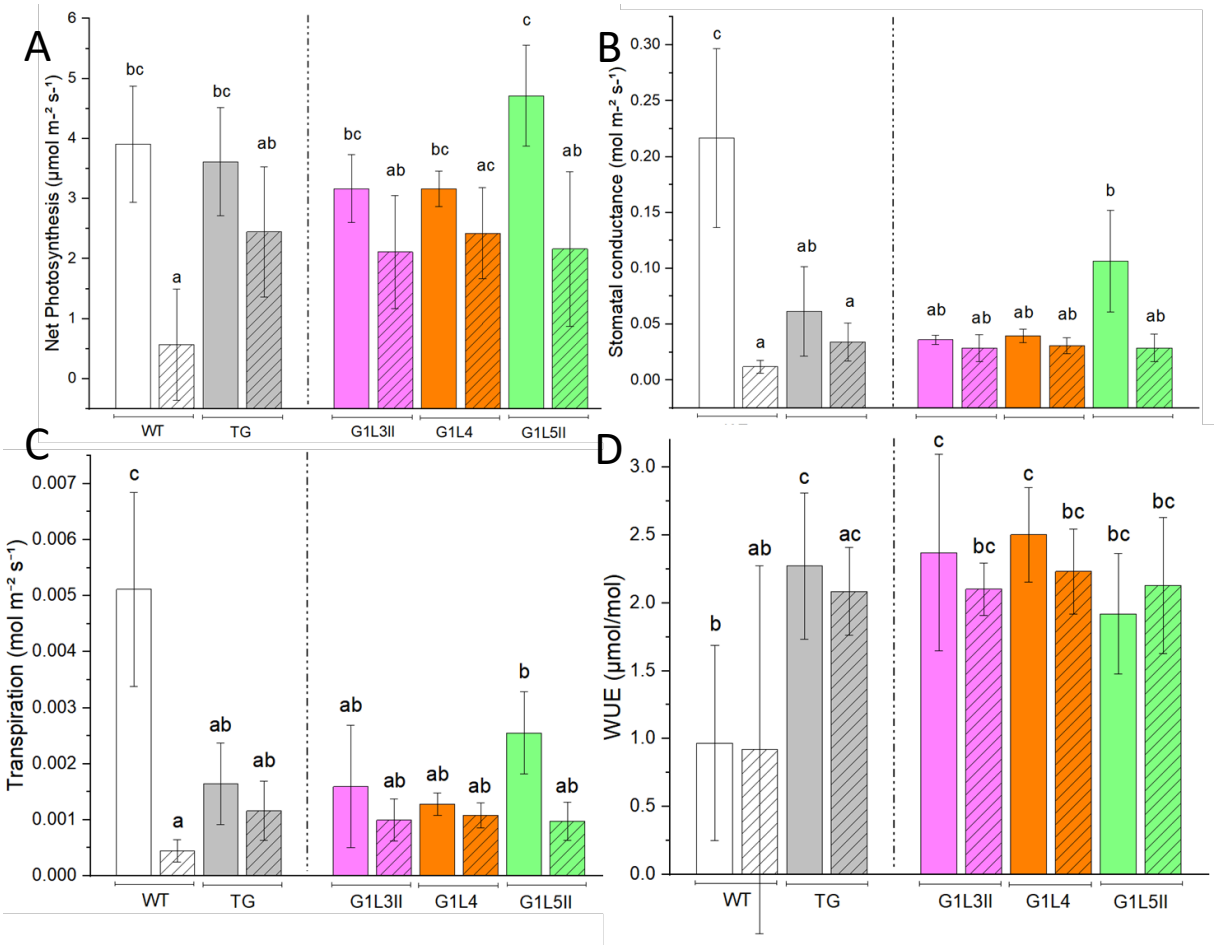

Figure 58: Photosynthesis of drought stressed *ScWS*-OE and WT poplar plants in Exp.1. The TG group indicated in grey is the mean of all transgenic plants tested, including the represented lines. **A.:** Net photosynthesis, **B.:** stomatal conductance, **C.:** transpiration and **D.:** water use efficiency (instantaneous). $N_{WT(w)} = 3$, $N_{WT(d)} = 3$, $N_{TG(w)} = 9$, $N_{TG(d)} = 9$, $N_{Line(w)} = 3$, $N_{Line(d)} = 3$. Measurement parameters: Tair = 26.1 to 27.2 °C, RH_{air} = 62-59%, CO_{2air} = 301.5 to 311.8 µmol mol^{-1}. Different letters indicate significant differences among lines at $P \leq 0.05$ (ANOVA). Values are given as means ± SD.

3.3.1.2. *Improved long term water usage of ScWS-OE lines*

The water use of TG and WT plants was investigated in short term measurements (Figure 59 A) by weight differences and in long term conditions (Figure 59 B) through measurements of the amount of water given to each plant (Exp.2) in a time period of 7 d. No significant difference in short term water usage was detected. The long-term water usage neither showed a significant difference between the WT and the TG plants but a tendency of less water consumption by the *ScWS*-OE plants was observed.

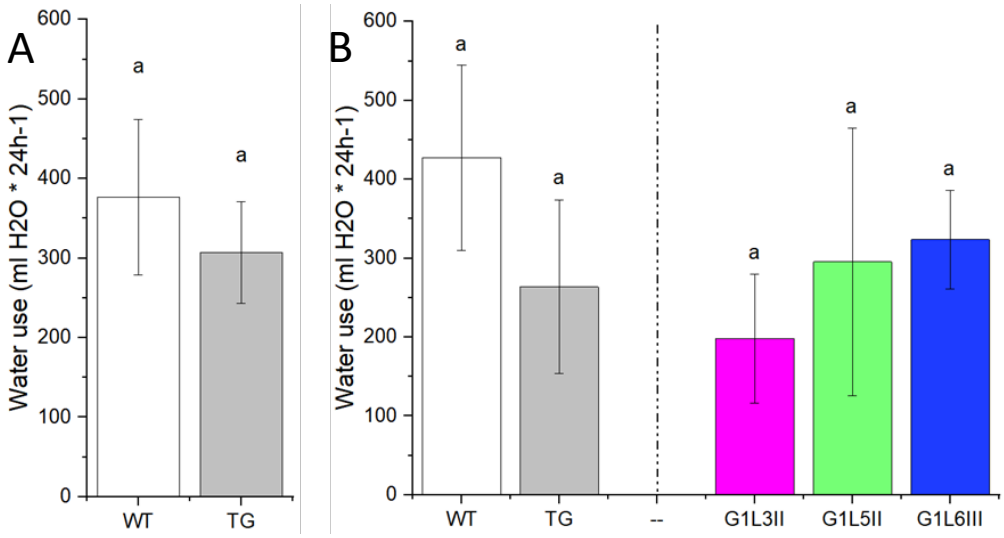

Figure 59: Water usage of *ScWS*-OE and WT plants in Exp.2. A.: Short-term water usage, 24 h. $N_{WT} = 5$, $N_{TG} = 11$. Plants of same height and appearance were taken for measurement. **B.:** Long term water use over 7 d. Only plants > 95 cm height were taken for measurement. Data were normalized to height. $N_{WT} = 10$, $N_{TG} = 11$, $N_{G1L3II} = 5$, $N_{G1L5II} = 3$, $N_{G1L6III} = 3$. The TG group indicated in grey is the mean of all transgenic plants tested. Different letters indicate significant differences among lines at $P \leq 0.05$ (ANOVA). Values are means ± SD.

3.3.1.3. *Wood anatomy and wood water content*

The vessel frequency (Figure 60 A) was not affected by overexpression of the *ScWS* compared to the WT, neither in drought-stressed nor in well-watered plants (Figure 50 A). However, a significant difference was found between the TG control and TG drought, in contrast to the WT control and WT drought. The vessel lumen area was similar to that of the WT (Figure 60 B).

The water uptake of dried wood of TG plants (Figure 61) demonstrated no significant differences compared to the WT after 24h.

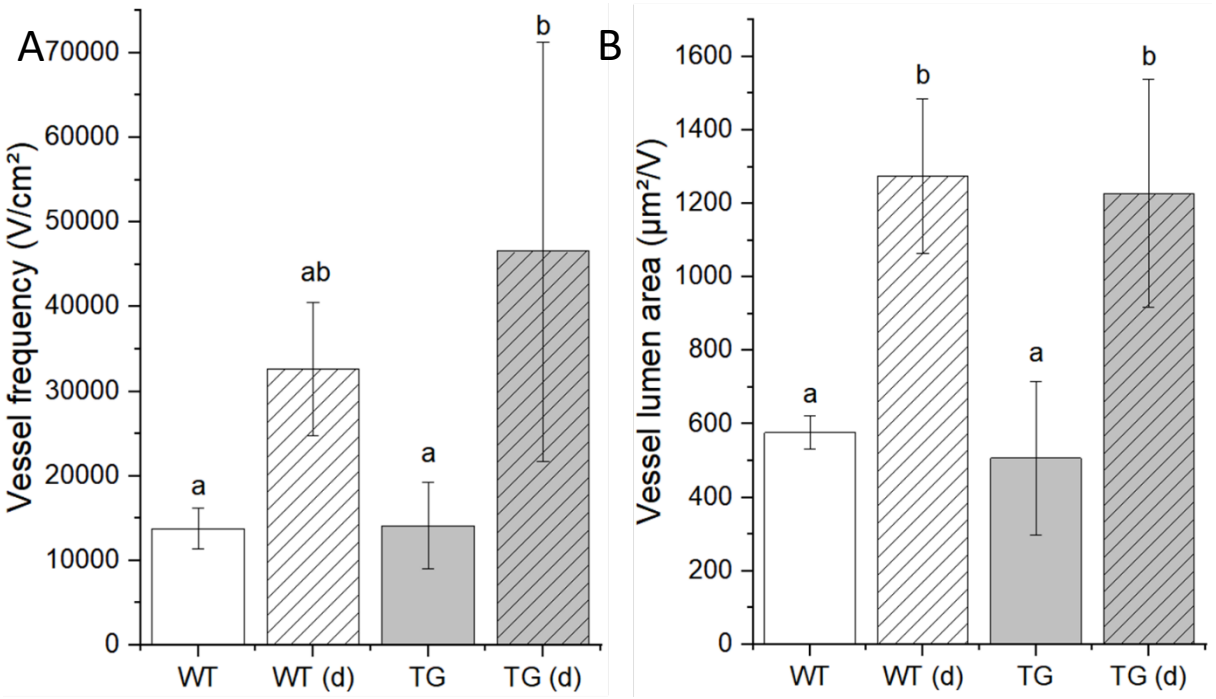

Figure 60: Vessel frequency (A) and area (B) of *ScWS*-OE plants (Exp.2). Wood formed in drought stresses plants conditions was compared with wood formed in plants in non-stressed conditions. N_{WT} = 3, N_{TG} = 6. Different letters indicate significant differences among lines at P ≤ 0.05 (ANOVA). Values are means ± SD.

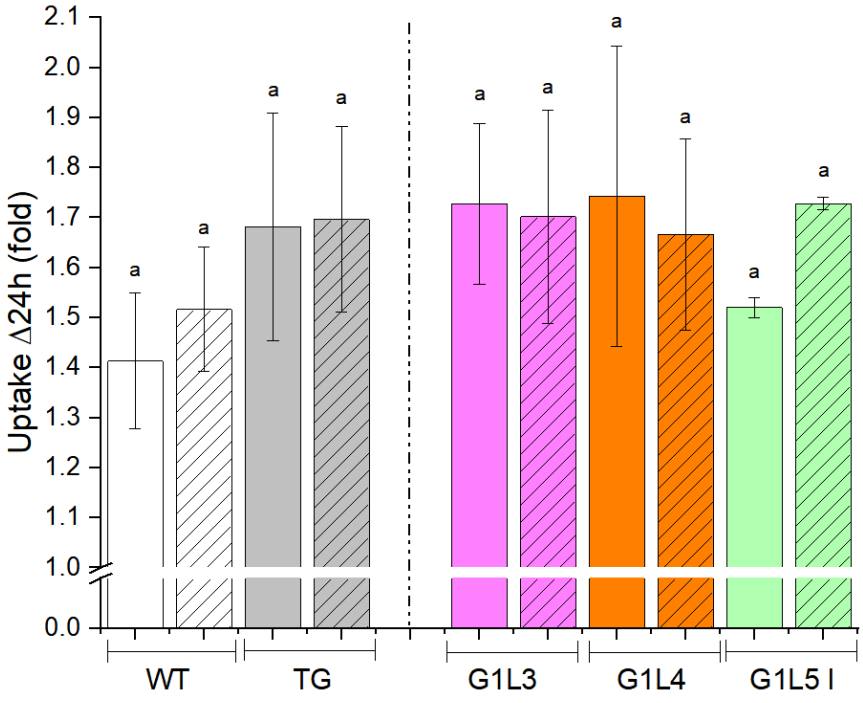

Figure 61: Relative water uptake of poplar wood of *35S::ScWS* and WT plants in Exp.2 in 24 h. The TG group indicated in grey is the mean of all transgenic lines tested. Drought treated groups are indicated by hatched bars. $N_{WT(w)}$ = 6, $N_{WT(d)}$ = 6, $N_{TG(w)}$ = 8, $N_{TG(d)}$ = 10, $N_{G1L3(w)}$ = 5, $N_{G1L3(d)}$ = 3, $N_{G1L4(w)}$ = 3, $N_{G1L4(d)}$ = 3, $N_{G1L5I(w)}$ = 2, $N_{G1L5I(d)}$ = 2. Different letters indicate significant differences among the lines at P ≤ 0.05 (ANOVA). Values are means ± SD.

3.3.1.4. *Stem cuticula*

To investigate the effects of drought treatment on stem surface and phelloderm, stem cross sections of 25 µm thickness were stained with Sudan III (2.3.6.1). Compared to the WT control (Figure 62 A1-3), drought stressed WT plants (Figure 62 B1-B3) show accumulation of lipids in the phelloderm as demonstrated by a brighter reddish colour. A similar observation was made when comparing TG control plants (Figure 62 C1-C3) with TG drought stressed plants (Figure 62 D1-D3). Comparing WT and TG plants did not reveal differences in the appearance of phelloderm and cuticula in watered conditions (Figure 62 A1-A3, C1-C3) or stress treatments (Figure 62 B1-B3, D1-D3).

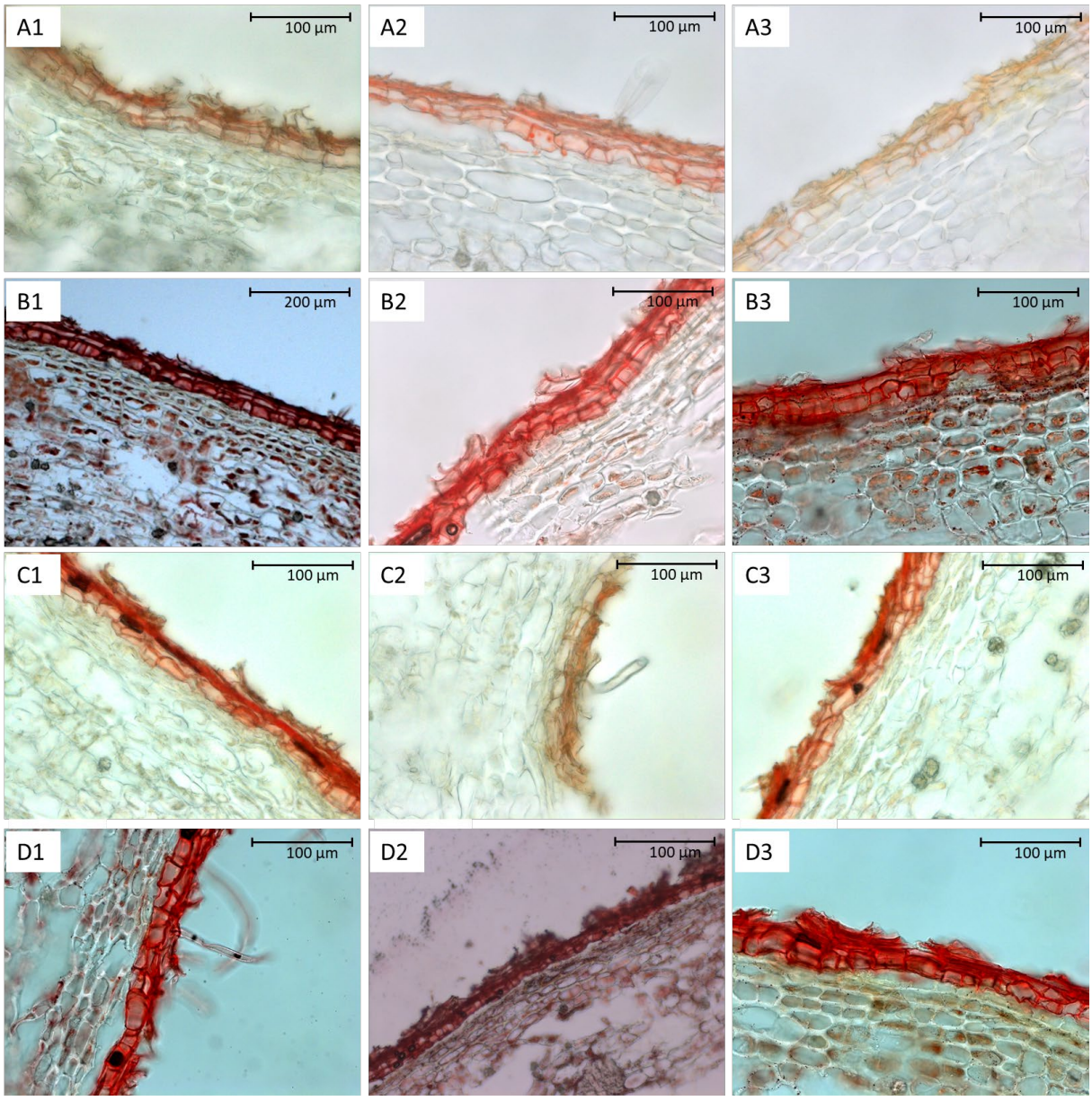

Figure 62: Comparison of stem cuticula and phelloderm of WT (A1-B3) and *35S::ScWS* plants (C1 – D3), stained with Sudan III. A1 – A3: WT, control. **B1 – B3:** WT, drought treatment. **C1 – C3:** TG, control. **D1 – D3:** TG, drought treatment. Plants are originated from Exp. 2: line G1L6I (C1, D1), line G1L4 (C2, D2) and line G4L1 (C3, D3).

4. Discussion

4.1. Production of transgenic *P.* x *canescens* lines

4.1.1. Binary vector system pCAMBIA versus pK7WG

For bio-engineering of *ScWS, DGAT1, WR1* or *FAR* -overexpressing plants, several different vector systems have been produced and tested by transformation of *P.* x *canescens* plants (Figure 12). Here, two different binary vector systems, pCAMBIA and pK7WG, were tested with several different gene and promoter combinations. Binary vector systems based upon the pCAMBIA vector are often used for *Agrobacteria*-mediated plant transformation (Leclercq et al., 2015) and positive transformation results were achieved also in woody species such as *P. angustifolia* and *P. balsamifera* (Maheshwari and Kovalchuk, 2016). In *P.* x *canescens*, pCAMBIA was used successfully in a transformation protocol similar to the one used in this work, with BASTA (Lu et al., 2015) and kanamycin (Meyer et al., 2004) as selection components. However, no stable transformation of different multiple- and single gene setups containing the pCAMBIA binary vector system was achieved in this work (Table 13).

In previous studies, stable poplar lines were produced by the use of the pK7WG vector system (Muhr et al. (2016), Allario et al. (2018)). In this work, contrary to the pCAMBIA system, the pk7WG system provided viable transgenic *P.* x *canescens* lines with different genes and promoter combinations (Table 23). Two pk7WG binary vectors were used: the pK7WG2, including a 35S promoter and the pK7WG, excluding a promoter. In the latter case, the promoter was introduced in the pEntry entry vector system first, which was then used to introduce the promoter/gene setup for the pK7WG and for the pCAMBIA system as well. Although the same promoter/gene combinations were introduced into poplar by both binary vector systems, only the pK7WG provided positive transformation results, indicating that the pCAMBIA system used in this work is not suitable for transformation in *P.* x *canescens* in this constellation.

In contrast to the rapid “floral dip” – method used for the transformation of the model organism *A. thaliana* (Clough and Bent, 1998), the transformation of *Populus* species requires plant tissue culture and regeneration and thus relies on highly optimized protocols regarding the incubation time of *Agrobacteria* (Han et al., 2013) or the addition of phytochemicals such as acetosyringon (Nilsson et al., 1992). Consequently, the transformation efficiency of poplar species is generally low (Han et al., 2000) compared to *A. thaliana;* satisfying results can only be reached by a high quantity of transformable material, which often is problematic to acquire (Figure 13). Additionally, transformation efficiency decreases with increasing size of the binary vector. Since several transformation attempts utilizing the pCAMBIA vector system which included multiple gene constructs of sizes bigger than 12.000 kb (Table 22; K30, K31 and K32), a positive transformation might have been prevented just by the size of the

construct. Additionally, multiple insertions of the 35S promoter might cause silencing effects. Multiple gene constructs were thus not applied further in the pK7WG system.

A low overall transformation rate, a demand for highly optimized protocols and binary vectors and low quantity of transformable material could be the reason for a negative outcome utilizing the pCambia system. Therefore, regarding the transformation protocol utilized in this work, the pCAMBIA system was not the system of choice for transformation of *P.* x *canescens.*

4.1.1.1. *35S promoter*

Although the pK7WG system accomplished much better transformation results than the pCAMBIA system, not every promoter/gene combination was transformed successfully. Consistently failing transformation attempts were often linked to the use of the 35S promoter. In the case of the transcription factor *AtWRI1* and the key enzyme in triacylglycerol production *AtDGAT1*, under the 35S promoter no viable plants after transformation were observed. On the contrary, a positive transformation was demonstrated with the *MaFAR* (K 71) and the *ScWS* under two different 35S promoters (K 60 and K 72) and additionally with the wood-specific promoter DX15 (K 78, Table 23). Utilizing the DX15 promoter, the transformation of *AtDGAT1* was also successful and led to a high number of stable lines (Table 23).

The 35S promoter is a widespread tool used in plant research for its lack of tissue specificity, its high expression levels and its applicability to different plant species. Nevertheless, several inconsistencies of the 35S promoter in scientific use have been discovered. For example, the impact of the 35S could be enhanced by duplication (Kay et al., 1987), different transcription levels were found in younger tissues of *Nicotiana benthamiana* compared to older tissues (Williamson et al., 1989) and evidence was found that the 35S promoter reacts sensitive to short photoperiods (Schnurr and Guerra, 2000). Also, a high diversity of different 35S promoter sequences exists; e.g., long variants of the promoter contain an open reading frame and might lead to unintended phenotypic changes (Podevin and Jardin, 2012). Nevertheless, the 35S promoter used in this work demonstrated a consistent overexpression of *ScWS* (K 60) in different transgenic lines (Figure 29 A) as well as in different tissues: leaf, developing xylem and roots (Figure 29 B). Therefore, it is unlikely that the 35S promoter was responsible for the continuously failing transformation of *AtDGAT1* and the inhibited growth of *AtWRI1* in *P.* x *canescens*. The lack of viable transformants rather suggests that the harsh impact of a constitutive overexpression of the key gene *AtDGAT1* or key transcription factor *AtWRI1* is the main reason for failing transformation results.

4.1.1.2. *DX15 promoter*

In order to drive expression of genes in developing xylem tissue, Ko et al. (2012) identified a group of specific and highly expressed genes in the DX *in silico* by GeneChip Poplar Genome Array (Affymetrix) analysis; the specific expression of a chosen subgroup of genes found *in silico* was confirmed *in planta* by fusing promoter regions with the β-glucuronidase (GUS)-reporter gene from *E. coli*. The promoter region of *PtrNAC073* (further referred to as DX5) has been found to be highly expressed in xylem tissue before (Grant et al., 2010) and the expression patterns of this gene were validated in the work of Ko *et al.* (2012). However, the promoter region of Fasciclin-like AGP8 (further referred to as DX15) was demonstrated to have higher expression rates in DX tissue compared to DX5 and was thus chosen to express the genes of interest in this work.

In contrast to the findings of Ko et al. (2012), the sequence analysis of the promoter region revealed a missing repetitive element (Figure 48). This missing element was consistently found in three different *P. trichocarpa* individuals. Since Ko et al. (2012) used hybrid poplar 'NM6' (*Populus maximowiczii* x *nigra*) for promoter sequence analyses, the missing element in our study is most likely due to the use of different species, *P. trichocarpa*.

In the developmental xylem of transformed plants, generally a high expression of the target gene under the DX15 promoter was found. In *ScWS*–transformed plants, a high variation of the expression level between different plants was observed (Figure 49 A). Additionally, in WT-plants, a basal expression was found, demonstrating that endogenous wax ester synthesis was taking place and that the primer was exclusively amplifying the transgene. On the contrary, no basal expression of diacylglycerol acyltransferases was found in plants transformed with the *DX15::AtDGAT1*-construct (Figure 49 B). The expression levels the *AtDGAT1*-OE lines were normalized against the reference genes *PtrPPR_2* (Potri.012G141400, referred to as Aref2) and *PtrRpp14* (Potri.015G001600, referred to as Cref1) and thus, appeared to be seemingly much lower than the expression levels of *ScWS* overexpression lines, in which stable basal expression of the endogenous wax ester synthase was used as the reference. Nevertheless, the *AtDGAT1* expression levels were up to 100-fold higher than those of the reference genes, clearly showing strong expression of *AtDGAT1* in DX tissue.

An important point is whether the DX15 promoter is tight, i.e. expressed only in wood. Therefore, the expression of target genes in different tissues was analysed. *AtDGAT1* was found to be expressed mainly in developing xylem tissue. In bark and leaf, *AtDGAT1* was also detected, but at very minor levels. Bark tissue had higher *ATDGAT1* expression levels than leaf tissue. However, these enhanced expression levels might be due to the RNA isolation from bark, which may comprise DX to a certain extent. This was observed specially in the *ScWS*-expressing line K78III (Figure 27), indicating a poor sample preparation. This has been addressed by Ko *et al.* (2012) as well to be the major problem to

identify tissue-specific promoters. Here, both genes, *AtDGAT1* and *ScWS* under the DX15 promoter principally showed strong enrichment for DX but not perfect tissue specificity.

4.1.1.3. *AtWRI1*

In this study, the *A. thaliana* gene *AtWRI1* was chosen and transformed into *P.* x *canescens*, utilizing the pCAMBIA or the pK7WG binary vector system. No stable line was produced with any of the binary vector systems. However, plantlets transformed with *35S::AtWRI1* demonstrated a significantly longer rooting period compared to plantlets transformed with the *AtDGAT1*. To counteract a possible deficiency in growth, several plantlets were transferred to culture media containing 4 % sucrose to increase carbon availability, but plantlets on 2 % and on 4 % sucrose containing medium died consistently after a rooting period of 9 to 12 weeks.

WRI1, a well-studied transcription factor closely linked to fatty acid synthesis (Focks and Benning, 1998), plays a key role in oil accumulation, e.g. in potato (Hofvander et al., 2016). In vegetative tissue, transformed WRI1 led to increased TAG quantities in leaves of *Nicotiana benthamiana* (Vanhercke et al., 2013) or *A. thaliana* (Sanjaya et al., 2011). Woody plants were affected by overexpression of *WRI1* as well, e.g. *Jatropha curcas,* in which overexpression of *JcWRI1* enhanced lipid contents and oleate levels in seeds (Ye et al., 2018). The poplar homolog of WRI1, derived from *P. trichocarpa* cambium, led to oil accumulation in leaves of DGAT1-co-transformed *Nicotiana benthamiana* (Grimberg et al., 2015), indicating a highly conserved function across different species. Contrary, overexpression of *PtWRI1* in *Populus tremula* × *tremuloides* (clone T89) under a 35S promoter did not lead to an additional TAG increase, indicating a more diverse and different role of *WRI1* in poplar stem storage lipid production (Grimberg et al., 2018). Grimberg et al. (2018) discussed that limitation of starch and thus carbon due to short day growing periods might be a possible explanation for steady TAG levels. Furthermore, the poplar *WRI1* orthologue is not expressed in long-day conditions.

The plantlets in this study transformed with the *AtWRI1* under a 35S promoter were grown in long-day conditions but with reduced light according to the protocol (2.2.4). This might have increased the endogenous *WRI1* orthologue leading to a carbon limitation that could not be rescued by the light conditions or the increased sucrose content in the media. However, the long rooting process without growth and lack of viability remains unclear and should be addressed in further studies by adjusting light intensity and sugar content of the media.

4.1.1.4. *AtDGAT1*

In this work, the *AtDGAT1 gene* was transformed in several construct and promoter combinations (Table 23), but viable lines were only found by utilizing the DX15 promoter in the pK7WG binary vector system. Since the DGAT1 is the key step and bottleneck in TAG synthesis, recent studies focused on its usability in altering seed storage TAG in *A. thaliana* (Savadi et al., 2015) as well as the possibility to increase TAG levels in vegetative tissues, such as stem tissue of tobacco (Nookaraju et al., 2014) by utilizing a 35S promoter. Apart from the present thesis (December 2019), no other studies regarding overexpression of *DGAT1* have been accomplished in woody, perennial plants.

No viable poplar lines obtained utilizing the 35S promoter. In contrast, with the tissue-specific DX15 promoter, viable lines were generated in which *AtDGAT1* was expressed (Table 23). This indicates that the *AtDGAT1* plays a crucial role for TAG synthesis and a massive overexpression caused by a 35S promoter might alter the balance in lipid synthesis too harshly and thus preventing the production of viable transgenic poplar plants. Here, due to time constraints a detailed phenotypic analyses of the *DX15::ATDGAT1* poplars were not possible. A glimpse into its possible impact on wood properties were promising because we found a trend towards decreased swelling of the wood (Figure 52). This phenotype was expected, if the hydrophobicity of the wood was increased. It will be important to investigate this phenotype further, using more mature and field-grown transgenic plants.

4.1.1.5. *ScWS*

The *ScWS* was transformed in several construct and promoter combinations (Table 23) and viable lines were achieved with both promoters (35S and DX15) utilizing the pk7WG and pk7WG2 binary vector system. Contrary to WSDs (1.2.2), the role of ScWS is dedicated to the production of wax esters used as seed storage compound*,* demonstrated by high expression rates of *ScWS* and the fatty alcohol reductase (*ScFAR)* in cotyledonary tissue in *Simmondsia chinensis* (Sturtevant et al., 2020). Because of its dedication to the storage function and exploitability of WE in technical applications (Jetter and Kunst, 2008), research mainly focussed on the possibility to increase WE in seed tissues in higher plants under seed specific promoters (Iven et al., 2016; Ivarson et al., 2017b; Yu et al., 2018). So far, studies regarding the expression of *ScWS* in other vegetative tissues such as leaf or xylem have not been executed yet (April 2020).

In most cases, co-expression of a fatty alcohol reductase led to significant increases in seed oil yield (Iven et al., 2013), since fatty alcohols are the limiting compounds in synthesis of wax esters (Iven et al., 2016). A co-transformation with both genes (*ScWS* and *MaFAR*) was not achieved in this work most probably due to the size of the used binary vector system (4.1.1). However, in single-gene attempts, the *ScWS* were transformed successfully under both promoters. Although no intensive accumulation of lipids were observed under the 35S promoter (3.3.1.4), plants demonstrated changes in physiology

and leaf surface wax ester composition (3.2.1) similar to the results of overexpression studies with different WS, with special regard to drought performance (4.2). Thus, contrary to the results of *AtDGAT1*-transformed plants (4.1.1.4), the *ScWS* might affect the wax ester synthesis just enough to allow viable transformed plants and detectable changes in the leaf surface wax ester composition, but not enough to detect increased wax ester accumulation in the tissues. Since the *AtDGAT1* was positively transformed under the DX15 promoter, a tissue specific expression of *ScWS* might decrease the impact of altered wax ester synthesis even more. Because of time constraints, detailed phenotypic analyses of *DX15::ScWS* plants were not possible, but expression of *ScWS* in DX tissue was observed (3.2.2). To accumulate wax esters in vegetative tissues in larger quantities, a co-expression of *ScWS* and *MaFAR* under the constitutive 35S and in particular the tissue-specific DX15 promoter should be the subject of further research.

4.2. Impact of overexpressed *ScWS* on poplar drought performance

Many studies with annual plants such as rice (Zhou et al., 2013), camelina (Lee et al., 2014) and maize (Li et al., 2019) have shown correspondence between increased cuticular waxes and enhanced drought resistance. In this study, overexpressing the *ScWS* gene in *P.* x *canescens* resulted in decreased stomatal conductance (Figure 41), smaller stomata (Figure 44) and reduced amounts of wax ester precursors (Figure 47, for a schematic overview see Figure 63). These phenotypic consequences of *WS*-expression in poplar led to increased water use efficiency (Figure 42), drought avoidance and better performance under severe stress (Figure 56). Additionally, the plants showed a trend towards lower long-term water use (Figure 52). These findings concur with the results of Ni et al. (2015), who observed that a larger amount of wax deposited on the cuticula negatively affected the stomatal conductance. Ni et al. (2015) studied the leaf total wax deposition of different cultivars of the woody species mulberry (*Morus alba*) with GC-MS. Additionally, they found a smaller stomata aperture, but contrary to our results, the net photosynthetic rate and the transpiration rate were reduced as well. Ni et al. (2015) concluded that the total wax deposition can have a direct influence to the stomata apertures by preventing additional loss of water by an enforced cuticula.

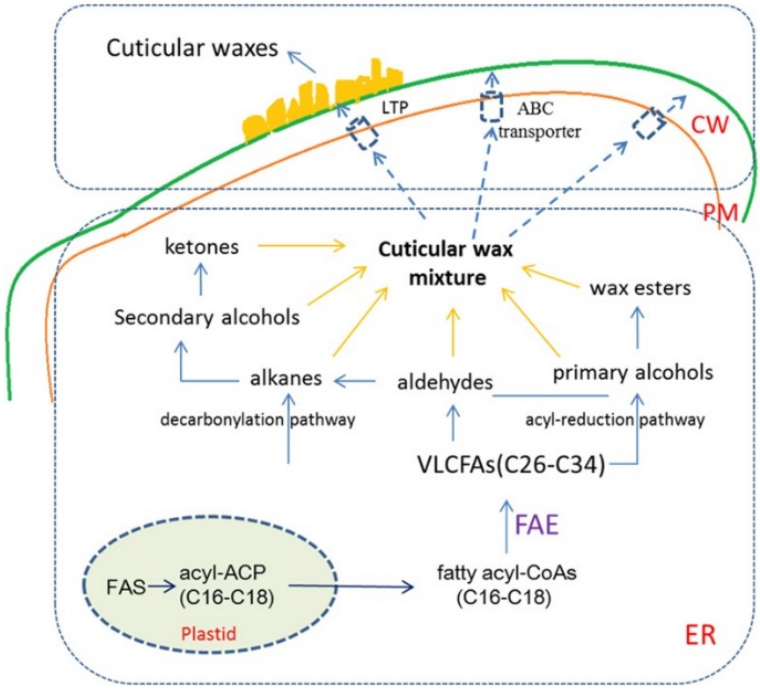

Figure 63: Schematic overview over cuticular wax synthesis in plants. C_{16} and C_{18} fatty acyl-CoA from plastidial origin are elongated in the ER (endoplasmatic reticulum) to very long chain fatty acids (VLCFAs), the precursor pool for aldehydes and primary alcohols. The cuticular wax mixture is transported through the cell wall (CW) onto the cuticula by ABC transporter (ATP binding cassette transporter) and LTP (lipid transfer protein). CW: cell wall, PM: plasma membrane, FAE: fatty acid elongase. Derived from Xue et al. (2017).

While an enhanced cuticula barrier was found to be the long-term answer of several species to drought stress as mentioned before, e.g. in tree tobacco (Cameron et al., 2006), a fast response to drought stress is the reduction of the stomatal conductance, triggered by abscisic acid (ABA) (Negin and Moshelion, 2016). ABA forms a complex network of genes and transcription factors that contribute to drought stress, e.g. reduction of stomatal conductance, root water uptake and biosynthesis of osmoprotectants (Kumar et al., 2012, 2018). Also, several links of ABA to cuticular waxes and altered cuticular composition were found in Arabidopsis (Macková et al., 2013), by actively switching on the promoter region of 3-KETOACYL-COA SYNTHASE 6 (*CER 6*) gene (Hooker et al., 2002). Macková et al. (2013) discovered significant increases in long chain fatty acids (C28, C30) and alkanes (C25, C27) in Arabidopsis. In the same study, decreases in long-chain alcohols (C22, C24, C26, C30, C32) in ABA-treated *Lepidium sativum* were discovered. This is at variance to our findings that the alkanes (C25, C27) were decreased and that fatty acids (C28) were unaffected. Although the cuticula composition responds to ABA signalling, a subset of genes contributing to wax biosynthesis was found to be affected by water deficit and NaCl treatment independently from ABA treatment, indicating the existence of another cuticula regulatory network induced by drought (Kosma et al., 2009). The link between ABA and wax production was found to be MYB96 (Figure 64), a transcription factor induced by ABA, influencing the stomatal aperture via RD22 (Seo et al., 2009) and also regulating the wax biosynthesis (Seo and Park, 2011).

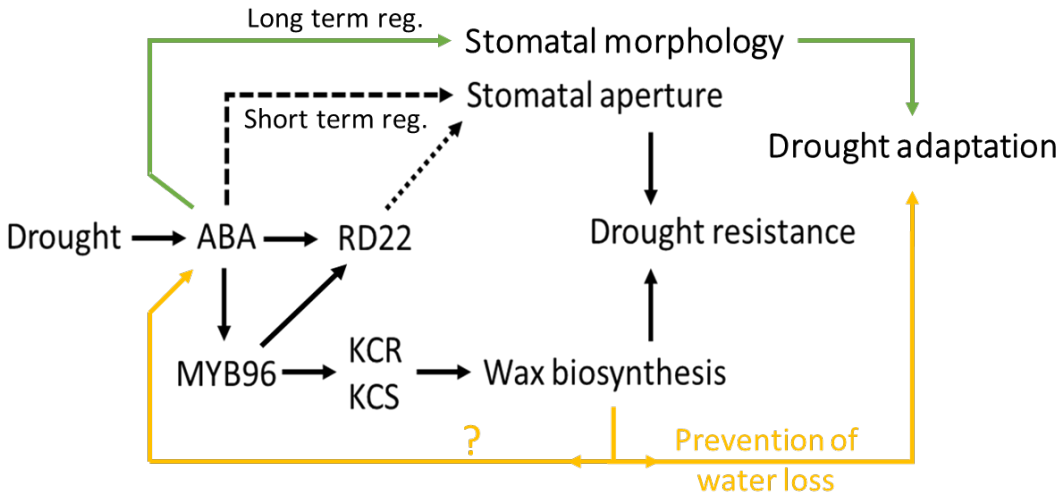

Figure 64: Schematic regulatory pathway of wax biosynthesis involved in drought resistance. The transcription factor MYB96 is upregulated in response to ABA and directly interacts with the promoter region of 3-ketoacyl-CoA reductases (KCR) and 3-ketoacyl-CoA synthetases (KCS). Putatively feed-back effects of wax biosynthesis to ABA is shown in orange. Derived from Seo et al. (2009, 2011).

Smaller sized stomata and reduced stomatal conductance without decreased photosynthesis capacity, i.e. enhanced photosynthetic efficiencies, have often been found in plants undergoing long term drought stress or long-term exposure to high ABA concentrations, an effect firstly described by Bradford et al. (1983) and confirmed by the finding of (Franks and Farquhar, 2001). Our findings agree with these reports because we observed (i) smaller stomata, (ii) decreased stomatal conductance but unchanged net photosynthesis rates and (iii) no significant differences in biomass of transgenic compared to WT plants. Furthermore, the pre-dawn leaf water potential of mild-drought treated *ScWS*-OE plants and WT plants did not differ (Figure 57 B, C) but under severe stress conditions (Figure 57 A, D), the transgenic plants had a higher pre-dawn leaf water potential, indicating lower stress levels compared to WT plants.

Taken together, the results of this thesis indicate a “pre-adaptation” of *ScWS*-OE plants to drought stress conditions that might be linked to a long-term regulating function of ABA. No significant changes in the root-to-shoot ratio, another ABA–dependent response to drought (McAdam et al., 2016), were found between WT and TG plants (Figure 35). However, when grown for a longer period, the biomass of leaves and roots of untreated plants were smaller in TG plants compared to the WT (Figure 37). This is consistent to previous findings (Arend et al., 2009; Yu et al., 2019) in which ABA was discussed to act independently from drought stress as a positive regulator of growth in leaves and roots.

The leaf area of TG plants did not significantly differ to the WT plants in drought and watered conditions in short time experiments (Figure 33 A, C), but a significant decreased leaf area in TG plants in long-term experiments was observed (Figure 33 B). Consistently to our findings, a linkage of ABA to

leaf area was elaborately described by Yu et al. (2019); several different TF and ABA receptors were found to regulate the leaf area and implicitly wood biomass production. Additionally, a strong dependency of ABA and stomatal conductance was observed.

ABA regulates cuticula wax composition via transcription factor MYB96, but it is unknown whether changes in the wax composition, which were induced here by the overexpression of *ScWS*, can have a feed-back effect on ABA (Figure 64). The overexpression of the *ScWS* led to reduced precursor molecules for wax esters (Figure 47), which might have regulating effects. Because especially long chain alkanes were found to decrease drought resistance when reduced (Park et al., 2010) and an increase of long chain alkanes is contributing positively to drought resistance (Kosma and Jenks, 2007), alkane synthesis might be considered to be the key player in cuticular stress response. The contribution of the sheer thickness of the wax layer to drought stress response is, however, discussed controversially; several studies have demonstrated that water loss is not directly related to the thickness of the wax layer (Schreiber and Riederer, 1996), (Sánchez et al., 2001). Therefore, the composition of the cuticular waxes may be more important than changes in the thickness of this layer.

In this study, alkanes were the most significant group found to be decreased by overexpression of *ScWS*. Because a trend for a reduction in alcohols and in fatty acids was demonstrated as well (Figure 47), a possible explanation can be that carbon in the form of lipid-derived precursor molecules are channelled towards the *ScWS* and quickly turned over to produce higher amounts wax esters. If the reduction of the precursors indicates a depletion of the pool because of enhanced wax biosynthesis, the basal drought tolerance of transformed poplars might have been increased, thus, resulting in the “pre-adapted” phenotype.

5. Overall conclusion / outlook

In conclusion, this study demonstrates that changes in the lipid metabolism, in particular boosting the wax ester synthesis, can result in benefits regarding the plant's adaptation to dry environments. Overexpression of *ScWS* in poplar plants caused a decrease in the stomatal conductance because of morphological changes in the stomata size. Since the photosynthesis rates were unaffected, the water use efficiency was increased. This led to pre-adapted poplar plants with lower water use that can withstand short-term drought periods. Because the plant hormone ABA is the key player in drought stress responses and seems to have the potential to influence the composition of the cuticula, the role of ABA regarding the phenotype of *ScWS*-OE plants should be investigated in greater detail. Further experiments therefore should focus on the concentration of ABA in plants overexpressing *ScWS* in drought and watered conditions. Since the water balance is regulated through a widespread network of ABA - sensitive genes and transcription factors, the postulated feed - back effect of wax biosynthesis towards ABA could be clarified by RNA sequence analysis, concentrating on genes crucial for wax ester synthesis such as KCR or the transcription factor MYB96.

How the composition of the cuticula on leaves and stems was altered could not be directly measured because methods to determine wax load were not available. The decrease in the amounts of precursor molecules needed for wax ester synthesis suggests that alterations may occur. Light microscopic studies did not show conclusive results regarding morphological changes in the surface. Further research on the composition of the cuticula is needed to understand its involvement in the plant's water balance.

The biomass accumulation was not affected significantly, however, a tendency for lower biomass yield was observed. This has to be examined further and should be tested in experiments in long-term growing periods. Nevertheless, a stable phenotype was reproduced in three different experiments under greenhouse conditions. However, since the measured effects might be diminished by other stress-related influences outdoors, field testing is necessary.

To modify wood, the promoter DX15 was cloned into a binary vector system and was proven to express genes of interest in DX tissue. Genes that could not be transformed into poplar system using the highly overexpressing 35S promoter, were able to be transformed using the DX15 promoter. Therefore, this promoter might be a valuable step in wood biotechnology.

6. References

Allario, T., Tixier, A., Awad, H., Lemaire, C., Brunel, N., Badel, E., Barigah, T.S., Julien, J.-L., Peyret, P., Mellerowicz, E.J., et al. (2018). *PtxtPME1* and homogalacturonans influence xylem hydraulic properties in poplar. Physiol. Plant. *163*, 502–515.

Arend, M., Schnitzler, J.-P., Ehlting, B., Hänsch, R., Lange, T., Rennenberg, H., Himmelbach, A., Grill, E., and Fromm, J. (2009). Expression of the Arabidopsis Mutant *abi1* Gene Alters Abscisic Acid Sensitivity, Stomatal Development, and Growth Morphology in Gray Poplars. Plant Physiol. *151*, 2110–2119.

Bates, P.D., Durrett, T.P., Ohlrogge, J.B., and Pollard, M. (2009). Analysis of Acyl Fluxes through Multiple Pathways of Triacylglycerol Synthesis in Developing Soybean Embryos. Plant Physiol. *150*, 55–72.

Begum, S., Nakaba, S., Oribe, Y., Kubo, T., and Funada, R. (2010). Changes in the localization and levels of starch and lipids in cambium and phloem during cambial reactivation by artificial heating of main stems of Cryptomeria japonica trees. Ann. Bot. *106*, 885–895.

Bourdenx, B., Bernard, A., Domergue, F., Pascal, S., Léger, A., Roby, D., Pervent, M., Vile, D., Haslam, R.P., Napier, J.A., et al. (2011). Overexpression of Arabidopsis *ECERIFERUM1* Promotes Wax Very-Long-Chain Alkane Biosynthesis and Influences Plant Response to Biotic and Abiotic Stresses. Plant Physiol. *156*, 29–45.

Bouvier-Navé, P., Benveniste, P., Oelkers, P., Sturley, S.L., and Schaller, H. (2000). Expression in yeast and tobacco of plant cDNAs encoding acyl CoA:diacylglycerol acyltransferase. Eur. J. Biochem. FEBS *267*, 85–96.

Bruegmann, T., Polak, O., Deecke, K., Nietsch, J., and Fladung, M. (2019). Poplar Transformation. In Transgenic Plants: Methods and Protocols, S. Kumar, P. Barone, and M. Smith, eds. (New York, NY: Springer New York), pp. 165–177.

Cagliari, A., Margis, R., Maraschin, F. dos S., Turchetto-Zolet, A.C., Loss, G., and Margis-Pinheiro, M. (2011). Biosynthesis of Triacylglycerols (TAGs) in plants and algae. Int. J. Plant Biol. *2*, e10–e10.

Cameron, K.D., Teece, M.A., and Smart, L.B. (2006). Increased accumulation of cuticular wax and expression of lipid transfer protein in response to periodic drying events in leaves of tree tobacco. Plant Physiol. *140*, 176–183.

Cernac, A., and Benning, C. (2004). WRINKLED1 encodes an AP2/EREB domain protein involved in the control of storage compound biosynthesis in Arabidopsis. Plant J. *40*, 575–585.

Chang, S., Puryear, J., and Cairney, J. (1993). A simple and efficient method for isolating RNA from pine trees. Plant Mol. Biol. Report. *11*, 113–116.

Chen, T.H.H., and Gusta, L.V. (1983). Abscisic Acid-Induced Freezing Resistance in Cultured Plant Cells. Plant Physiol. *73*, 71–75.

Clough, S.J., and Bent, A.F. (1998). Floral dip: a simplified method for Agrobacterium -mediated transformation of Arabidopsis thaliana. Plant J. *16*, 735–743.

Cramer, G.R. (2002). Response of abscisic acid mutants of Arabidopsis to salinity. Funct. Plant Biol. *29*, 561–567.

Cui, F., Brosché, M., Lehtonen, M.T., Amiryousefi, A., Xu, E., Punkkinen, M., Valkonen, J.P.T., Fujii, H., and Overmyer, K. (2016). Dissecting Abscisic Acid Signaling Pathways Involved in Cuticle Formation. Mol. Plant *9*, 926–938.

Dost, M. Epicuticular waxes of Populus trichocarpa: their chemistry and role in the host recognition. 36.

Durrett, T.P., Benning, C., and Ohlrogge, J. (2008). Plant triacylglycerols as feedstocks for the production of biofuels. Plant J. *54*, 593–607.

Dyer, J.M., Stymne, S., Green, A.G., and Carlsson, A.S. (2008). High-value oils from plants. Plant J. *54*, 640–655.

Eckert, C., Sharmin, S., Kogel, A., Yu, D., Kins, L., Strijkstra, G.-J., and Polle, A. (2019). What Makes the Wood? Exploring the Molecular Mechanisms of Xylem Acclimation in Hardwoods to an Ever-Changing Environment. Forests *10*, 358.

Focks, N., and Benning, C. (1998). wrinkled1: A Novel, Low-Seed-Oil Mutant of Arabidopsis with a Deficiency in the Seed-Specific Regulation of Carbohydrate Metabolism. Plant Physiol. *118*, 91–101.

Franich, R.A., Goodin, S.J., and Volkman, J.K. (1985). Alkyl esters from pinus radiata foliage epicuticular wax. Phytochemistry *24*, 2949–2952.

Franks, P.J., and Farquhar, G.D. (2001). The Effect of Exogenous Abscisic Acid on Stomatal Development, Stomatal Mechanics, and Leaf Gas Exchange in Tradescantia virginiana. Plant Physiol. *125*, 935–942.

Giovannelli, A., Emiliani, G., Traversi, M.L., Deslauriers, A., and Rossi, S. (2011). Sampling cambial region and mature xylem for non structural carbohydrates and starch analyses. Dendrochronologia *29*, 177–182.

Grant, E.H., Fujino, T., Beers, E.P., and Brunner, A.M. (2010). Characterization of NAC domain transcription factors implicated in control of vascular cell differentiation in Arabidopsis and Populus. Planta *232*, 337–352.

Griffiths, G., and Harwood, J.L. (1991). The regulation of triacylglycerol biosynthesis in cocoa (Theobroma cacao) L. Planta *184*, 279–284.

Grimberg, Å., Carlsson, A., Marttila, S., Bhalerao, R., and Hofvander, P. (2015). Transcriptional transitions in Nicotiana benthamiana leaves upon induction of oil synthesis by WRINKLED1 homologs from diverse species and tissues. BMC Plant Biol. *15*, 192.

Grimberg, Å., Lager, I., Street, N.R., Robinson, K.M., Marttila, S., Mähler, N., Ingvarsson, P.K., and Bhalerao, R.P. (2018). Storage lipid accumulation is controlled by photoperiodic signal acting via regulators of growth cessation and dormancy in hybrid aspen. New Phytol. *219*, 619–630.

Han, K.-H., Meilan, R., Ma, C., and Strauss, S.H. (2000). An Agrobacterium tumefaciens transformation protocol effective on a variety of cottonwood hybrids (genus Populus). Plant Cell Rep. *19*, 315–320.

Han, X., Ma, S., Kong, X., Takano, T., and Liu, S. (2013). Efficient Agrobacterium-Mediated Transformation of Hybrid Poplar Populus davidiana Dode × Populus bollena Lauche. Int. J. Mol. Sci. *14*, 2515–2528.

Hilhorst, H.W.M., and Karssen, C.M. (1992). Seed dormancy and germination: the role of abscisic acid and gibberellins and the importance of hormone mutants. Plant Growth Regul. *11*, 225–238.

Hoang, M.H.T., Nguyen, X.C., Lee, K., Kwon, Y.S., Pham, H.T.T., Park, H.C., Yun, D.-J., Lim, C.O., and Chung, W.S. (2012). Phosphorylation by AtMPK6 is required for the biological function of AtMYB41 in Arabidopsis. Biochem. Biophys. Res. Commun. *422*, 181–186.

Hobbs, D.H., Lu, C., and Hills, M.J. (1999). Cloning of a cDNA encoding diacylglycerol acyltransferase from Arabidopsis thaliana and its functional expression. FEBS Lett. *452*, 145–149.

Hofvander, P., Ischebeck, T., Turesson, H., Kushwaha, S.K., Feussner, I., Carlsson, A.S., and Andersson, M. (2016). Potato tuber expression of Arabidopsis WRINKLED1 increase triacylglycerol and membrane lipids while affecting central carbohydrate metabolism. Plant Biotechnol. J. *14*, 1883–1898.

Hooker, T.S., Millar, A.A., and Kunst, L. (2002). Significance of the expression of the CER6 condensing enzyme for cuticular wax production in Arabidopsis. Plant Physiol. *129*, 1568–1580.

Hubbard, K.E., Nishimura, N., Hitomi, K., Getzoff, E.D., and Schroeder, J.I. (2010). Early abscisic acid signal transduction mechanisms: newly discovered components and newly emerging questions. Genes Dev. *24*, 1695–1708.

Huerlimann, R., Steinig, E.J., Loxton, H., Zenger, K.R., Jerry, D.R., and Heimann, K. (2014). The effect of nitrogen limitation on acetyl-CoA carboxylase expression and fatty acid content in Chromera velia and Isochrysis aff. galbana (TISO). Gene *543*, 204–211.

Ishitani, M., Xiong, L., Stevenson, B., and Zhu, J.K. (1997). Genetic analysis of osmotic and cold stress signal transduction in Arabidopsis: interactions and convergence of abscisic acid-dependent and abscisic acid-independent pathways. Plant Cell *9*, 1935–1949.

Ivarson, E., Leiva-Eriksson, N., Ahlman, A., Kanagarajan, S., Bülow, L., and Zhu, L.-H. (2017a). Effects of Overexpression of WRI1 and Hemoglobin Genes on the Seed Oil Content of Lepidium campestre. Front. Plant Sci. *7*.

Ivarson, E., Iven, T., Sturtevant, D., Ahlman, A., Cai, Y., Chapman, K., Feussner, I., and Zhu, L.-H. (2017b). Production of wax esters in the wild oil species Lepidium campestre. Ind. Crops Prod. *108*, 535–542.

Iven, T., Herrfurth, C., Hornung, E., Heilmann, M., Hofvander, P., Stymne, S., Zhu, L.-H., and Feussner, I. (2013). Wax ester profiling of seed oil by nano-electrospray ionization tandem mass spectrometry. Plant Methods *9*, 24.

Iven, T., Hornung, E., Heilmann, M., and Feussner, I. (2016). Synthesis of oleyl oleate wax esters in Arabidopsis thaliana and Camelina sativa seed oil. Plant Biotechnol. J. *14*, 252–259.

Jako, C., Kumar, A., Wei, Y., Zou, J., Barton, D.L., Giblin, E.M., Covello, P.S., and Taylor, D.C. (2001). Seed-Specific Over-Expression of an Arabidopsis cDNA Encoding a Diacylglycerol Acyltransferase Enhances Seed Oil Content and Seed Weight. Plant Physiol. *126*, 861–874.

Jetter, R., and Kunst, L. (2008). Plant surface lipid biosynthetic pathways and their utility for metabolic engineering of waxes and hydrocarbon biofuels. Plant J. *54*, 670–683.

Jiang, L., Wang, Y., Björn, L.O., and Li, S. (2009). Arabidopsis RADICAL-INDUCED CELL DEATH1 is involved in UV-B signaling. Photochem. Photobiol. Sci. *8*, 838.

Jones, R.J., and Mansfield, T.A. (1970). Suppression of Stomatal Opening in Leaves Treated with Abscisic Acid. J. Exp. Bot. *21*, 714–719.

Kalscheuer, R., Stöveken, T., Luftmann, H., Malkus, U., Reichelt, R., and Steinbüchel, A. (2006). Neutral Lipid Biosynthesis in Engineered Escherichia coli: Jojoba Oil-Like Wax Esters and Fatty Acid Butyl Esters. Appl. Environ. Microbiol. *72*, 1373–1379.

Katavic, V., Reed, D.W., Taylor, D.C., Giblin, E.M., Barton, D.L., Zou, J., MacKenzie, S.L., Covello, P.S., and Kunst, L. (1995). Alteration of Seed Fatty Acid Composition by an Ethyl Methanesulfonate-Induced Mutation in Arabidopsis thaliana Affecting Diacylglycerol Acyltransferase Activity. Plant Physiol. *108*, 399–409.

Kaup, M.T., Froese, C.D., and Thompson, J.E. (2002). A Role for Diacylglycerol Acyltransferase during Leaf Senescence. Plant Physiol. *129*, 1616–1626.

Kawelke, S., and Feussner, I. (2015). Two Predicted Transmembrane Domains Exclude Very Long Chain Fatty acyl-CoAs from the Active Site of Mouse Wax Synthase. PLOS ONE *10*, e0145797.

Kay, R., Chan, A., Daly, M., and Mcpherson, J. (1987). Duplication of CaMV 35S Promoter Sequences Creates a Strong Enhancer for Plant Genes. Science *236*, 1299–1302.

Kennedy, E.P. (1961). Biosynthesis of complex lipids. Fed. Proc. *20*, 934–940.

Ko, J.-H., Kim, H.-T., Hwang, I., and Han, K.-H. (2012). Tissue-type-specific transcriptome analysis identifies developing xylem-specific promoters in poplar. Plant Biotechnol. J. *10*, 587–596.

Kong, Y., Chen, S., Yang, Y., and An, C. (2013). ABA-insensitive (ABI) 4 and ABI5 synergistically regulate DGAT1 expression in Arabidopsis seedlings under stress. FEBS Lett. *587*, 3076–3082.

Kosma, D.K., and Jenks, M.A. (2007). Eco-Physiological and Molecular-Genetic Determinants of Plant Cuticle Function in Drought and Salt Stress Tolerance. In Advances in Molecular Breeding Toward Drought and Salt Tolerant Crops, M.A. Jenks, P.M. Hasegawa, and S.M. Jain, eds. (Dordrecht: Springer Netherlands), pp. 91–120.

Kosma, D.K., Bourdenx, B., Bernard, A., Parsons, E.P., Lü, S., Joubès, J., and Jenks, M.A. (2009). The Impact of Water Deficiency on Leaf Cuticle Lipids of Arabidopsis. Plant Physiol. *151*, 1918–1929.

Kumar, S., Kaushal, N., Nayyar, H., and Gaur, P. (2012). Abscisic acid induces heat tolerance in chickpea (Cicer arietinum L.) seedlings by facilitated accumulation of osmoprotectants. Acta Physiol. Plant. *34*, 1651–1658.

Kumar, S., Sachdeva, S., Bhat, K.V., and Vats, S. (2018). Plant Responses to Drought Stress: Physiological, Biochemical and Molecular Basis. In Biotic and Abiotic Stress Tolerance in Plants, S. Vats, ed. (Singapore: Springer Singapore), pp. 1–25.

Larisch, C., Dittrich, M., Wildhagen, H., Lautner, S., Fromm, J., Polle, A., Hedrich, R., Rennenberg, H., Müller, T., and Ache, P. (2012). Poplar Wood Rays Are Involved in Seasonal Remodeling of Tree Physiology. Plant Physiol. *160*, 1515–1529.

Leclercq, J., Szabolcs, T., Martin, F., and Montoro, P. (2015). Development of a new pCAMBIA binary vector using Gateway® technology. Plasmid *81*, 50–54.

Lee, S.B., Kim, H., Kim, R.J., and Suh, M.C. (2014). Overexpression of Arabidopsis MYB96 confers drought resistance in Camelina sativa via cuticular wax accumulation. Plant Cell Rep. *33*, 1535–1546.

Li, L., Du, Y., He, C., Dietrich, C.R., Li, J., Ma, X., Wang, R., Liu, Q., Liu, S., Wang, G., et al. (2019). Maize glossy6 is involved in cuticular wax deposition and drought tolerance. J. Exp. Bot. *70*, 3089–3099.

Li-Beisson, Y., Shorrosh, B., Beisson, F., Andersson, M.X., Arondel, V., Bates, P.D., Baud, S., Bird, D., DeBono, A., Durrett, T.P., et al. (2010). Acyl-Lipid Metabolism. Arab. Book *2010*.

Lu, H., Viswanath, V., Ma, C., Etherington, E., Dharmawardhana, P., Shevchenko, O., Strauss, S.H., Pearce, D.W., Rood, S.B., and Busov, V. (2015). Recombinant DNA modification of gibberellin metabolism alters growth rate and biomass allocation in Populus. Tree Genet. Genomes *11*, 127.

Ma, W., Kong, Q., Arondel, V., Kilaru, A., Bates, P.D., Thrower, N.A., Benning, C., and Ohlrogge, J.B. (2013). WRINKLED1, A Ubiquitous Regulator in Oil Accumulating Tissues from Arabidopsis Embryos to Oil Palm Mesocarp. PLoS ONE *8*.

Macková, J., Vašková, M., Macek, P., Hronková, M., Schreiber, L., and Šantrůček, J. (2013). Plant response to drought stress simulated by ABA application: Changes in chemical composition of cuticular waxes. Environ. Exp. Bot. *86*, 70–75.

Mader, M., Le Paslier, M.-C., Bounon, R., Bérard, A., Rampant, P.F., Fladung, M., Leplé, J.-C., and Kersten, B. (2016). Whole-genome draft assembly of Populus tremula x P. alba clone INRA 717-1B4. Silvae Genet. *65*, 74–79.

Maheshwari, P., and Kovalchuk, I. (2016). Agrobacterium-Mediated Stable Genetic Transformation of Populus angustifolia and Populus balsamifera. Front. Plant Sci. *7*.

Maiti R and Rodriguez Hg (2016). Variability in Epicuticular Wax in 35 Woody Plants in Linares, Northeast Mexico. For. Res. Open Access *05*.

Maravi, D.K., Kumar, S., Sharma, P.K., Kobayashi, Y., Goud, V.V., Sakurai, N., Koyama, H., and Sahoo, L. (2016). Ectopic expression of AtDGAT1, encoding diacylglycerol O-acyltransferase exclusively committed to TAG biosynthesis, enhances oil accumulation in seeds and leaves of Jatropha. Biotechnol. Biofuels *9*, 226.

Martin, L.B.B., Romero, P., Fich, E.A., Domozych, D.S., and Rose, J.K.C. (2017). Cuticle Biosynthesis in Tomato Leaves Is Developmentally Regulated by Abscisic Acid. Plant Physiol. *174*, 1384–1398.

McAdam, S.A.M., Brodribb, T.J., and Ross, J.J. (2016). Shoot-derived abscisic acid promotes root growth. Plant Cell Environ. *39*, 652–659.

Meyer, S., Nowak, K., Sharma, V.K., Schulze, J., Mendel, R.R., and Hänsch, R. (2004). Vectors for RNAi Technology in Poplar. Plant Biol. *7*, 100–104.

Miwa, T.K. (1971). Jojoba oil wax esters and derived fatty acids and alcohols: Gas chromatographic analyses. J. Am. Oil Chem. Soc. *48*, 259–264.

Muhr, M., Prüfer, N., Paulat, M., and Teichmann, T. (2016). Knockdown of strigolactone biosynthesis genes in Populus affects BRANCHED1 expression and shoot architecture. New Phytol. *212*, 613–626.

Murashige, T., and Skoog, F. (1962). A Revised Medium for Rapid Growth and Bio Assays with Tobacco Tissue Cultures. Physiol. Plant. *15*, 473–497.

Negin, B., and Moshelion, M. (2016). The evolution of the role of ABA in the regulation of water-use efficiency: From biochemical mechanisms to stomatal conductance. Plant Sci. *251*, 82–89.

Ni, Y., Sun, Z., Huang, X., Huang, C., and Guo, Y. (2015). Variations of cuticular wax in mulberry trees and their effects on gas exchange and post-harvest water loss. Acta Physiol. Plant. *37*, 112.

Nookaraju, A., Pandey, S.K., Fujino, T., Kim, J.Y., Suh, M.C., and Joshi, C.P. (2014). Enhanced accumulation of fatty acids and triacylglycerols in transgenic tobacco stems for enhanced bioenergy production. Plant Cell Rep. *33*, 1041–1052.

Park, J.-J., Jin, P., Yoon, J., Yang, J.-I., Jeong, H.J., Ranathunge, K., Schreiber, L., Franke, R., Lee, I.-J., and An, G. (2010). Mutation in Wilted Dwarf and Lethal 1 (WDL1) causes abnormal cuticle formation and rapid water loss in rice. Plant Mol. Biol. *74*, 91–103.

Patwari, P., Salewski, V., Gutbrod, K., Kreszies, T., Dresen-Scholz, B., Peisker, H., Steiner, U., Meyer, A.J., Schreiber, L., and Dörmann, P. (2019). Surface wax esters contribute to drought tolerance in Arabidopsis. Plant J. *98*, 727–744.

Paux, E., Tamasloukht, M., Ladouce, N., Sivadon, P., and Grima-Pettenati, J. (2004). Identification of genes preferentially expressed during wood formation in <Emphasis Type="Italic">Eucalyptus</Emphasis>. Plant Mol. Biol. *55*, 263–280.

Podevin, N., and Jardin, P. du (2012). Possible consequences of the overlap between the CaMV 35S promoter regions in plant transformation vectors used and the viral gene VI in transgenic plants. GM Crops Food *3*, 296–300.

Sachse, D., Kahmen, A., and Gleixner, G. (2009). Significant seasonal variation in the hydrogen isotopic composition of leaf-wax lipids for two deciduous tree ecosystems (Fagus sylvativa and Acerpseudoplatanus). Org. Geochem. *40*, 732–742.

Sánchez, F., Manzanares, M., Andrés, E., Tenorio, J.L., and Ayerbe, L. (2001). Residual transpiration rate, epicuticular wax load and leaf colour of pea plants in drought conditions. Influence on harvest index and canopy temperature. Eur. J. Agron. - EUR J AGRON *15*, 57–70.

Sanjaya, Durrett, T.P., Weise, S.E., and Benning, C. (2011). Increasing the energy density of vegetative tissues by diverting carbon from starch to oil biosynthesis in transgenic Arabidopsis. Plant Biotechnol. J. *9*, 874–883.

Sauter, J.J., and Cleve, B. van (1994). Storage, mobilization and interrelations of starch, sugars, protein and fat in the ray storage tissue of poplar trees. Trees *8*, 297–304.

Savadi, S., Naresh, V., Kumar, V., and Bhat, S.R. (2015). Seed-specific overexpression of Arabidopsis DGAT1 in Indian mustard (Brassica juncea) increases seed oil content and seed weight. Botany *94*, 177–184.

Schnurr, J.A., and Guerra, D.J. (2000). The CaMV-35S promoter is sensitive to shortened photoperiod in transgenic tobacco. Plant Cell Rep. *19*, 279–282.

Scholander, P.F., Hammel, H.T., Hemmingsen, E.A., and Bradstreet, E.D. (1964). HYDROSTATIC PRESSURE AND OSMOTIC POTENTIAL IN LEAVES OF MANGROVES AND SOME OTHER PLANTS*. Proc. Natl. Acad. Sci. U. S. A. *52*, 119–125.

Schreiber, L., and Riederer, M. (1996). Ecophysiology of cuticular transpiration: comparative investigation of cuticular water permeability of plant species from different habitats. Oecologia *107*, 426–432.

Seo, P.J., and Park, C.-M. (2011). Cuticular wax biosynthesis as a way of inducing drought resistance. Plant Signal. Behav. *6*, 1043–1045.

Seo, P.J., Xiang, F., Qiao, M., Park, J.-Y., Lee, Y.N., Kim, S.-G., Lee, Y.-H., Park, W.J., and Park, C.-M. (2009). The MYB96 transcription factor mediates abscisic acid signaling during drought stress response in Arabidopsis. Plant Physiol. *151*, 275–289.

Sham, A., and Aly, M. (2012). Bioinformatics Based Comparative Analysis of Omega-3 Fatty Acids in Desert Plants and Their Role in Stress Resistance and Tolerance. Int. J. Plant Res. *2*, 80–89.

Sharp, R.E., and LeNoble, M.E. (2002). ABA, ethylene and the control of shoot and root growth under water stress. J. Exp. Bot. *53*, 33–37.

Shepherd, T., and Griffiths, D.W. (2006). The effects of stress on plant cuticular waxes. New Phytol. *171*, 469–499.

Shockey, J.M., Gidda, S.K., Chapital, D.C., Kuan, J.-C., Dhanoa, P.K., Bland, J.M., Rothstein, S.J., Mullen, R.T., and Dyer, J.M. (2006). Tung Tree DGAT1 and DGAT2 Have Nonredundant Functions in Triacylglycerol Biosynthesis and Are Localized to Different Subdomains of the Endoplasmic Reticulum. Plant Cell *18*, 2294–2313.

Sinnott, E.W. (1918). Factors Determining Character and Distribution of Food Reserve in Woody Plants. Bot. Gaz. *66*, 162–175.

Stark, R.E., and Tian, S. (2018). The Cutin Biopolymer Matrix. In Annual Plant Reviews Online, (American Cancer Society), pp. 126–144.

Sturtevant, D., Lu, S., Zhou, Z.-W., Shen, Y., Wang, S., Song, J.-M., Zhong, J., Burks, D.J., Yang, Z.-Q., Yang, Q.-Y., et al. (2020). The genome of jojoba (Simmondsia chinensis): A taxonomically isolated species that directs wax ester accumulation in its seeds. Sci. Adv. *6*, eaay3240.

Takeda, S., Iwasaki, A., Tatematsu, K., and Okada, K. (2014). The Half-Size ABC Transporter FOLDED PETALS 2/ABCG13 Is Involved in Petal Elongation through Narrow Spaces in Arabidopsis thaliana Floral Buds. Plants *3*, 348–358.

Turchetto-Zolet, A.C., Maraschin, F.S., de Morais, G.L., Cagliari, A., Andrade, C.M., Margis-Pinheiro, M., and Margis, R. (2011). Evolutionary view of acyl-CoA diacylglycerol acyltransferase (DGAT), a key enzyme in neutral lipid biosynthesis. BMC Evol. Biol. *11*, 263.

Tuskan, G.A., Difazio, S., Jansson, S., Bohlmann, J., Grigoriev, I., Hellsten, U., Putnam, N., Ralph, S., Rombauts, S., Salamov, A., et al. (2006). The genome of black cottonwood, Populus trichocarpa (Torr. & Gray). Science *313*, 1596–1604.

Tylewicz, S., Petterle, A., Marttila, S., Miskolczi, P., Azeez, A., Singh, R.K., Immanen, J., Mähler, N., Hvidsten, T.R., Eklund, D.M., et al. (2018). Photoperiodic control of seasonal growth is mediated by ABA acting on cell-cell communication. Science *360*, 212–215.

Van Erp, H., Kelly, A., Menard, G., and Eastmond, P. (2014). Multigene Engineering of Triacylglycerol Metabolism Boosts Seed Oil Content in Arabidopsis. Plant Physiol. *165*.

Vanhercke, T., Tahchy, A.E., Shrestha, P., Zhou, X.-R., Singh, S.P., and Petrie, J.R. (2013). Synergistic effect of WRI1 and DGAT1 coexpression on triacylglycerol biosynthesis in plants. FEBS Lett. *587*, 364–369.

Wang, L., Shen, W., Kazachkov, M., Chen, G., Chen, Q., Carlsson, A.S., Stymne, S., Weselake, R.J., and Zou, J. (2012). Metabolic Interactions between the Lands Cycle and the Kennedy Pathway of Glycerolipid Synthesis in Arabidopsis Developing Seeds. Plant Cell *24*, 4652–4669.

Wang, P., Wang, Z., Dou, Y., Zhang, X., Wang, M., and Tian, X. (2013). Genome-wide identification and analysis of membrane-bound O-acyltransferase (MBOAT) gene family in plants. Planta *238*, 907–922.

Weselake, R.J., Shah, S., Tang, M., Quant, P.A., Snyder, C.L., Furukawa-Stoffer, T.L., Zhu, W., Taylor, D.C., Zou, J., Kumar, A., et al. (2008). Metabolic control analysis is helpful for informed genetic manipulation of oilseed rape (Brassica napus) to increase seed oil content. J. Exp. Bot. *59*, 3543–3549.

Williamson, J.D., Hirsch-Wyncott, M.E., Larkins, B.A., and Gelvin, S.B. (1989). Differential Accumulation of a Transcript Driven by the CaMV 35S Promoter in Transgenic Tobacco. Plant Physiol. *90*, 1570–1576.

Xue, D., Zhang, X., Lu, X., Chen, G., and Chen, Z.-H. (2017). Molecular and Evolutionary Mechanisms of Cuticular Wax for Plant Drought Tolerance. Front. Plant Sci. *8*.

Ye, J., Wang, C., Sun, Y., Qu, J., Mao, H., and Chua, N.-H. (2018). Overexpression of a Transcription Factor Increases Lipid Content in a Woody Perennial Jatropha curcas. Front. Plant Sci. *9*.

Yeap, W.-C., Lee, F.-C., Shan, D.K.S., Musa, H., Appleton, D.R., and Kulaveerasingam, H. (2017). WRI1-1, ABI5, NF-YA3 and NF-YC2 increase oil biosynthesis in coordination with hormonal signaling during fruit development in oil palm. Plant J. *91*, 97–113.

Yu, D., Hornung, E., Iven, T., and Feussner, I. (2018). High-level accumulation of oleyl oleate in plant seed oil by abundant supply of oleic acid substrates to efficient wax ester synthesis enzymes. Biotechnol. Biofuels *11*.

Yu, D., Wildhagen, H., Tylewicz, S., Miskolczi, P.C., Bhalerao, R.P., and Polle, A. (2019). Abscisic acid signalling mediates biomass trade-off and allocation in poplar. New Phytol. *223*, 1192–1203.

Zale, J., Jung, J.H., Kim, J.Y., Pathak, B., Karan, R., Liu, H., Chen, X., Wu, H., Candreva, J., Zhai, Z., et al. (2016). Metabolic engineering of sugarcane to accumulate energy-dense triacylglycerols in vegetative biomass. Plant Biotechnol. J. *14*, 661–669.

Zhang, F.-Y., Yang, M.-F., and Xu, Y.-N. (2005). Silencing of DGAT1 in tobacco causes a reduction in seed oil content. Plant Sci. *169*, 689–694.

Zhao, Y., Chan, Z., Gao, J., Xing, L., Cao, M., Yu, C., Hu, Y., You, J., Shi, H., Zhu, Y., et al. (2016). ABA receptor PYL9 promotes drought resistance and leaf senescence. Proc. Natl. Acad. Sci. *113*, 1949–1954.

Zheng, Y., Schumaker, K.S., and Guo, Y. (2012). Sumoylation of transcription factor MYB30 by the small ubiquitin-like modifier E3 ligase SIZ1 mediates abscisic acid response in Arabidopsis thaliana. Proc. Natl. Acad. Sci. U. S. A. *109*, 12822–12827.

Zhou, L., Ni, E., Yang, J., Zhou, H., Liang, H., Li, J., Jiang, D., Wang, Z., Liu, Z., and Zhuang, C. (2013). Rice OsGL1-6 Is Involved in Leaf Cuticular Wax Accumulation and Drought Resistance. PLOS ONE *8*, e65139.

7. Supplemental information

7.1. Sequences

7.1.1. Genes

>AtDGAT1

ATGGCGATTTTGGATTCTGCTGGCGTTACTACGGTGACGGAGAACGGTGGCGGAGAGTTCGTCGATCTTGATAGGCTTCGTCGACGGAA
ATCGAGATCGGATTCTTCTAACGGACTTCTTCTCTCTGGTTCCGATAATAATTCTCCTTCGGATGATGTTGGAGCTCCCGCCGACGTTAGG
GATCGGATTGATTCCGTTGTTAACGATGACGCTCAGGGAACAGCCAATTTGGCCGGAGATAATAACGGTGGTGGCGATAATAACGGTG
GTGGAAGAGGCGGCGGAGAAGGAAGAGGAAACGCCGATGCTACGTTTACGTATCGACCGTCGGTTCCAGCTCATCGGAGGGCGAGAG
AGAGTCCACTTAGCTCCGACGCAATCTTCAAACAGAGCCATGCCGGATTATTCAACCTCTGTGTAGTAGTTCTTATTGCTGTAAACAGTAG
ACTCATCATCGAAAATCTTATGAAGTATGGTTGGTTGATCAGAACGGATTTCTGGTTTAGTTCAAGATCGCTGCGAGATTGGCCGCTTTTC
ATGTGTTGTATATCCCTTTCGATCTTTCCTTTGGCTGCCTTTACGGTTGAGAAATTGGTACTTCAGAAATACATATCAGAACCTGTTGTCAT
CTTTCTTCATATTATTATCACCATGACAGAGGTTTTGTATCCAGTTTACGTCACCCTAAGGTGTGATTCTGCTTTTTTATCAGGTGTCACTTT
GATGCTCCTCACTTGCATTGTGTGGCTAAAGTTGGTTTCTTATGCTCATACTAGCTATGACATAAGATCCCTAGCCAATGCAGCTGATAAG
GCCAATCCTGAAGTCTCCTACTACGTTAGCTTGAAGAGCTTGGCATATTTCATGGTCGCTCCCACATTGTGTTATCAGCCAAGTTATCCAC
GTTCTGCATGTATACGGAAGGGTTGGGTGGCTCGTCAATTTGCAAAACTGGTCATATTCACCGGATTCATGGGATTTATAATAGAACAAT
ATATAAATCCTATTGTCAGGAACTCAAAGCATCCTTTGAAAGGCGATCTTCTATATGCTATTGAAAGAGTGTTGAAGCTTTCAGTTCCAAA
TTTATATGTGTGGCTCTGCATGTTCTACTGCTTCTTCCACCTTTGGTTAAACATATTGGCAGAGCTTCTCTGCTTCGGGGATCGTGAATTCT
ACAAAGATTGGTGGAATGCAAAAAGTGTGGGAGATTACTGGAGAATGTGGAATATGCCTGTTCATAAATGGATGGTTCGACATATATAC
TTCCCGTGCTTGCGCAGCAAGATACCAAAGACACTCGCCATTATCATTGCTTTCCTAGTCTCTGCAGTCTTTCATGAGCTATGCATCGCAGT
TCCTTGTCGTCTCTTCAAGCTATGGGCTTTTCTTGGGATTATGTTTCAGGTGCCTTTGGTCTTCATCACAAACTATCTACAGGAAAGGTTTG
GCTCAACGGTGGGGAACATGATCTTCTGGTTCATCTTCTGCATTTTCGGACAACCGATGTGTGTGCTTCTTTATTACCACGACCTGATGAA
CCGAAAAGGATCGATGTCATGA

Figure 65: Sequence *AtDGAT1*.

>AtWRI1

ATGAAGAAGCGCTTAACCACTTCCACTTGTTCTTCTTCTCCATCTTCCTCTGTTTCTTCTTCTACTACTACTTCCTCTCCTATTCAGTCGGAGG
CTCCAAGGCCTAAACGAGCCAAAAGGGCTAAGAAATCTTCTCCTTCTGGTGATAAATCTCATAACCCGACAAGCCCTGCTTCTACCCGAC
GCAGCTCTATCTACAGAGGAGTCACTAGACATAGATGGACTGGGAGATTCGAGGCTCATCTTTGGGACAAAAGCTCTTGGAATTCGATT
CAGAACAAGAAAGGCAAACAAGTTTATCTGGGAGCATATGACAGTGAAGAAGCAGCAGCACATACGTACGATCTGGCTGCTCTCAAGTA
CTGGGGACCCGACACCATCTTGAATTTTCCGGCAGAGACGTACACAAAGGAATTGGAAGAAATGCAGAGAGTGACAAAGGAAGAATAT
TTGGCTTCTCTCCGCCGCCAGAGCAGTGGTTTCTCCAGAGGCGTCTCTAAATATCGCGGCGTCGCTAGGCATCACCACAACGGAAGATGG
GAGGCTCGGATCGGAAGAGTGTTTGGGAACAAGTACTTGTACCTCGGCACCTATAATACGCAGGAGGAAGCTGCTGCAGCATATGACAT
GGCTGCGATTGAGTATCGAGGCGCAAACGCGGTTACTAATTTCGACATTAGTAATTACATTGACCGGTTAAAGAAGAAAGGTGTTTTCCC
GTTCCCTGTGAACCAAGCTAACCATCAAGAGGGTATTCTTGTTGAAGCCAAACAAGAAGTTGAAACGAGAGAAGCGAAGGAAGAGCCT
AGAGAAGAAGTGAAACAACAGTACGTGGAAGAACCACCGCAAGAAGAAGAAGAGAAGGAAGAAGAGAAAGCAGAGCAACAAGAAGC
AGAGATTGTAGGATATTCAGAAGAAGCAGCAGTGGTCAATTGCTGCATAGACTCTTCAACCATAATGGAAATGGATCGTTGTGGGGACA
ACAATGAGCTGGCTTGGAACTTCTGTATGATGGATACAGGGTTTTCTCCGTTTTTGACTGATCAGAATCTCGCGAATGAGAATCCCATAG
AGTATCCGGAGCTATTCAATGAGTTAGCATTTGAGGACAACATCGACTTCATGTTCGATGATGGGAAGCACGAGTGCTTGAACTTGGAA
AATCTGGATTGTTGCGTGGTGGGAAGAGAGAGCCCACCCTCTTCTTCTTCACCATTGTCTTGCTTATCTACTGACTCTGCTTCATCAACAAC
AACAACAACAACCTCGGTTTCTTGTAACTATTTGGTCTGA

Figure 66: Sequence *AtWRI1*.

>ScWS

ATGGAGGTGGAGAAGGAGCTAAAGACCTTCTCAGAGGTATGGATCTCCGCCATAGCCGCCGCCTGCTACTGCCGCTTCGTCCCCGCCGT
TGCCCCTCACGGCGGCGCTCTCCGCCTCCTCCTCCTCCTCCCCGTCGTCCTCCTCTTCATTTTCCTCCCCCTCCGCCTCTCCTCCTTCCACCTC
GGCGGGCCCACCGCCTTGTATCTCGTCTGGCTTGCCAACTTCAAGCTCCTTCTCTTCGCCTTTCATCTTGGCCCTTTATCTAACCCCTCTCTC
TCTCTCCTTCACTTCATCTCCACCACCCTCCTCCCCATCAAGTTCAGAGATGACCCATCTAATGATCATGAGAAAAACAAGAGAACTCTGAG
TTTTGAGTGGCGTAAAGTTGTTCTTTTTGTTGCTAAGTTGGTGTTTTTTGCGGGTATTTTAAAGATTTATGAGTTTAGAAAAGATTTGCCTC
ATTTTGTGATCTCGGTGCTTTACTGTTTTCACTTCTATCTCGGGACGGAGATCACCTTAGCAGCAAGCGCAGTCATAGCTCGAGCCACGCT
AGGGTTAGACCTATACCCCCAGTTCAACGAGCCATACTTAGCCACCTCGCTGCAAGACTTCTGGGGGCGCAGGTGGAACCTCATGGTGTC
AGACATCTTGGGGTTGACAACATACCAGCCTGTCCGGCGTGTCCTCTCGAGGTGGGTCAGGCTGCGGTGGGAGGTCGCCGGCGCAATG
TTGGTGGCGTTCACGGTGTCGGGGCTAATGCATGAAGTGTTTTTCTTCTACTTAACTCGCGCGAGGCCCTCGTGGGAGGTGACGGGGTT
CTTTGTGTTGCATGGGGTTTGCACAGCCGTGGAGATGGTGGTGAAGAAGGCGGTTTCAGGCAAGGTGCGGCTGCGCCGGGAGGTGTCA
GGGGCGCTGACGGTGGGGTTCGTGATGGTGACTGGAGGGTGGTTGTTTTTGCCGCAGCTGGTGAGGCATGGGGTAGATTTGAAGACCA
TTGATGAGTATCCTGTCATGTTTAATTATACTCAGAAGAAATTGATGGGTTTGTTGGGGTGGTGAGGATCC

Figure 67: Sequence *ScWS*.

>*MaFAR*
ATGGCAATCCAGCAGGTCCACCACGCGGATACATCCTCATCAAAAGTGCTTGGCCAGCTTCGTGGCAAGCGCGTCTTGATCACCGGCACT
ACTGGGTTCCTGGGCAAGGTCGTCCTAGAGCGTCTAATCCGTGCCGTGCCGGACATTGGTGCGATTTATTTGCTGATTCGCGGTAATAAA
CGACATCCTGATGCCCGCTCAAGATTCTTGGAAGAGATTGCCACCTCGTCCGTTTTTGATCGCCTTCGTGAAGCTGACTCTGAAGGGTTTG
ACGCCTTCTTAGAAGAGAGGATTCATTGCGTCACCGGAGAGGTGACGGAAGCGGGATTCGGTATCGGCCAAGAAGACTACCGAAAACT
CGCTACAGAGTTAGATGCTGTAATCAATTCAGCCGCATCCGTGAACTTTCGAGAAGAATTAGACAAGGCTCTGGCCATCAACACCTTGTG
CTTACGGAATATTGCCGGGATGGTTGATTTAAATCCCAAGTTGGCCGTGCTTCAAGTGTCCACTTGCTACGTGAATGGGATGAATAGCGG
ACAGGTTACCGAAAGCGTTATCAAGCCGGCAGGTGAAGCAGTGCCTCGCTCTCCTGACGGGTTTTATGAAATCGAGGAGCTTGTTCGGC
TCCTCCAGGATAAGATCGAAGATGTTCAGGCCCGGTACAGTGGTAAAGTGCTTGAACGTAAATTAGTAGATCTTGGCATTCGCGAAGCC
AATCGGTACGGGTGGAGCGACACGTATACCTTTACGAAATGGCTCGGTGAGCAATTGCTCATGAAAGCGCTGAATGGTCGCACATTGAC
CATTTTGCGCCCGTCTATTATCGAAAGTGCCTTAGAAGAACCGGCACCGGGTTGGATTGAAGGAGTAAAAGTGGCTGATGCAATTATTTT
AGCGTATGCCCGTGAAAAAGTCACCCTCTTTCCGGGCAAACGGTCGGGTATAATCGACGTGATCCCAGTTGACTTAGTCGCGAATAGTAT
TATCTTAAGCCTCGCCGAAGCGCTGGGTGAGCCGGGTCGTCGTAGAATATATCAGTGTTGTAGTGGTGGCGGCAACCCGATCAGCCTTG
GCGAATTTATCGATCATCTCATGGCAGAGTCGAAAGCGAACTACGCAGCATACGACCATCTCTTTTACCGCCAACCCAGCAAACCATTCCT
GGCTGTAAACCGCGCGCTGTTCGATCTGGTAATCAGCGGCGTGCGCCTGCCACTGAGCCTGACGGATCGTGTTCTGAAACTGCTGGGCA
ACAGCCGCGATCTGAAAATGCTGCGTAACCTGGATACCACGCAGTCGCTGGCTACCATTTTTGGTTTTTATACCGCGCCGGATTATATCTT
CCGCAACGATGAACTGATGGCGCTGGCGAACCGCATGGGCGAAGTTGATAAAGGCCTGTTCCCCGTGGATGCGCGCCTGATTGATTGG
GAACTGTATCTGCGTAAAATACACCTGGCCGGCCTGAACCGTTATGCGCTGAAAGAACGTAAAGTGTATTCGCTGAAAACGGCCCGTCA
ACGTAAAAAAGCGGCATGAGGATCC

Figure 68: Sequence *MaFAR*.

7.1.2. Promoter

>DX15_Ko_et_al
TTCCCCCTTTTGGTTCAATGCCTTTTATTCTTCCAAAATTATTTCATATTTTGTATCCGGAGGACATATTTGTTTCAAAAGGTGTCAGAAAAT
CAAAGCCCATTGAAAATATATAAACATATATAGATATAAAAACTCAAGGGTTCATTCCAAAATATAAGAACAAACTGATTGAATTAATTTG
TTATTTTAAGAACACTGTCTATATGTTTATATAGTGGGAGGTAGTGTTTTTTAAATCATATACTAACTTATTATAAAAATAAATCATAAAAA
AGGAACCTCAAGCATCCCCTGGTAAGCTCGTATGTAGGAATACTCGGAGATCAAATGTCCGAATGTCAAATGTTAAGGCAAGTGAAATA
TCCCTGACTTTTTAGCAAGCAAATTGTTGAGTAGCTAAAATGAATTATTTTAATATTTTTAAATCATTTTAATATATTAATATTAAAAAAAAT
TAAATATTTTTTTTAATACATTTTCAATAACAAACACTTTAAAATATAATCTTTGTCACACTCTTAAACAGTAACAGCAGAAAGCATATGTG
AGTGATATAGCTATAGTTGCTGTTTGACACGGACAATCTCCATCTAAATTCATGAATAATAAAGTTTTGCCTACACACCCACTTGAAATCTC
CTCCTAGTTTTCCTGATTTGCCATGCTAACTACAAGAACAAGATGCTAGCTAGTATCTTGTTCTGTCTCTCGCTCTCTCTCTATCTCTCCAG**T**
TGATAGTTGATAGTTGATAGTTGATAGCTGATACCCTCCCACCTTTCCCAGAAAGATGATTGAGGAACTAGTCACTGTGTTCGTGTAACT
AATACTGTTCATGGC**ACCTAAC**TTGATCCTCTCTTCACCAGACCACTATAAAAACCCTATCTGTCCTCCTCATAATCATATCACTACACCCAA
CACTTCTGCAAGCACAACTCCATTCAAGAACATCAAGAGTATAGGCCGCCGCTGCAACAAAACAGCACTCCTAGCTACTTCAAGATGAGG
CCACAATCTTTCATCTT

Figure 69: Sequence of DX15 promoter region, published by Ko et al. (2012). Repetitive TTGATAG element is highlighted with a grey box. The AC element (ACCTAAC) is highlighted in bold.

>DX15_Sequence
TTCCCCCTTTTGGTTCAATGCCTTTTATTCTTCCAAATTAATTTCAATATTTTGTATCCGGAGGAACATATTTGTTTCAAAAGGTGTCAGAAA
ATCAAAGCCCATTGAAAATATATAAACATATATAGATATAAAAACTCAAGGATTCATTCCAAAATATAAGAACAAACTGATTGAATTAATT
TGTTATTTTAAGAACACTGTCTATATGTTTATATAGTGGTAGGTAGTGTTTTTAAAATCATATACTAACTTATTATAAAAATAAATCATAAA
AAAGGAACCTCAAGCATCCCCTGGTAAGCTCGTATGTAGGAATACTCGGAGGTCAAATGTCCGAATGTCAAATGTTAAGGCAAGTGAAA
TATCCCTGACTTTTTAGCAAGCAAATTGTTGAGTAGCTAAAATGAATTATTTTAATATTTTCAAATCATTTTAATATATTAATATTAAAAAAA
ATTAAATATTTTTTTTAATACATTTTCAATAACAAACACTTTAAAATATAATCTTTGTCACACTCTTAAACAGTAACAGCAGAAAGCATATGT
GAGTGATATAGCTATAGTTGCTGTTTGACACGGACAATCTCCATCTAAATTCATGAATAATAAAGTTTTGCCTACACACCCACTTGAAATC
TCCTCCTAGTTTTCCTGATTTGCCATGCTAACTACAAGAACAAGATGCTAGCTAGTATCTTGTTCTGTCTCTCGCTCTCTCTCTACCTCTCCA
G**TTGATAGTTGATAGTTGATAG**CTGATACCCTCCCACCTTTCCCAGAAAGATGATTGAGGAACTAGTCACTGTGTTCGTGTAACTAATAC
TGTTCATGGC**ACCTAAC**TTGATCCTATCTTCACCAGACCACTATAAAAACCCTATCTGTCCTCCTCATAATCATATCACTACACCCAACACTT
CTGCAAGCACAACTCCATTCAAGAACATCAAGAGTATAGGCCGCCGCTGCAACAAAACAGCACTCCTAGCTACTTCAAGATGAGGCCACA
ATCTTTCATCTT

Figure 70: Sequence of DX15 promoter cloned in this study. Repetitive TTGATAG element is highlighted with a grey box. The AC element (ACCTAAC) is highlighted in bold.

>35S_P-entry_gateway_system
AGAGCAGCTTGCCAACATGGTGGAGCACGACACTCTCGTCTACTCCAAGAATATCAAAGATACAGTCTCAGAAGACCAAAGGGCTATTG
AGACTTTTCAACAAAGGGTAATATCGGGAAACCTCCTCGGATTCCATTGCCCAGCTATCTGTCACTTCATCAAAAGGACAGTAGAAAAGG
AAGGTGGCACCTACAAATGCCATCATTGCGATAAAGGAAAGGCTATCGTTCAAGATGCCTCTGCCGACAGTGGTCCCAAAGATGGACCC
CCACCCACGAGGAGCATCGTGGAAAAAGAAGACGTTCCAACCACGTCTTCAAAGCAAGTGGATTGATGTGATAACATGGTGGAGCACG
ACACTCTCGTCTACTCCAAGAATATCAAAGATACAGTCTCAGAAGACCAAAGGGCTATTGAGACTTTTCAACAAAGGGTAATATCGGGAA
ACCTCCTCGGATTCCATTGCCCAGCTATCTGTCACTTCATCAAAAGGACAGTAGAAAAGGAAGGTGGCACCTACAAATGCCATCATTGCG
ATAAAGGAAAGGCTATCGTTCAAGATGCCTCTGCCGACAGTGGTCCCAAAGATGGACCCCCACCCACGAGGAGCATCGTGGAAAAAGA
AGACGTTCCAACCACGTCTTCAAAGCAAGTGGATTGATGTGATATCTCCACTGACGTAAGGGATGACGCACAATCCCACTATCCTTCGCA
AGACCTTCCTCTATATAAGGAAGTTCATTTCATTTGGAGAGGACACGCTGAAATCACCAGTCTCTCTCTACAAATCTATCTCTG

Figure 71: Sequence of the 35S promoter used in the pEntry vector system.

>35S_pK7WG2
GATCTCCTTTGCCCCGGAGATCACCATGGACGACTTTCTCTATCTCTACGATCTAGGAAGAAAGTTCGACGGAGAAGGTGACGATACCAT
GTTCACCACCGATAATGAGAAGATTAGCCTCTTCAATTTCAGAAAGAATGCTGACCCACAGATGGTTAGAGAGGCCTACGCGGCAGGTC
TCATCAAGACGATCTACCCGAGTAATAATCTCCAGGAGATCAAATACCTTCCCAAGAAGGTTAAAGATGCAGTCAAAAGATTCAGGACTA
ACTGCATCAAGAACACAGAGAAAGATATATTTCTCAAGATCAGAAGTACTATTCCAGTATGGACGATTCAAGGCTTGCTTCATAAACCAA
GGCAAGTAATAGAGATTGGAGTCTCTAAGAAAGTAGTTCCTACTGAATCAAAGGCCATGGAGTCAAAAATTCAGATCGAGGATCTAACA
GAACTCGCCGTGAAGACTGGCGAACAGTTCATACAGAGTCTTTTACGACTCAATGACAAGAAGAAAATCTTCGTCAACATGGTGGAGCA
CGACACTCTCGTCTACTCCAAGAATATCAAAGATACAGTCTCAGAAGACCAAAGGGCTATTGAGACTTTTCAACAAAGGGTAATATCGGG
AAACCTCCTCGGATTCCATTGCCCAGCTATCTGTCACTTCATCAAAAGGACAGTAGAAAAGGAAGGTGGCACCTACAAATGCCATCATTG
CGATAAAGGAAAGGCTATCGTTCAAGATGCCTCTGCCGACAGTGGTCCCAAAGATGGACCCCCACCCACGAGGAGCATCGTGGAAAAA
GAAGACGTTCCAACCACGTCTTCAAAGCAAGTGGATTGATGTGATATCTCCACTGACGTAAGGGATGACGCACAATCCCACTATCCTTCG
CAAGACCCTTCCTCTATATAAGGAAGTTCATTTCATTTGGAGAGGACTGCAGGACGATCCGTATTTTTACAACAATTACCACAACAAAACA
AACAACAAACAACATTACAATTTACTATTCTAG

Figure 72: Sequence of the 35S promoter used in the pK7WG-pDONR vector system.

8. Appendix

8.1. Danksagung

Mein größter Dank gilt Prof. Dr. A. Polle für die Möglichkeit der Promotion in der Abteilung Forstbotanik und Baumphysiologie, ihren Einsatz für meine Person bezüglich des Stipendiums, ihre Hilfestellungen und Betreuung, für die Korrektur der schriftlichen Ausarbeitung und die Freiheiten, die ich hatte, um das Projekt weiterzuentwickeln.

Ich bedanke mich weiterhin bei Prof. Dr. C. Volkert und Prof. Dr. C. Mai für ihre Anregungen zum Projekt und als Mitglieder meines Thesis Komitees und Dr. habil. T. Teichmann für die Übernahme des Zweitgutachtens.

Ich möchte mich ebenfalls bei den Mitgliedern der Prüfungskommission bedanken: Prof. Dr. H. Militz, Prof. Dr. C. Mai, Prof. Dr. C. Volkert und bei Dr. C. Eckert.

Dem Niedersächsischen Ministerium für Wissenschaft und Kultur danke ich zudem für die finanzielle Unterstützung in Form eines Lichtenberg-Stipendiums, das mir die Teilnahme im Promotionsprogramm Materialforschung Holz ermöglicht hat.

Einen großen Dank gilt Dr. Merlin Muhr und Dr. habil. Thomas Teichmann für die Möglichkeit, die Methode des genetischen Transformierens von Pappeln zu erlernen und letztendlich zu etablieren. Ebenfalls bedanken möchte ich mich bei Dr. Ellen Hornung und Prof. Dr. Ivo Feussner für die Bereitstellung genetischen Materials und die Nutzung der Labors der Abteilung Biochemie der Pflanze, sowie bei Milena Lewandowska für die GC-MS – Messungen.

Weiterhin möchte ich mich bei allen Mitgliedern der Abteilung bedanken, die mir häufig mit gutem Rat und Tat zur Seite standen. Im Speziellen möchte ich mich bei Dr. Christian Eckert bedanken, für diverse Anregungen und Hilfestellungen beim Klonieren und bei Photosynthese-Messungen, Dr. Ulrike Lipka und Felix Häffner für die REM- Mikroskopie, Thomas Klein für die molekularbiologische Unterstützung, Dr. Dennis Janz für Hilfestellungen in der Statistik, Ashkan Amirkhosravi für diverse Nachtmessungen und alle Kollegen und Kolleginnen der Arbeitsgruppe, die mir als Erntehelfer und Unterstützer mehr als einmal zur Seite standen. Insbesondere bedanke ich mich bei Merle Fastenrath für eine gute Zusammenarbeit in anatomischen Fragestellungen, und zusammen mit Cathrin Leibecke und Marianne Smiatacz für die tolle Umsorgung meiner Pappeln.

Ich möchte mich ebenfalls bei meinen ehemaligen Bürokolleginnen Dr. Lisa Kins, Dr. Dade Yu und Dr. Aileen Kogel für ein paar tolle Jahre bedanken, für kreative Ideen und Diskussionen in wissenschaftlichen Fragestellungen aber auch für humorvolle Zeiten in diversen Kaffeerunden, Krimidinnern und abendlichen Veranstaltungen. Karl Kasper und Johannes Ballauff möchte ich für die

schöne Zeit danken, in der wir den neuen Ph.D. – Wagen für die Forstbotanik bastelten. Möge er viele Ph.D. – Generationen zur Gänseliesel bringen!

Weiterhin möchte ich mich bei meinen Eltern bedanken, die mich immer unterstützt haben und an mich glaubten, auch wenn ich es nicht tat. Danke für den Rückhalt!

Zuletzt möchte ich mich bei meiner Frau bedanken, für ihre Liebe, Geduld und Zusprache!

8.2. Declaration of academic honesty

Eidesstattliche Erklärung

Hiermit erkläre ich, Gerrit-Jan Strijkstra, dass ich die vorliegende Arbeit selbstständig und ohne unzulässige Hilfe oder Benutzung anderer als der angegebenen Quellen und Hilfsmittel angefertigt habe. Es wurden alle Personen genannt, die direkt und indirekt an der Entstehung der vorliegenden Arbeit beteiligt waren. Alle Textstellen, die wörtlich oder sinngemäß aus veröffentlichten oder nichtveröffentlichten Schriften entnommen sind, wurden als solche kenntlich gemacht.

Die vorliegende Arbeit wurde weder im Inland noch im Ausland in gleicher oder ähnlicher Form einer anderen Prüfungsbehörde zum Zweck einer Promotion oder eines anderen Prüfungsverfahrens vorgelegt.

Varel, den

_____

Gerrit-Jan Strijkstra